



**VALIDATE SMALL UNMANNED AIRCRAFT SYSTEMS (SUAS) DETECT AND
AVOID (DAA) WELL CLEAR REQUIREMENTS
(A11L.UAS.117): FINAL REPORT**

November 21, 2025

NOTICE

This document is disseminated under the sponsorship of the U.S. Department of Transportation in the interest of information exchange. The U.S. Government assumes no liability for the contents or use thereof. The U.S. Government does not endorse products or manufacturers. Trade or manufacturers' names appear herein solely because they are considered essential to the objective of this report. The findings and conclusions in this report are those of the author(s) and do not necessarily represent the views of the funding agency. This document does not constitute FAA policy. Consult the FAA sponsoring organization listed on the Technical Documentation page as to its use.

LEGAL DISCLAIMER

The information provided herein may include content supplied by third parties. Although the data and information contained herein has been produced or processed from sources believed to be reliable, the Federal Aviation Administration makes no warranty, expressed or implied, regarding the accuracy, adequacy, completeness, legality, reliability or usefulness of any information, conclusions or recommendations provided herein. Distribution of the information contained herein does not constitute an endorsement or warranty of the data or information provided herein by the Federal Aviation Administration or the U.S. Department of Transportation. Neither the Federal Aviation Administration nor the U.S. Department of Transportation shall be held liable for any improper or incorrect use of the information contained herein and assumes no responsibility for anyone's use of the information. The Federal Aviation Administration and U.S. Department of Transportation shall not be liable for any claim for any loss, harm, or other damages arising from access to or use of data or information, including without limitation any direct, indirect, incidental, exemplary, special or consequential damages, even if advised of the possibility of such damages. The Federal Aviation Administration shall not be liable to anyone for any decision made or action taken, or not taken, in reliance on the information contained herein.

TECHNICAL REPORT DOCUMENTATION PAGE

1. Report No. A11L.UAS.117 A68	2. Government Accession No.	3. Recipient's Catalog No.	
4. Title and Subtitle Validate Small Unmanned Aircraft Systems (sUAS) Detect and Avoid (DAA) Well Clear Requirements - Final Report	5. Report Date November 21, 2025		6. Performing Organization Code ASSURE
	8. Performing Organization Report No.		
7. Author(s) Bouteina Driouche, PhD- https://orcid.org/0000-0001-7034-0930 Walaa Al-Qwider, PhD- https://orcid.org/0000-0001-9888-7890 Armando De Abreu – https://orcid.org/0000-0002-7398-7294 Gerardo Arboleda – https://orcid.org/0000-0002-1953-4673 Gerardo Olivares, PhD – https://orcid.org/0000-0003-0748-3917 Luis Gomez – https://orcid.org/0000-0002-8768-9060 Mark Askelson: https://orcid.org/0000-0002-8521-7158 Prasad Pothana: https://orcid.org/0000-0001-7321-5625 Sreejith Nair: https://orcid.org/0000-0002-0529-4269 Mark S. Ewing, PhD, https://orcid.org/0000-0001-5982-6219 Hady Benyamen, PhD, https://orcid.org/0000-0001-9885-5004	10. Work Unit No.		
9. Performing Organization Name and Address Raspet Flight Research Laboratory, Mississippi State University, 114 Airport Rd, Starkville, MS 39759 National Institute for Aviation Research, Wichita State University, 1845 Fairmount St, Wichita, KS, 67260-0193. University of North Dakota Tech Accelerator Room 2050, 4201 James Ray Dr Stop 8367 Grand Forks, ND 58202-8367 University of Kansas Aerospace Engineering, 1530 West 15 th Street, Lawrence, KS 66045	11. Contract or Grant No. 15-C-UAS		
	13. Type of Report and Period Covered Final Report		
10. Sponsoring Agency Name and Address U.S. Department of Transportation Federal Aviation Administration Washington, DC 20591	14. Sponsoring Agency Code 5401		
	15. Supplementary Notes		
16. Abstract The ASSURE A68 project was established to conduct a holistic assessment of the currently accepted small UAS (sUAS) Well-Clear (WC) separation requirements, defined as 2,000 ft horizontal and 250 ft vertical in the American Society for Testing and Materials (ASTM) International standard F3442/F3442M-23. The research sought to determine whether these criteria remain adequate for today's sUAS operational environment or if refinements to either the horizontal or vertical separation distances are recommended. The study examined WC from operational, regulatory and human performance, and surveillance system perspectives using mitigated encounter simulations, pilot Right-of-Way (RoW) performance assessments, Remote ID (RID) field evaluations, and UAS Traffic Management (UTM) service testing. Project findings indicate that the 2,000'×250' separation remains appropriate for sUAS-MA encounters, though in cases where this separation distance creates significant operational burdens, the horizontal dimension could be reasonably reduced to 1,500 ft for non-cooperative encounters, provided the surveillance system reliably meets the minimum required detection performance. This approach maintains safety while supporting industry interest in reducing surveillance range where technically justified. Encounter simulation results show that collision likelihood remains within the safety targets proposed by ASTM for a 1500-ft horizontal separation under ideal sensor performance. In the RoW impact studies, both Virtual Reality (VR) and daytime test results indicate that there is a potential to reduce the 2000-ft horizontal separation to 1500 ft. This is further supported by using Class 3 UAS in these tests to enable visual acquisition and, therefore, collection of RoW impact data. Based on the VR tests, pilot responses support the adequacy of the current 250-ft vertical WC. As part of UTM field testing, simulations were performed to determine the minimum detection range required for UTM-enabled separation. Results indicate that a 1,500-ft separation reduced the required minimum detection range by roughly 1,000 ft (to ~2,250 ft) compared to the 2000-ft separation, although some flight tests revealed that in real-world flights, encounter setup, sensor latencies, position biases, and environmental effects (e.g., wind, terrain) introduce variability that the surveillance system must accommodate. Overall, the recommendation is that when there is not a significant cost, integration, or operational efficiency need to reduce the well clear dimension, such as in the case for most cooperative encounters and many UTM concepts, that the larger 2,000 ft dimension be used to maximize safety. For sUAS-to-sUAS interactions, RID and UTM testing demonstrated achievable separations of ~100–300 ft for small quadcopters and ~400–600 ft for larger platforms under current ASTM RID performance. Project findings provide a consolidated basis for FAA and standards bodies to consider adjustments to sUAS WC thresholds where operationally justified and to guide future refinement to DAA performance requirements.			
17. Key Words Well Clear, Mid-Air Collision, Encounter models, Right of Way, See and Avoid, Detect and Avoid, Beyond Visual Line of Sight, Remote Identification, Packet Reception Rate, UAS Traffic management, Minimum Detection Distance, Radar Range Bias, Azimuth Bias		18. Distribution Statement No restrictions. This document is available through the National Technical Information Service, Springfield, VA 22161. Enter any other agency mandated distribution statements. Remove NTIS statement if it does not apply.	
19. Security Classification (of this report) Unclassified	20. Security Classification (of this page) Unclassified	21. No. of Pages 102	22. Price

TABLE OF CONTENTS

NOTICE.....	I
LEGAL DISCLAIMER.....	II
TECHNICAL REPORT DOCUMENTATION PAGE.....	III
TABLE OF FIGURES.....	V
TABLE OF TABLES.....	VII
TABLE OF ACRONYMS.....	IX
EXECUTIVE SUMMARY.....	XI
1 INTRODUCTION, BACKGROUND, AND OBJECTIVES.....	1
1.1 Introduction.....	1
1.2 Background.....	3
1.2.1 Historical Basis of Risk Ratios.....	3
1.2.2 Derivation of Well-Clear Distances.....	4
1.2.3 Right-of-Way Rules and Well-Clear.....	6
1.2.4 Drone-to-Drone Operations.....	6
1.3 Motivation.....	7
1.4 Objectives.....	8
2 RESEARCH TASKS.....	9
2.1 sUAS-MA Well Clear Assessment.....	9
2.1.1 sUAS Well Clear Volume Validation.....	9
2.1.2 Right of Way Quantification.....	16
2.1.3 UTM Services Field testing.....	25
2.2 sUAS-sUAS Separation and Enabling Technologies.....	47
2.2.1 UTM Services Field Testing.....	47
2.2.2 Remote ID Field Testing.....	58
3 CONCLUSIONS AND RECCOMENDATIONS.....	78
3.1 sUAS-MA Separation.....	78
3.2 sUAS-sUAS Separation.....	85
4 REFERENCES.....	87

TABLE OF FIGURES

Figure 1.1: Well-clear and NMAC volume (ASTM F3442/F3442M-20, 2020)	5
Figure 2.1: MAC ratio $[P(\text{MAC} \text{enc})]$, NMAC risk ratio & LoWC ratio – 1200 code-exclude (coop).	13
Figure 2.2: MAC ratio $[P(\text{MAC} \text{enc})]$, NMAC risk ratio & LoWC ratio – 1200 code-only (non-coop).	14
Figure 2.3: Average MAC mitigation ratio for each aircraft pair	16
Figure 2.4: A stationary potential field (left) and a morphing potential field (right).	26
Figure 2.5: Morphing potential field geometry.....	27
Figure 2.6: Aircraft used in this work: (a) SkyHunter sUAS, (b) Cessna 172, (c) Cessna L319. 28	
Figure 2.7: Intruder aircraft heading angle definition.....	29
Figure 2.8:sUAS-Manned Aircraft Approach 1: ADS-B receives messages through Unifly	30
Figure 2.9: sUAS-Manned Aircraft Approach 2: Using Unifly UTM.....	31
Figure 2.10: sUAS-Manned Aircraft Approach 3: Simulated radar data sent to Unifly UTM. ...	31
Figure 2.11: sUAS-Manned Aircraft Approach 4: Actual radar data sent to Unifly UTM.	31
Figure 2.12: UTM messages received on the ground using a laptop.....	32
Figure 2.13: Diagram of corridor scenario for trailing sUAS with manned intruder interception ratios.....	34
Figure 2.14: Simulated sUAS-manned aircraft encounters: minimum detection distance at different relative encounter angles and three Cessna airspeeds. Results are for a 2000 ft horizontal well clear volume. Broken lines show the detection distances allowing 50% of the sUAS-manned aircraft simulated encounters to be well clear.	35
Figure 2.15: Minimum required detection distances to maintain 1500 and 2000 ft horizontal well clear separation between sUAS and manned aircraft. Manned intruder’s speed is 145 ft/s.	36
Figure 2.16: Comparison between Cessna L319 trajectories as obtained from radar detections and from the aircraft flight logs.	42
Figure 2.17: Error between detected radar positions and ADS-B positions: North error, East error, and magnitude of error. Errors are presented for the duration of Encounter 17.....	42
Figure 2.18: Latency in obtaining radar detection using the UTM system, as observed during the duration of Encounter 17.	45
Figure 2.19: sUAS-sUAS Approach 1: Using Unifly UTM.....	49
Figure 2.20: sUAS-sUAS Approach 2: Using 900 MHz communication.	49
Figure 2.21:sUAS Approach 3: Using network RID through Unifly UTM.	50
Figure 2.22: Simulated sUAS-sUAS encounters: minimum detection distance at different relative encounter angles and three intruder sUAS airspeeds. Results are for a 500 ft horizontal well clear volume. Broken lines show the detection distances allowing 50% of the sUAS-sUAS encounters to be well clear.	51
Figure 2.23: Minimum required detection distances to maintain the six studied sUAS-sUAS horizontal well clear separations. sUAS intruder’s speed is 45 ft/s.....	52
Figure 2.24: Minimum required detection distances to maintain the six studied sUAS-sUAS horizontal well clear separations. sUAS intruder’s speed is 60 ft/s.....	53
Figure 2.25: Minimum required detection distances to maintain the six studied sUAS-sUAS horizontal well clear separations. sUAS intruder’s speed is 90 ft/s.....	53

Figure 2.26: Observed UTM communication latencies in the flight containing sUAS-sUAS Encounters 1 and 2. The left plot shows the observed latency over the duration of the flight. The right plot shows the same data using a histogram plot. 55

Figure 2.27: Simplified testing matrix for evaluating RID performance..... 61

Figure 2.28: Simulated sUAS-sUAS encounters- minimum required detection distances to remain well clear across sHWC distances, and relative encounter angles. Left column: basic avoidance tuning ($\sigma = \text{sHWC}$), right column stronger avoidance tuning ($\sigma = \text{sHWC} + 50\text{ft}$). Rows show intruder speeds of 45 ft/s, 60 ft/s, and 90 ft/s..... 63

Figure 2.29: Packet reception rate (Hz) versus horizontal distance for all RID module configurations. 71

Figure 2.30: RID packet update rate (Hz) versus horizontal distance for all RID modules. 72

Figure 2.31: Packet reception rate versus horizontal distances during the inbound flight profile.74

Figure 2.32: RID packet update rate versus horizontal distances during the inbound flight profile. 75

TABLE OF TABLES

Table 1-1: Risk ratio and loss of well-clear requirements for cooperative and non-cooperative aircraft (ASTM F3442/F3442M-20, 2020).....	5
Table 2-1: Proposed WCVs for analysis.....	10
Table 2-2: Minimum detection distances which allow 100% and 50% of the sUAS-Manned aircraft encounters to be well clear, based on simulation. Results are for a 2000 ft horizontal well clear radius.....	36
Table 2-3: Minimum detection distances which allow 100% and 50% of the sUAS-manned aircraft encounters to be well clear, based on simulation. Results are for two horizontal well clear dimensions: 1500 ft and 2000 ft. Avoidance algorithm is set to have $\sigma =$ horizontal well clear radius + 50.	36
Table 2-4: Sample head-on flight test encounter.	37
Table 2-5: Summary of sUAS-manned aircraft head-on flight test encounters.....	38
Table 2-6: Summary of sUAS-manned aircraft 90-degree flight test encounters.	39
Table 2-7: Summary of sUAS-manned aircraft 30-degree flight test encounters.	40
Table 2-8: Summary of sUAS-manned aircraft overtaking flight test encounters.	40
Table 2-9: Head-on sUAS-manned aircraft encounters using real radar data sent to Unifyfly	41
Table 2-10: Summarized comparison of simulation and flight test detection distances.....	43
Table 2-11: Summary of latency statistics for the ten sUAS-manned aircraft flight tests.	44
Table 2-12: Statistics of the observed latencies and update periods for the Cessna 172 flight data. 4,867 data points were collected (~81.1 minutes of flight).	45
Table 2-13: Minimum detection distances which allow 100% and 50% of the sUAS-sUAS encounters to be well clear, based on simulation. Results are for a 500 ft horizontal well clear radius.....	52
Table 2-14: Minimum detection distances which allow 100% and 50% of the sUAS-sUAS encounters to be well clear, based on simulation. Results are for six horizontal well clear separations. Avoidance algorithm is set to have $\sigma =$ horizontal well clear radius + 50.....	54
Table 2-15: Summary of sUAS-sUAS head-on flight test encounters	55
Table 2-16: Statistics of latencies observed with network RID data forwarded to Unifyfly.	56
Table 2-17: Statistics of the observed latencies and update periods for the sUAS flight data at Lawrence, KS. 13,488 data points were collected (~224.8 minutes of flight).....	56
Table 2-18: Statistics of the observed latencies and update periods for the sUAS flight data at Starkville, MS. 1980 data points were collected (~33 minutes of flight).	56
Table 2-19: Proposed Well -Clear Volumes for sUAS-vs-sUAS.....	60
Table 2-20: Minimum Detection Distances which allow 50% of the sUAS-sUAS encounters to be well clear, based on simulation across sHWC distances, intruder speeds and avoidance algorithm tuning.	63
Table 2-21: Minimum Detection Distances which allow 100% of the sUAS-sUAS encounters to be well clear, based on simulation across sHWC, intruder speeds and avoidance algorithm tuning.	64
Table 2-22: Mean and standard deviation of horizontal position error (in feet) for different aircraft – RID (WiFi) module configurations across varying distances.....	66
Table 2-23: Mean and standard deviation of horizontal position error (in feet) for different aircraft – RID (BLE) module configurations across varying distances.	67

Table 2-24: Mean and standard deviation of horizontal position error (in feet) for different aircraft – RID (WiFi) module configurations across varying speeds.....	68
Table 2-25: Mean and standard deviation of horizontal position error (in feet) for different aircraft – RID (BLE) module configurations across varying speeds.	69
Table 2-26: Hover time and total number of received RID packets for each aircraft–RID module configuration across horizontal separation distances.....	70
Table 2-27: Hover time and number of unique (non-duplicate) RID packets for each aircraft–RID module configuration across horizontal separation distances.....	72
Table 2-28: Inbound flight results showing segment travel time and number of received RID packets.....	73
Table 2.29-: Inbound flight results showing segment travel time and number of received RID packets.....	74
Table 2-30: sUAS-sUAS horizontal well clear separation: A brief assessment.....	76

TABLE OF ACRONYMS

ADS-B	Automatic Dependent Surveillance-Broadcast
AGL	Above Ground Level
ARC	Aviation Rulemaking Committee
ASTM	American Society for Testing and Materials
BVLOS	Beyond Visual Line of Sight
CFR	Code of Federal Regulations
COTS	Commercial Off-the-Shelf
DAA	Detect and Avoid
DAIDALUS	DAA Alerting Logic for Unmanned Systems
DEGAS	DAA Evaluation of Guidance, Alerting, and Surveillance
FAA	Federal Aviation Administration
FWME	Fixed Wing Multi-Engine
FWSE	Fixed Wing Single-Engine
GPS	Global Positioning System
ICAO	International Civil Aviation Organization
KU	University of Kansas
LoWC	Loss of Well Clear
LoWCR	Loss-of-Well-Clear Risk Ratio
LTE	Long Term Evolution
MA	Manned Aircraft
MAC	Mid-Air Collision
MHz	MegaHertz
MDD	Minimum Detection Distances
MIT LL	Massachusetts Institute of Technology Lincoln Laboratory
MOPS	Minimum Operational Performance Standards
MPF	Morphing Potential Field
MSU	Mississippi State University
NAS	National Airspace System
NMAC	Near Mid-Air Collision
NPRM	Notices of Proposed Rulemaking
RID	Remote Identification
RF	Radio Frequency
RoW	Right-of-Way
RTCA	Radio Technical Commission for Aeronautics
sHWC	sUAS Horizontal “Well Clear”
SME	Subject Matter Expert
sNMAC	Small Near Mid-Air Collision
sUAS	Small Unmanned Aircraft System
TCAS	Traffic Collision Avoidance System
TICS	Test Information Collection System
TLS	Target Level of Safety
UAS	Unmanned Aircraft Systems
USC	United States Code

UTM	UAS Traffic Management
VR	Virtual Reality
WC	Well Clear
WCR	Well Clear Requirements
WCV	Well Clear Volume

EXECUTIVE SUMMARY

The ASSURE A68 project was established to initiate a holistic assessment of the currently accepted small UAS (sUAS) Well-Clear (WC) separation requirements, defined as 2,000 ft horizontal and 250 ft vertical in the American Society for Testing and Materials (ASTM) standard F3442/F3442M-23, and to determine whether these criteria remain adequate for today's sUAS operational environment or if refinements to the horizontal and/or vertical separation distances are recommended. Current WC thresholds were originally developed during a period when few fielded Detect and Avoid (DAA) systems existed and operational data were limited. As a result, the current standard emerged from unmitigated encounter simulations, first-order analytical estimates, and expert judgment rather than from a fully validated systems engineering process. A68 initiates the most comprehensive assessment of these criteria to date, integrating mitigated encounter simulations, pilot Right-of-Way (RoW) performance, Remote ID (RID) field testing, and UAS Traffic Management (UTM) system evaluations. Encounter simulations suggest a moderate reduction of the horizontal WC threshold, from 2,000 ft to 1,500 ft, maintains ASTM safety thresholds for cooperative encounters and remains near-threshold for non-cooperative scenarios when supported by adequate surveillance performance. For RoW impact pilots expressed a desire to maneuver at a significant rate at ~ 1531 ft in VR and 1,712 ft during real-world daytime flights for the encounter conditions that were tested. Vertical RoW impacts observed in the VR tests support the adequacy of the current 250-ft vertical standard. These results also support the potential use of a 300-ft vertical separation for well clear, with the understanding that the VR findings may be biased high due to the use of a larger Group 3 UAS. UTM field testing showed that UTM-supported horizontal separation between sUAS and manned aircraft is feasible at 1,500-ft and 2,000-ft WC thresholds, when detection ranges meet the simulation derived minimum detection distances, position errors are small relative to separation distances, and communication latencies remain low. Flight tests demonstrated reliable cellular connectivity, but also highlighted that position error (e.g., 500-ft radar biases), occasional latency spikes, and high-density encounters can require substantially larger detection distances. Since sensor tracking range is not a constraint for detecting and avoiding cooperative aircraft, reducing the cooperative well clear distance does not offer meaningful benefits for sensor design or integration in the same way it might for non-cooperative traffic. To preserve safety while minimizing operational impacts, the recommended approach is to retain the 2,000-ft well-clear distance for cooperative traffic while allowing well clear against non-cooperative intruders to be reduced to 1,500 ft, provided the surveillance system can reliably detect the intruder at the reduced WC boundary. Cooperative traffic is also likely to operate at higher speeds, providing an additional rationale for maintaining a larger standoff distance when doing so does not create significant operational burdens.

For drone-to-drone operations, candidate horizontal separations between 100 ft and 600 ft emerge as feasible starting points when supported by RID and UTM, though accuracy, latency, and message dropouts remain important constraints when operating at tighter separation distances

1 INTRODUCTION, BACKGROUND, AND OBJECTIVES

1.1 Introduction

The safe integration of small Unmanned Aircraft Systems (sUAS) into the National Airspace Systems (NAS) requires a clear and validated definition of Well-Clear (WC) – the separation needed to avoid creating a collision hazard or interfering with Right-of-Way (RoW) responsibilities. Current WC separation criteria for sUAS as reflected in American Society for Testing and Materials (ASTM) International standard F3442/F3442M-23 (ASTM F3442/F3442M-23, 2023) and other Detect and Avoid (DAA) performance standards, were developed during a period when operational data, fielded DAA systems, and empirical validation sources were limited. As a result, the existing WC criteria emerged from a series of unmitigated encounter analyses, first-order assumptions, and expert judgment rather than from a fully traceable systems engineering process.

As sUAS operations rapidly expand, particularly in Beyond Visual Line of Sight (BVLOS) operations, low altitude airspace, and environments involving both cooperative and non-cooperative traffic, the adequacy of the current WC criteria needed to be further verified and validated.

Among others, factors such as surveillance accuracy, latency, sensor performance, pilot response, and compliance with RoW rules all influence whether the established WC dimensions remain sufficient for today’s operational landscape. Likewise, emerging needs such as UAS Traffic Management (UTM), and high-density drone operations introduce additional separation challenges that were not considered during early WC development.

Recognizing these gaps, the ASSURE A68 project was established to initiate a holistic assessment of WC for sUAS. The project builds on the analytical foundations of previous ASSURE efforts and the Massachusetts Institute of Technology Lincoln Laboratory (MIT LL) encounter set research and extends the investigation to address areas not previously evaluated. A68 aims to answer the following research questions:

1. *How do different potential DAA WCRs impact collision likelihood for UAS equipped with DAA?*
2. *Concerning the proposed ASTM sUAS WC criteria of 2,000’ horizontal and 250’ vertical, is the vertical distance sufficient? Can the horizontal dimension be reduced? Are the proposed distances sized correctly to 1) not interfere with manned operations while also balancing 2) the industry desires to reduce surveillance range if it is safe to do so? Are different well clear distances recommended based on the equipment of the crewed aircraft?*
3. *What should the separation and performance requirements be for BVLOS sUAS to remain separated from other sUAS that broadcast their Remote ID (RID)?*
4. *What is the list of factors that should be considered when assessing and validating proposed WC Ratios? What factors are more important than others?*

5. *What data elements are needed for information that is presented to a remote pilot to be useable for decision making when a pilot maneuvers to remain well clear?*
6. *What is the performance of on-board pilots to remain well clear of other aircraft that have the right-of-way?*
7. *The BVLOS Aviation Rulemaking Committee (ARC) report recommends that non-cooperative aircraft below 500' Above Ground Level (AGL) give way to BVLOS drones. How well can an onboard pilot using see-and-avoid do this for different manned low altitude operations? What are estimated probability of visual acquisition at range and example closest points of approach when trying to give way to a small or medium drone? Do lights or paint schemes help at all during the day?*

To address these research questions, the A68 project was structured as a three-phase effort and organized into a set of research tasks spanning foundational research, analytical modeling and simulation, flight testing, and system-level assessments. Each task involves dedicated research activities that contribute to a specific component needed to holistically assess Well Clear for sUAS, while also enabling integration of results across both sUAS vs Manned Aircraft (MA) and sUAS vs sUAS encounters.

The following outlines the project's corresponding phase I, II, and III tasks planned to generate the analytical, experimental, and operational insights needed to evaluate whether existing ASTM WC criteria remain suitable, identify refinements where needed, and establish a more traceable and comprehensive basis for future WC criteria.

0. Project Management:
Management of the overall project, including project kick-off, the project research task plan, technical interchange meetings, research summaries, leadership briefings, industry standards engagement, and project close out.
1. Phase I: Background Report
Assessment of international, U.S. government, standards body, and industry work to create well clear separation criteria for DAA systems. Literature review identifies research gaps concerning ensuring well clear requirements between sUAS to sUAS and sUAS to MA encounters and assesses the state of the art in UTM services.
2. Phase II: Creation of Planning Documents
 - a. sUAS Well Clear Volume Validation
 - b. RoW Quantification
 - c. Remote Identification Field Testing
 - d. UTM Services Field Testing
 Development of comprehensive work plans with the dual objectives of refining and/or validating well clear separation criteria and proposing and/or validating well clear separation criteria.
3. Phase III: Test Plan Execution:
 - a. sUAS Well Clear Volume Validation

- b. RoW Quantification
- c. Remote Identification Field Testing
- d. UTM Services Field Testing
- e. Final Briefing and Report

Execute the approved test, simulation, and analysis plans for each topic and deliver the final briefing and report.

This final report consolidates the project phases and the key findings from each task to provide the concise insights needed to support a comprehensive and operationally relevant assessment of Well Clear criteria for small UAS.

1.2 Background

Over the past decade, the development of DAA WC separation requirement (WCRs) has evolved through a series of first-order analytical estimates and Subject Matter Expert (SME) judgment. Early approaches for WC thresholds and associated risk ratios were derived from manned aviation “see-and-avoid” performance models and later adapted to support UAS integration into the NAS. The resulting nominal values were subsequently formalized as recognized benchmarks by the International Civil Aviation Organization (ICAO) and adopted by the Radio Technical Commission for Aeronautics (RTCA) and the ASTM, forming the groundwork for subsequent DAA system performance evaluations. Over time, this layering of assumptions, approximations, and unmitigated analyses has introduced uncertainty regarding the adequacy of the existing WC standards across cooperative and non-cooperative operations, especially for sUAS operations. The main goal of this project is to conduct a holistic evaluation to verify and validate the proposed WC criteria. This includes performing mitigated analyses that incorporate DAA system behavior, assessing how well-clear thresholds are perceived by other pilots, revisiting foundational assumptions, and integrating results across multiple operational and surveillance contexts.

1.2.1 Historical Basis of Risk Ratios

(Hendrickson, 2015) provided one of the earliest systematic efforts to quantify pilot’s “see-and-avoid” performance using collision data and traffic densities across the NAS to derive baseline risk ratios. The study estimated the pilot Field of Regard Near Mid-Air Collision (NMAC) risk ratio as 0.3115 which later informed ICAO and other standards efforts. ICAO adopted this value and established a non-cooperative DAA NMAC risk ratio of 0.3, representing the probability that a DAA system could prevent an NMAC under nominal conditions (ICAO, 2018). ICAO SMEs introduced a conceptual linkage between NMAC risk ratio and WC risk ratio, assuming that remaining well clear must contribute about half of the overall collision avoidance. The Loss of Well Clear (LoWC) risk ratio was estimated through a rough first-order relationship as $\sqrt{0.3} \approx 0.54$, rounded to 0.5 for non-cooperative operations (ICAO, 2018). Though this estimate is mathematically incorrect, it was considered operationally acceptable for early DAA performance standards and served as a pragmatic benchmark in the absence of detailed validation data. The rationale was that a safety requirement should ensure compliance in at least half of operational cases (ICAO, 2018). The same approach was used for cooperative intruders where the Traffic Collision Avoidance System (TCAS) served as the reference benchmark. ICAO lists a minimum NMAC risk ratio of 0.18 for TCAS and the corresponding WC requirement for cooperative

operations was set to $\sqrt{0.18} \approx 0.42$, formalized as 0.4 in DAA standards development (ICAO, 2018).

1.2.2 Derivation of Well-Clear Distances

With risk ratios established, subsequent efforts by MIT LL conducted large-scale unmitigated encounter analyses using models representative of NAS traffic, to determine WC separation distances that would satisfy the adopted risk ratios for cooperative and non-cooperative intruders (Weinert, Campbell, Vela, Schuldt, & Kurucar, 2018). Because a few functional DAA systems existed at that time, the intent was to define a WC standard that is independent of the DAA system (unmitigated).

The analyses relied on encounter set simulations to generate conditional probability curves, $P(\text{MAC}|\text{NMAC})$ and $P(\text{NMAC}|\text{LoWC})$, from which WC distance thresholds were derived. However, part of the analysis was based on a historical but unverified assumption that the probability of a Mid-Air Collision (MAC) if an NMAC occurs, $P(\text{MAC}|\text{NMAC})$ was 10% (RTCA, 2005). This assumption originated from early aviation studies and was carried forward largely for continuity, despite evidence that the value varies significantly with aircraft size and geometry. Later research for general aviation aircraft demonstrated that a value of 10% for $P(\text{MAC}|\text{NMAC})$ may not correlate with many types of manned vs manned aircraft encounters (Kochenderfer et al., 2010). However, the value was retained in MIT LL unmitigated encounter analysis for $P(\text{NMAC}|\text{LoWC})$ when selecting WC separation distances (Weinert, Campbell, Vela, Schuldt, & Kurucar, 2018), even though the domains are different. This highlights that the 10% value for $P(\text{MAC}|\text{NMAC})$ was applied to a different domain for $P(\text{NMAC}|\text{LoWC})$. While this approach lacked traceability between risk ratios and separation distances, it was the only feasible approach at the time. The resulting Well-Clear volume (WCV) recommended by MIT LL based on an unmitigated $P(\text{NMAC}|\text{LoWC}) \approx 0.1$ was 2000ft horizontal separation and 250ft vertical separation. This WCV was subsequently adopted by industry standards and formalized as the benchmark for DAA system performance requirements. RTCA Special Committee 147 (SC-147) incorporated this volume into the Minimum Operational Performance Standards for Airborne Collision Avoidance System sXu, DO-396 (RTCA, 2022) and ASTM International established the separation thresholds within ASTM F38 (ASTM F3442/F3442M-20, 2020), the Standard Specification for DAA System Performance Requirements. Current Well Clear and NMAC volumes suggested by ASTM are illustrated in Figure 1.1 while Table 1-1 lists the risk ratio target requirements established by ASTM. ICAO, on the other hand, has not provided a specific definition of WCV for UAS. The proposed WC definition remains under consideration at the ICAO level and is expected to reflect a holistic approach that goes beyond nominal conditions and incorporates traceability to regulations, mitigated analysis, human factors, system performance and interdependencies and other aspects recognized as essential to ensure Target Level of Safety (TLS) across NAS-representative operations (ICAO, 2018).

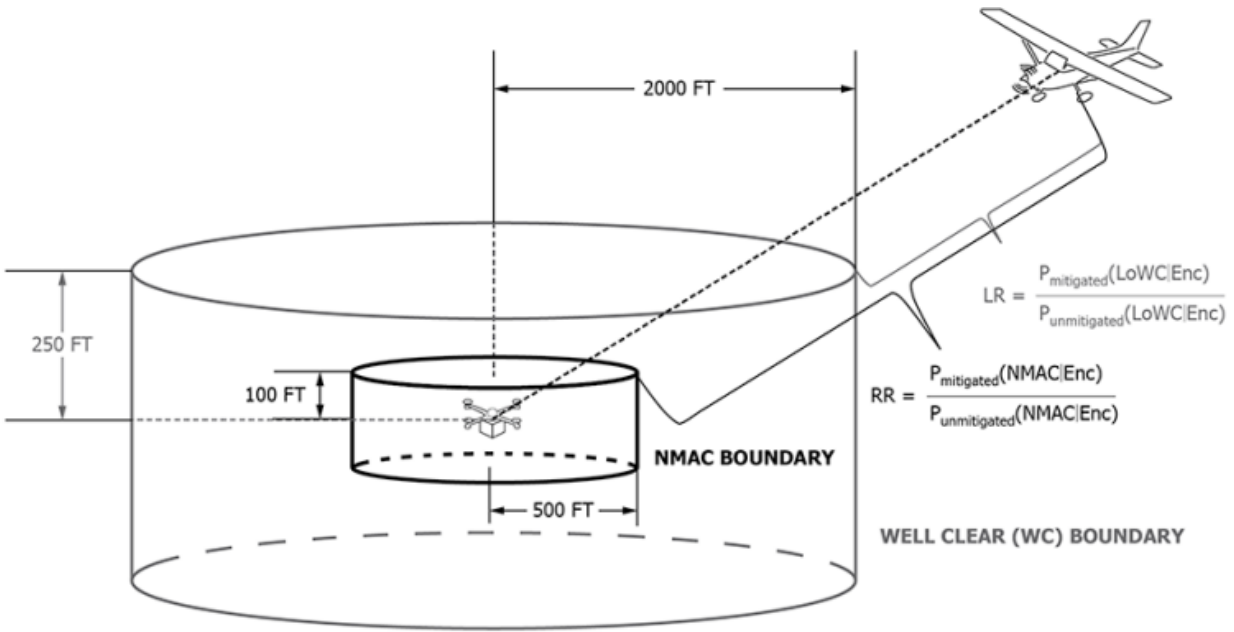


Figure 1.1: Well-clear and NMAC volume (ASTM F3442/F3442M-20, 2020)

Table 1-1: Risk ratio and loss of well-clear requirements for cooperative and non-cooperative aircraft (ASTM F3442/F3442M-20, 2020).

	Cooperative Intruder	Non-cooperative Intruder
ASTM NMAC RR	0.18	0.30
ASTM LoWCR	0.40	0.50

While unmitigated analyses provide a useful starting point, they lack the operational, human, and system-integration factors required to fully validate WC criteria for modern DAA-equipped sUAS operations. By definition, an unmitigated analysis does not account for real-world DAA system characteristics—such as sensor accuracies, latencies, avoidance timelines, or sUAS maneuverability—and is therefore limited in its ability to inform safety targets for operational DAA systems. It also omits several key considerations necessary for a holistic safety assessment, including:

- Operational efficiency impacts (e.g., additional flight time from avoidance maneuvers and the relationship between WC size, false tracks, and false alerts);
- Onboard pilot perceptions regarding the acceptability or perceived hazard of close encounters; and
- System-to-system interactions, such as the role of intruder ADS-B Out, Remote ID messages, UTM services, or ATC coordination

1.2.3 Right-of-Way Rules and Well-Clear

(Weinert, Campbell, Vela, Schuldt, & Kurucar, 2018) proposed a WC definition commonly referred to as the “hockey-puck” volume, defined as 2,000 ft horizontal and 250 ft vertical separation. Within the U.S. aviation regulations, the concept of “remaining well clear” is defined in terms of RoW rules. In the Code of Federal Regulations (CFR) (14 CFR §91.113, 2025) (section 113 is “Right-of-Way Rules: Except Water Operations” for Part 91 which is for “General Operating and Flight Rules”; e-CFR 2025a), pilots are required to maintain vigilance to see and avoid other aircraft and must maneuver to not interfere with another aircraft’s RoW. The regulation specifies how aircraft must yield or maneuver based on aircraft category and encounter geometry. Well-Clear is therefore defined in this context according to whether one interferes with the RoW of another aircraft.

Similarly, in (14 CFR §107.37, 2025) (section 37 is “Operation Near Aircraft: Right-of-Way-Rules” for part 107 which is for “Small Unmanned Aircraft Systems”; e-CFR 2025b), requires that sUAS must yield right-of-way to all aircraft and must not operate so close to another aircraft as to create a collision hazard. The regulation also specifies that sUAS may not pass over, under, or ahead of a manned aircraft unless well clear. In practice, this means that sUAS must give way and maintain sufficient distance to not interfere with the RoW of another aircraft. The recent FAA Notice of Proposed Rulemaking (NPRM) for BVLOS operations, commonly referred to as Part 108, proposes to relax requirements placed upon UAS that are not operating in a shielded area in that they have the RoW at low altitudes unless other aircraft are transponding, departing, or arriving from an airport or heliport. Even with this relaxation of a requirement, maintenance of WC (safe distance) is required which occurs within the context of RoW.

While the proposed “hockey-puck” volume provides an interpretation of WC for analytical and system-design purposes, the regulatory definition of WC is inherently behavioral and focuses on whether one aircraft interferes with another aircraft’s Right-of-Way

1.2.4 Drone-to-Drone Operations

The challenges observed in establishing WC criteria for sUAS–manned aircraft (sUAS-MA) encounters are also reflected in early attempts to define separation thresholds for small UAS–to–small UAS (sUAS–sUAS) interactions. One widely cited starting point for sUAS-sUAS interactions is the small NMAC (sNMAC) threshold, characterized as approximately 50 ft horizontal and ± 15 ft vertical separation (RTCA, 2022). This threshold was originally derived from a simplified 10% conditional collision probability assumption, similar to the historical assumption used in earlier manned aviation studies. Subsequent research has shown that this value is not consistently representative of actual collision likelihood and, in many cases, is smaller than the navigation and surveillance position uncertainty associated with sUAS platforms. As a result, a sNMAC event in real-world NAS operations may not be detectable or verifiable, particularly in BVLOS operations where operators rely on onboard navigation sensors, Automatic Dependent Surveillance-Broadcast (ADS-B), RID, or UTM services. Differences in altimetry sources (e.g., GPS vs. barometric) and surveillance update rates may introduce additional ambiguity in determining whether aircraft were within sNMAC proximity. Thus, the currently referenced sNMAC criteria function more as first-order placeholders rather than operationally meaningful separation metrics.

Initial “back of the envelope” rationale intended to frame the exploration of more appropriate “well-clear” distances for sUAS–sUAS encounters begins with observations leveraged from FAA Order 8040.6A (FAA, 8040.6A, 2023), which links severity categories to allowable event probabilities (it is important to note that Order 8040.6A does not currently provide fully developed, operation specific severity categories for all classes of sUAS and that further maturation of those tables may be required):

- A sUAS-sUAS collision poses lower severity than a collision between a sUAS and a MA, as no person is onboard either platform. Consequences are primarily related to aircraft hull loss, mission disruption, and potential effects on people, property, and infrastructure on the ground.
- A one level reduction in severity (e.g., Hazardous to Major) corresponds to ten (10) times increase in allowable event probability

A working assumption can therefore suggest that a sUAS-MA collision scenario could be treated at a higher severity level (e.g., “hazardous”) while a sUAS-sUAS collision could, in many cases, be treated at a lower severity level (e.g., “major”), depending on operating environment. Based on this conceptual reasoning, it can be proposed that the current ASTM sUAS WCV of 2000 ft by ± 250 (designed to reduce the unmitigated 500 ft by ± 100 ft NMAC likelihood by approximately 10 times), could be scaled down for sUAS-sUAS interactions. A starting point of investigation for sUAS–sUAS “well-clear” volume each with 13 ft wingspan (representative of the average airframes considered in (ASTM F3442/F3442M-23, 2023) well clear work) could therefore be closer to the sUAS-MA NMAC cylinder (500 ft \times ± 100). While this estimate is not a formal standard, it follows FAA risk matrix logic and may be applicable to interactions between sUAS larger than 55 lb and a wingspan less than 13 ft.

For interaction between sUAS under 55 lb, collisions between two such small drones are expected to present lower severity levels than collisions involving larger sUAS or manned aircraft, particularly outside densely populated environments. Using the same 8040.6A logic, a further reduction in severity would imply another 10 times increase in allowable event probability. A candidate sUAS–sUAS “well clear” volume of 100 ft horizontal by ± 50 ft vertical can be proposed as a working exploratory range, rather than a recommended standard. It is critical to note that such small volume must be evaluated against the combined effects of sensor uncertainty (e.g., RID) such as positional accuracy, latency, and update rate. If the total uncertainty in relative position is comparable to or larger than the candidate small “well clear” volume, then the resulting well clear definition may not provide reliable operational buffer.

These candidate values (500 ft \times ± 100 for larger sUAS and 13 ft wingspan and 100 ft \times ± 50 ft for ≤ 55 lb sUAS) should therefore be treated as initial analytical starting point rather than validated design targets.

1.3 Motivation

Current DAA WC separation criteria were developed at a time when operational data, fielded DAA systems, and empirical validation sources were limited. The resulting WC thresholds were established primarily through unmitigated encounter analyses (without DAA), first-order analytical estimates, and subject matter expert judgment. These values served as a necessary

foundation for early UAS integration; however, a fully traceable systems engineering basis for WC remains incomplete. Among other things, previous efforts often lacked:

- Clear traceability back to regulatory RoW intent
- A holistic assessment of how WC criteria are used across different system functions
- Integration of human factors perspectives (e.g., how onboard pilots or remote operators perceive and act upon WC)
- Alignment of WC distance thresholds with the safety risk ratios and representative encounter sets
- Other operational, procedural, and environmental influences

These limitations take on greater importance as UAS operations move toward routine BVLOS operations and begin to include a broader range of aircraft sizes and surveillance capabilities. The continued reliance on legacy assumptions and simplified analytical models introduce increasing uncertainty regarding the suitability of the current WC standards for sUAS BVLOS operations. The existing WC thresholds were originally derived from manned aviation and larger UAS concepts and may not fully reflect key factors that shape sUAS operations, particularly at low altitudes and in an airspace shared with other aircraft types. As a result, questions persist regarding whether the current WC separation volume remain appropriately sized across:

- Cooperative and non-cooperative surveillance environments,
- Different manned aircraft categories and encounter geometries,
- Regulatory RoW compliance and pilot/system response behavior,
- Sensor performance limitations, including detection range, accuracy, and latency, and
- Low-altitude sUAS-sUAS interactions

1.4 Objectives

The ASSURE A68 project is established to initiate a holistic assessment of WC separation requirements for sUAS. This effort builds directly on foundational analytical and experimental work from MIT LL and previous ASSURE projects, including A47 – *Small UAS Mid-Air Collision Likelihood*, A65 – *Detect and Avoid Risk Ratio Validation* and A23 – *Validation of Low-Altitude Detect and Avoid Standards*.

The primary objective of A68 is to determine whether the existing ASTM WC criteria (ASTM F3442/F3442M-23, 2023) continue to provide an acceptable level of safety for NAS-representative sUAS operations—or whether refinements to the horizontal and/or vertical separation distances are recommended. This includes evaluating whether the current WC volume remains appropriately sized across cooperative and non-cooperative encounters, and different manned aircraft categories and encounter geometries. Additionally, as WC is defined in regulations within the framework of RoW compliance, the project also assesses how onboard pilots’ behavior affects the ability to maintain WC when encountering a sUAS. This includes examining the performance of onboard pilots in visually acquiring the sUAS and the distances at which MA pilots feel their RoW is impacted by sUAS at low altitudes.

Beyond sUAS–MA aircraft interactions, the project explores separation requirements for drone-to-drone (sUAS–sUAS) encounters, particularly for BVLOS operations that rely on broadcast RID or other surveillance sources. The intent is to determine whether currently fielded RID systems, operating at ASTM minimum update rates and transmission power, can reliably meet the

communication and accuracy performance needed to support DAA functions. These evaluations help inform the broadcast power levels and broadcast rates needed so that RID can support drone-to-drone avoidance to maintain safe separation across different candidate small “well-clear” horizontal distances and ultimately support the recommendation of a small “well clear” horizontal separation distance.

A68 further includes assessing the role of UTM services in maintaining safe separation between both sUAS and MA and sUAS and other sUAS operating in the same airspace. In this context, the UTM system receives aircraft position information from different data sources to enable avoidance functions based on shared situational awareness and defines the minimum detection distances required to maintain WC across different horizontal separation distances, aircraft speeds and encounter geometries. The project also addresses an emerging area of interest focusing on how UTM could support high-density drone operations. Such environments create new challenges for safe separation, including higher detection range, sensor accuracy limitation, and communication delays.

This work offers several other important benefits that add value to the community regarding the assessment and development of sUAS DAA WC requirements. The findings provide a consolidated basis for FAA and standards bodies to consider adjustments to sUAS WC thresholds where technically justified and to guide future refinement to DAA performance requirements.

2 RESEARCH TASKS

2.1 sUAS-MA Well Clear Assessment

This section focuses on assessing and validating WC separation criteria between sUAS and manned aircraft (sUAS-MA) through a combination of simulations, flight testing, and human-in-the-loop evaluations. This section provides a summary of the results obtained from the tasks established to address the research questions for the project. Comprehensive task details are available in the individual Task Execution Reports published on the ASSURE website. The following research tasks were performed:

- sUAS Well Clear Volume Validation
- Right of Way Quantification
- Remote Identification Field Testing
- UTM Service Field Testing

2.1.1 sUAS Well Clear Volume Validation

2.1.1.1 Task Overview

This task applies a modeling and simulation approach to evaluate sUAS DAA well-clear criteria defined in (ASTM F3442/F3442M-23, 2023), building on ASSURE Project A47 *Small UAS Mid-Air Collision Likelihood* (De Abreu, et al., 2023) and using encounter sets derived from MIT Lincoln Laboratory ((Underhill & Weinert, 2021) (Weinert, Underhill, & Wicks, 2019)) encounter models. This research analyzes interactions between sUAS and rotorcraft, fixed-wing single-engine, and fixed-wing multi-engine aircraft. Performance is quantified using near mid-air collision risk ratio, loss-of-well-clear ratio, and the probability of mid-air collision; evaluated against the (ASTM F3442/F3442M-23, 2023) standard requirements for cooperative and non-cooperative operations. The main question considered in this evaluation is whether the horizontal

well-clear requirement can be reduced while maintaining safety levels, thereby informing a practical standard for BVLOS operations without increasing collision risk.

2.1.1.2 Method and Approach

This section describes the methodology used to generate and analyze the encounter sets, evaluate well-clear performance, and define the assumptions that bound the analysis. The objective was to test six well-clear volumes (WCVs), shown in Table 2-1, and determine how the horizontal and vertical distances affect mid-air collision probabilities. Moreover, the results of this analysis served to determine if smaller volumes satisfy the (ASTM F3442/F3442M-23, 2023) requirements while maintaining a safe probability of mid-air collision.

Table 2-1: Proposed WCVs for analysis

Well-Clear Volume	HMD (ft)	VMD (ft)
1	2000	450
2	2000	250
3	1500	250
4	1000	250
5	1000	100
6	500	100

A Monte Carlo simulation framework (Espindle, Griffith, & Kuchar, 2009), (RTCA DO-365B SC-228, 2021) was used to evaluate the sUAS-manned aircraft encounters derived. This analysis estimated NMAC and MAC outcomes under two conditions: mitigated, with a DAA system, and unmitigated, with no DAA logic applied.

Manned aircraft trajectories were produced from MIT Lincoln Laboratory uncorrelated encounter models, version 2.1 (Weinert, et al., 2021) for rotorcraft, fixed-wing single-engine (FWSE), and, and fixed-wing multi-engine (FWME) aircraft. Small UAS trajectories were produced by the geospatial encounter model (Weinert, 2021). A pairing process created encounters across multiple regions and filtered them to the small-UAS operating band from 50 to 1,200 feet above ground level and ownship speeds from 5 to 100 knots. This task leveraged the encounter sets produced on the previous ASSURE A47 project (De Abreu, et al., 2023).

Simulations ran in the DAA Evaluation of Guidance, Alerting, and Surveillance (DEGAS) (Serres, et al., 2020) environment using six-degree-of-freedom point-mass dynamics. Unmitigated runs held both aircraft on nominal paths. Mitigated runs allowed the sUAS to maneuver in response to DAA alerts. Detect and Avoid Alerting Logic for Unmanned Systems (DAIDALUS) v2.0.1c (Muñoz, et al., 2015), provided warning-level alerts in the form of directive guidance. The issued

alerts were executed as a system response with a one-second delay, a maximum turn rate of 7 degs/s, and climb or descent capability of plus or minus 1000 ft/min.

Surveillance sensors were utilized to support cooperative and non-cooperative encounter models. Cooperative encounters used ADS-B 1090ES with representative position and velocity accuracy specifying NACp and NACv errors. Non-cooperative encounters used an omnidirectional air-to-air (ATAR) radar with a 2 km declaration range and full circular (360 degs) field of regard. The detection probability was assumed at 80% throughout the declaration range.

Mid-air collision checks were applied to all encounters that resulted in an NMAC within DEGAS. Each case was reconstructed and evaluated with V-COLLIDE (Hudson, Lin, Cohen, Gottschalk, & Manocha, 2000) libraries using polygonal geometries representative of general aviation, rotorcraft, and business jet intruders, and sUAS quadcopter and fixed-wing geometries of up to 25 ft wingspan.

Assumptions in this analysis included uncorrelated traffic, no maneuver by the manned aircraft, nominal sensor performance without false-track modeling, no wind or environmental disturbances, and uniform sampling across the small-UAS altitude band. These assumptions bound the interpretation of results and are consistent with prior ASSURE analyses.

2.1.1.3 Common Analytical Metrics

In this study, simulation metrics are computed in DEGAS over the encounter sets analyzed; probabilities use weights, which were set to 1.

The risk ratio is a quantity that helps measure the performance of the Collision Avoidance System or DAA logic in use for a given encounter set. The risk ratio compares the number of encounters that resulted in an NMAC equipped with DAA to the number of encounters that resulted in an NMAC without a DAA, as given by Eq. (1)

$$Risk\ Ratio = \frac{\sum \{mitigated P(NMAC)\}}{\sum \{unmitigated P(NMAC)\}} \quad (1)$$

An NMAC is defined as penetration of a cylindrical volume of fewer than 500 feet horizontally and 100 feet vertically. $P(NMAC)$ for a weighted encounter set is calculated using Eq. (2). w_i represents the weight of an individual encounter. An unweighted encounter set assumes a weight of 1 for each encounter ($w_i=1$)

$$P(NMAC) = \frac{\sum_{i=1}^N NMAC_i * w_i}{\sum_{i=1}^N w_i} \quad (1)$$

The LoWCR is also utilized as a metric to assess the performance of the DAA logic for a given encounter set. In the same manner, it establishes a relationship between the number of encounters that incurred a well-clear violation with an equipped DAA system to the number of encounters that incurred a well-clear violation without a DAA system

$$LoWC\ Ratio = \frac{mitigated\ P(LoWC)}{unmitigated\ P(LoWC)} \quad (2)$$

For this research, the MAC ratio compares the number of encounters that resulted in a MAC.

$$MAC\ Ratio = \frac{mitigated\ P(MAC)}{unmitigated\ P(MAC)} \quad (3)$$

2.1.1.4 Results and Discussion

2.1.1.4.1 Mitigated Cooperative Encounter Results

The objective of this task was to quantify how changes in the WCV influence collision risk between sUAS and manned aircraft. The analysis compared six volumes from 2,000 ft × 450 ft (WC1) to 500 ft × 100 ft (WC6), using the ASTM F3442/F3442M-23 requirements (WC2) as the baseline. The study assessed how horizontal and vertical separation distances affect Near Mid-Air Collision Risk Ratio (NMAC RR) and Loss-of-Well-Clear Risk Ratio (LoWCR), and how these translate into MAC Ratio. This section summarizes the mitigated cooperative results across rotorcraft, FWME, and FWSE.

The analysis of 1200 code-exclude (coop) mitigated encounter models shows that reducing the horizontal well-clear distance from 2,000 ft to 1,500 ft (WC2 to WC3) produces small increases in NMAC Risk Ratio and LoWCR while remaining within the ASTM requirements. Reducing vertical distances from 250 ft to 100 ft (WC5) has a weaker impact but contributes to higher NMAC RR at the smallest volumes. At WC6, metrics converge toward the NMAC volume, as expected.

The key finding for mitigated cooperative encounters is that WC3 (1,500 ft horizontal, 250 ft vertical) preserves acceptable safety margins relative to the ASTM requirements while offering a 25% reduction in horizontal separation. MAC ratios follow a similar trend. As the volumes decrease in size, WC3 shows a similar performance comparable to WC2, and keeps rising as volumes decrease in size to the NMAC volume (WC6).

Regarding the encounter model type, the FWME exhibits the highest RR and LoWCR. These show a steep increase as volumes tighten, FWSE follows, and rotorcraft is lowest. The WC2 to WC3 ratio increase is small for all classes and remain within acceptance limits. All of these findings are summarized in Figure 2.1.

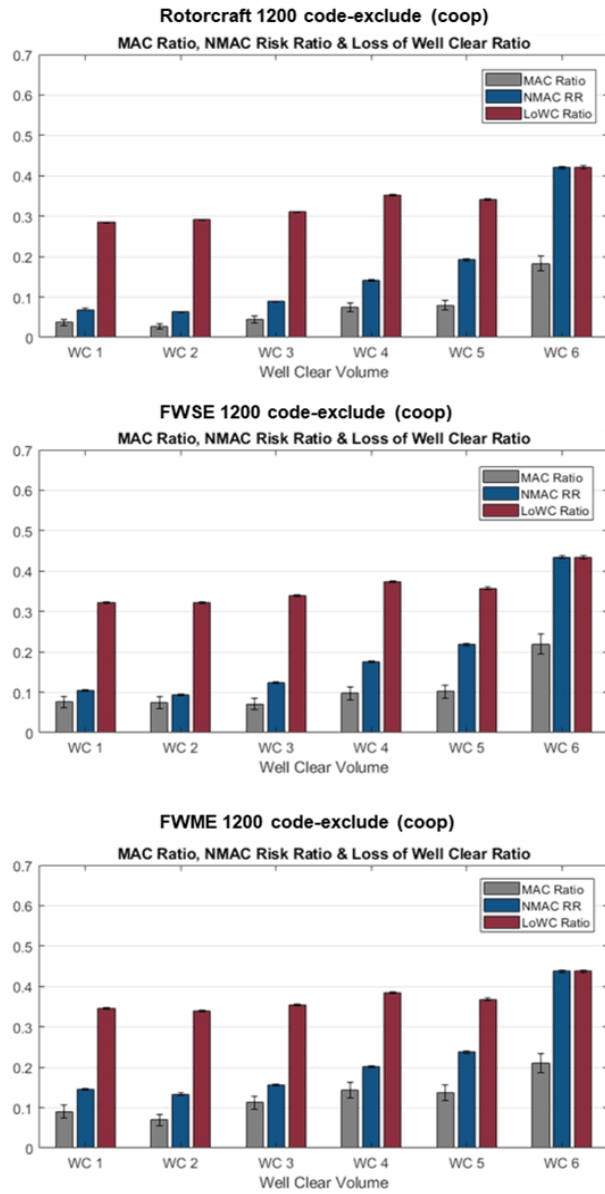


Figure 2.1: MAC ratio $[P(\text{MAC}|\text{enc})]$, NMAC risk ratio & LoWC ratio – 1200 code-exclude (coop).

2.1.1.4.2 Mitigated Non-cooperative Encounter Results

This section summarizes the analysis done on the 1200 code-only encounter models (non-cooperative). Six WCVs were assessed from 2,000×450 ft (WC1) to 500×100 ft (WC6), using the ASTM F3442/F3442M-23 requirement as the baseline (WC2: 2,000×250 ft). Similarly, metrics include NMAC Risk Ratio, LoWCR, and MAC Ratio. An air-to-air radar model with a fixed 2 km detection range was utilized alongside DAIDALUS as the DAA system.

In general, risk ratios are higher in magnitude than the ones reported in section 2.1.1.4.1. NMAC RR remains below the ASTM requirement at larger volumes and increases as volumes tighten, with exceedances appearing first in Fixed Wing Multi-Engine (FWME). LoWCR shows an

opposite trend: it is often above the limit at larger volumes and decreases as volumes shrink in size. This behavior is driven by the fixed radar detection range, which provides sufficient coverage at smaller volumes yet is insufficient to prevent LoWC at larger horizontal distances. However, the decrease in LoWCR should not be interpreted as a safety improvement as the MAC and NMAC Ratio increases steadily as volumes tighten toward WC6, as shown in Figure 2.2.

Key findings are that at WC3 (1,500 ft horizontal, 250 ft vertical), the NMAC RR increases to 0.148 (rotorcraft), 0.193 (Fixed Wing Single-Engine (FWSE)), and 0.276 (FWME), while LoWCR decreases to 0.402 (rotorcraft), 0.453 (FWSE), and 0.555 (FWME). These changes indicate a small rise in NMAC RR with a slight reduction in LoWCR when moving from WC2 to WC3.

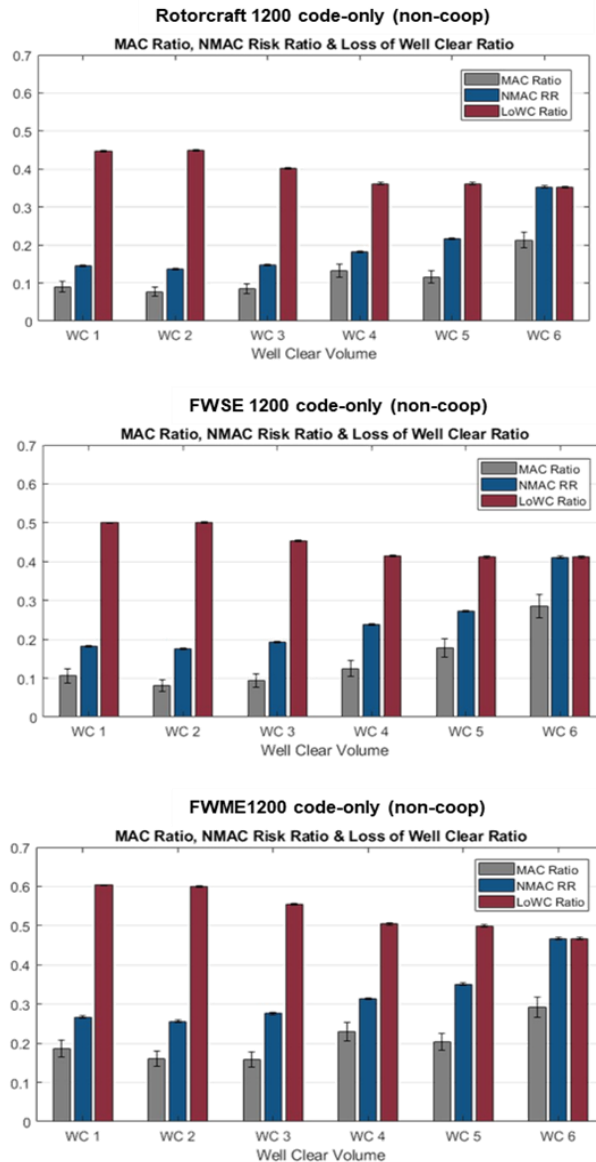


Figure 2.2: MAC ratio $[P(\text{MAC}|\text{enc})]$, NMAC risk ratio & LoWC ratio – 1200 code-only (non-coop).

2.1.1.4.3 MAC Results

Unmitigated MAC is $\sim 10^{-3}$ across scenarios; with DAA enabled it drops to $\sim 10^{-5}$. Prior work with ACAS sXu DO-396 (De Abreu, et al., 2023) reported $>99.4\%$ collision reduction for cooperative intruders and $\sim 95\text{--}98\%$ for non-cooperative.

In this study with DAIDALUS v2.0.1c, reductions are $\sim 78\text{--}97\%$ (cooperative) and $\sim 70\text{--}92\%$ (non-cooperative), depending on aircraft type and WCV analyzed. Research studies on visual acquisition show limited see-and-avoid performance: (Amerson, et al., 2023) found $\sim 57\%$ not seen at 1500 ft and $\sim 60\%$ not seen at 2000 ft, with simulated NMAC RR 0.508–0.717 and LoWCR 0.704–0.818; (NTSB, 1987) reported 56% unalerted detection (avg 0.99 nm) versus 86% alerted.

(Amerson, et al., 2024) reported $\geq 90\%$ acquisition of fixed-wing aircraft at 3000 ft in overtake, simulated NMAC RR 0.331–0.584 and LoWCR 0.596–0.650, and 44% acquisition of an 18-ft sUAS; Dolgov (2015) observed 67% acquisition with 22% false alerts (1.28 km [4200 ft] crewed, 0.76 km [2493 ft] sUAS), and (Wallace, et al., 2018) reported 7.7% sUAS detection (vs. 36.8% at ~ 0.1 SM [528 ft] in a separate study). These studies indicate that many aircraft are not seen even when approaching an NMAC, especially if they are small and/or have a fast approaching speed.

As shown in Figure 2.3, WC3 remains close to WC2 across the cooperative encounter models. In non-cooperative, MAC Ratio rises faster as volumes tighten, most notably for FWME which is driven mainly by horizontal distance reductions.

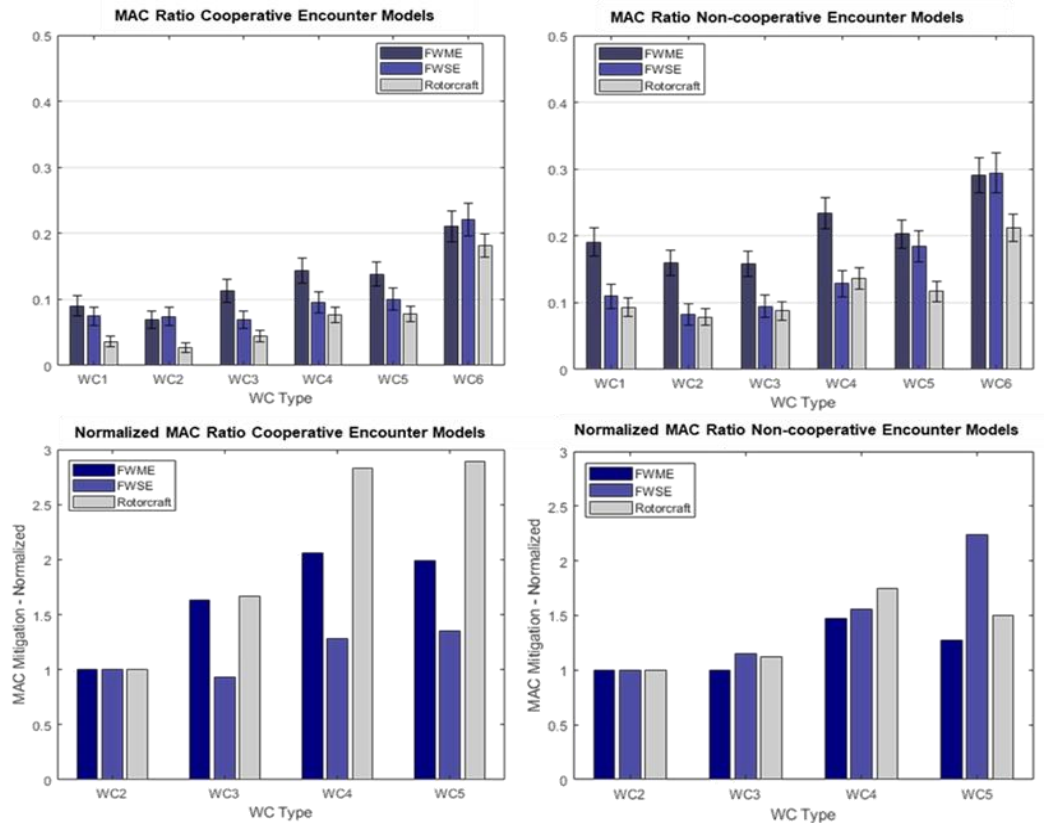


Figure 2.3: Average MAC mitigation ratio for each aircraft pair

2.1.1.5 Task Conclusions

This study comprehensively assessed the current ASTM F3442/F3442M 23 criteria for sUAS by quantifying the relationship between MAC probabilities and NMAC risk ratios. Utilizing over three million Monte Carlo simulations and incorporating both cooperative and non-cooperative encounter models, the analysis revealed that the current ASTM horizontal separation requirements can potentially be reduced without significantly increasing collision risk

The findings in this task indicate that a horizontal distance reduction to 1,500 ft is a viable candidate for redefining the ASTM F3442/F3442M-23. In cooperative encounters models, a volume of *1,500 horizontal x 250 vertical ft* produces small increases in NMAC RR and LoWCR that remain within the current ASTM requirements across rotorcraft, FWSE, and FWME, with a MAC Ratio close to the ASTM standard volume (2,000 horizontal x 250 vertical ft).

In non-cooperative encounter models, a similar trend is observed. The *1,500 horizontal x 250 vertical ft* volume shows a modest rise in NMAC RR and a decrease in LoWCR relative to *2,000 horizontal x 250 vertical ft*; MAC Ratio increases as volumes tighten, so applying *1,500 horizontal x 250 vertical ft* in non-cooperative operations depends on adequate surveillance performance: range, track quality, and coverage. Unless there are defined minimum performance requirements for non-coop sensors, whether a DAA system can perform well with a certain WCV will depend on the quality of the sensor. This study used a representative commercially available ATAR to demonstrate what is achievable with the current technology available and under ideal circumstances (no clutter and no false alerts).

Right-of-way evidence from the subsequent task (*Right of Way Quantification, section 2.1.2*) shows maneuver-desired thresholds near 1,500–1,700 ft under daytime/Virtual Reality (VR) conditions, which is consistent with the suggestions presented in this task. For the vertical separations, VR results indicate RoW impact at 281 ft (25% threshold) which supports retaining the current 250-ft vertical separation distance.

2.1.2 Right of Way Quantification

2.1.2.1 Task Overview

The main purpose of this research task was to validate sUAS well clear requirements and RoW impact distances. This was done by executing controlled flight tests and VR simulations to inform safe BVLOS operations. Towards this objective, a set of encounters between manned aircraft and UAS were executed at University of North Dakota facilities in June of 2025. The test matrix operationalized 75 planned encounters using two primary encounter geometries--head-on (0°), and converging (315°) to evaluate RoW impacts. These encounters were flown under both daytime and nighttime conditions to understand how ambient lighting affects when and how pilots visually detect intruder aircraft and decide to maneuver. In addition, the team used VR simulations to examine vertical separation scenarios at 0 ft, 100 ft, 250 ft, and 500 ft, providing a more complete picture of three-dimensional well clear volumes.

Throughout these activities, the team collected quantitative data regarding visual acquisition distances, desire-to-maneuver distances, strong-desire-to-maneuver distances, and closure rates, all aimed at defining practical RoW impact boundaries for sUAS operations. Safety was built into

every aspect of the campaign, with safety pilots, visual observers, and real-time telemetry monitoring ensuring that test encounters remained both realistic and risk-managed. The resulting empirical data were then compared against existing recommendations (Weinert, Campbell, Vela, Schuldt, & Kurucar, 2018), enabling proposition of a refined well clear volume tailored to sUAS operations. As key deliverables, the team provided statistical thresholds for pilot response distances and demonstrated that reduced well clear volumes could be applied to sUAS operations in the NAS.

2.1.2.2 Method and Approach

The team used VR simulations and flight tests to better understand RoW impacts. VR enabled execution of encounters with small separation distances that would be too risky to execute in the real world, while still grounding findings in actual flight operations so the results reflect what pilots and operators experience in practice.

2.1.2.2.1 VR Simulation Methodology

The team used VR simulations to study vertical separation impacts on RoW. Because it is not safe to fly manned aircraft and UAS with very little vertical separation in real life, VR enabled safe evaluation of “too-close” scenarios. Using this environment, a wide range of vertical encounter setups can be explored while keeping full control over conditions like distance, angle, and timing.

A total of 20 subjects with MA flying experience participated. Thus, the responses and decisions observed reflect how real pilots think and react. Each person went through multiple encounter scenarios in a within-subjects setup, which provided more reliable data while accounting for individual differences in how people fly.

For the VR scenario design, a standardized framework using fixed encounter geometries was used to enable reliable testing while key factors were manipulated. The MA flew straight and level at 80 kts and 600 ft AGL while the UAS (intruder) flew at 40 kts at a variety of altitude offsets. Their trajectories were defined as straight-line collision courses, which would result in collision if aircraft were co-altitude, which was the case for a subset, but not all, of the encounters. This provided a straightforward means to examine how and when pilots would choose to take action.

For the vertical separation, six differences in altitude between the aircraft (0, 100, 150, 200, 250, and 350 feet) were evaluated to see how pilot behavior vary as a function of vertical separation. These values were chosen to be around the commonly used 250 ft vertical “well clear” threshold. The order in which these scenarios appeared was randomized so participants could not predict what was coming next, helping to avoid learning effects and anticipatory reactions.

For data collection in VR, VR controller inputs were collected, so participants provided input log data from each encounter. Controller buttons were configured to capture the moment they first saw the intruder aircraft, and another button was configured for when they felt the need to start an avoidance maneuver. Each button press was logged as an event with an exact timestamp. These timestamps were synced with the aircraft position data to calculate separation distances for both of these types of events. Additionally, the team has the entire aircraft trajectories to obtain full kinematic records for analysis after each run.

Across all participants and conditions, a total of 638 encounter trials were executed. The scenarios were split between two approach angles, 0° head-on and 315° converging, so the team could

evaluate how geometry affects how pilots perceive RoW. Each participant completed ~32 encounters. Session lengths were limited to avoid fatigue while still giving everyone enough exposure to all key conditions.

To keep the focus on geometry rather than weather or display quirks, the visual environment was standardized. All scenarios used the same clear daytime conditions with effectively unlimited visibility, so changes in pilot response were not driven by clouds or haze. In addition, the UAS always looked the same size, color, and contrast—so any differences in detection came from how far apart the aircraft were.

Participant responses were monitored in real time so the team could quickly spot any technical issues or unusual behavior. For example, if a participant did not input any responses, it was automatically noted for review. After each session, the team members checked if the button presses matched a reasonable timeframe to consolidate only data that had meaning and value for analysis.

In VR, the participants were focused only on detection and decision-making, without the full workload of flying the aircraft. They also were not exposed to the same physiological stressors like motion, vibration, or real-world risk that pilots experience in the cockpit. To account for these differences, results were interpreted conservatively and compared with actual flight test data.

Some of the technical constraints the team encountered include the field of view was narrower than what pilots would have in a real cockpit and there were no true peripheral vision cues. Thus, the encounters were designed with frontal geometries to keep the intruder where pilots would naturally be looking. Display resolution can also make small objects harder to see, so the team used a larger Group 3 UAS representation to make sure targets were still visually acquirable despite those constraints.

This VR-based approach provided a safe, controlled way to understand how different vertical separations affect RoW. By systematically testing a full range of realistic height differences, the team collected meaningful data.

2.1.2.2.2 Flight Test Methodology

The flight testing component provided real-world data regarding RoW impact dependence on horizontal separation. These included real pilot workload, environmental variables, and aircraft dynamics. However, these impacts were somewhat ameliorated by the presence of a safety pilot (second pilot) in the MA.

For the flight-testing architecture, collision-geometry encounters between MA and UAS were used in which both aircraft arrive at the same horizontal location if the timing is perfect. A 400 ft vertical separation was used to ensure safety. As with the VR tests, two encounter geometries were used (0° and 315°). MA personnel were instructed to treat the encounters as if the aircraft were co-altitude.

To ensure safety, a safety pilot was present in the MA along with the pilot-in-command to focus specifically on looking for traffic and to record data, while the Flight Test Director was attentive to every encounter and had the ability to call an immediate abort if any issues arose. Both aircraft were tracked with real-time telemetry.

Data was collected using tablets and custom software known as the Test Information Collection System (TICS). The system support time-synchronization of test data from different locations during test campaigns.

The MA was a Piper Archer. For daytime tests, both a Gabriel G25 and a DJI M300 were used. For nighttime tests, a ScanEagle equipped with both a flashing strobe and with a red-green light pair was used.

2.1.2.3 Results and Discussion

2.1.2.3.1 Virtual Reality Results

The VR simulations provided a rich dataset from 638 controlled encounters with 20 participants, offering strong statistical support for understanding RoW-impact dependence upon vertical separation. Overall, participants successfully spotted UAS 98.4% of the time, with only 10 encounters ending without a visual detection. This showed that the VR setup was very effective at presenting a clearly detectable intruder. In addition, the high detection rates were consistent across both approach geometries, with 317 successful head-on (0°) encounters and 311 successful converging (315°) encounters, suggesting that approach angle was not an important factor in whether pilots could visually acquire the intruder in this simulated environment.

One of the most important insights from the VR study was how strongly vertical separation influenced whether pilots felt the need to maneuver. When the UAS was at the same altitude as the manned aircraft (0 ft separation), pilots wanted to take evasive action in each of 38 encounters. As the vertical gap increased, the desire to maneuver dropped off sharply: 83% of encounters at 100 ft, 71% at 150 ft, then falling to 34% at 200 ft, 24% at 250 ft, and just 13% at 350 ft. Using logistic regression, the key “shift point” was identified at ~281 ft of vertical separation, where the likelihood of wanting to maneuver dropped below 25%. This lines up closely with the commonly used 250 ft vertical well clear threshold and, importantly, provides real pilot perception data to back up a standard that had previously been driven by unmitigated collision risk models. It is noted that these results also support use of 300 ft vertical separation for well clear, with the caveat that the 281 ft value likely has a high bias relative to sUAS owing to the use of Group 3 UAS in the VR tests.

Analysis of horizontal distances where key events happened illustrated a clear difference between when pilots first spotted the UAS and when they actually felt the need to maneuver. On average, the pilots detected the intruder at about 1,040 ft away (with a median of 1,002 ft), showing that pilots could usually see the UAS well before they felt pressured to act. Spotting distances varied quite a bit from person to person: 90% of detections happened beyond 516 ft, while some pilots visually identified it as far out as 1,624 ft. In contrast, maneuver-desired was noticeably closer to ownship, with an average of 749 ft and a median of 680 ft, highlighting that detection and decision to evade are two distinct steps. In probabilistic terms, *for the subset of encounters with 0 ft vertical separation* 50% of the pilots wanted to maneuver by the time the aircraft were within 1,285 ft horizontally, 25% wanted to maneuver at 1,531 ft and beyond, and only 10% still wanted to maneuver beyond 1,703 ft. Together, these results provide clear, data-driven boundaries for where RoW impacts occur.

It is noted that maneuver-desired distances could be strongly driven by visual acquisition distances. The differences in distances identified herein correspond, conceptually, to roughly a 3-5 s

processing time (or less) in which pilots, once an aircraft is visually acquired, determine a conflict exists and express a desire to maneuver. Thus, it can be argued that the true maneuver-desired distances are actually larger than reported herein. To evaluate this, VR data were segregated according to the amount of time between visual acquisition and expression of a desire to maneuver. The threshold used was 5 s, with the idea that if more time existed between visual acquisition and desire to maneuver, those encounters provide better data regarding actual maneuver-desired distances (since the amount of time is greater than the suggested processing/cognition time). The results, however, indicate that for the data having > 5 s between visual acquisition and expression of a desire to maneuver, *while the visual acquisition distances are generally greater, the maneuver-desired distances are actually smaller*. Thus, while it is difficult to argue that visual acquisition does not influence maneuver-desired results since one has to see an intruder to have a desire to maneuver away from it, the hypothesis that maneuver-desired would be larger when the time between the two events is larger was not supported by these data. Moreover, the amount of time between visual acquisition and expression of a desire to maneuver was commonly < 3 s, especially for encounters having vertical separations of 150 ft or less.

Comparison between 0° head-on and 315° converging encounters revealed minimal influence of approach angle on both visual acquisition and desire to maneuver, though subtle differences were observed in the response patterns. For visual acquisition, the mean spotted distances were remarkably similar between the two geometries (1,065 ft for 0° versus 1,015 ft for 315°), with overlapping confidence intervals suggesting no statistically significant difference. However, maneuver-desired distances showed a slight tendency toward earlier response initiation in head-on encounters, with mean distances of 795 ft at 0° compared to 702 ft at 315° , and median values of 720 ft and 648 ft respectively. This pattern suggests that head-on encounters, despite having similar visual acquisition ranges, may be perceived as slightly more threatening, possibly due to the higher closure rates and more direct collision trajectory.

The team did a separate analysis to understand the visual growth rate. This analysis is done to investigate whether pilot responses were driven by the angular growth rate of the intruder aircraft and was conducted through both theoretical modeling and empirical validation using VR video frame analysis. Theoretical calculations demonstrated that angular size increases exponentially as separation distance decreases, with the growth rate being proportional to both aircraft width and closure velocity. Frame-by-frame analysis of VR recordings for aircraft having 10 ft, 15 ft, and 20 ft widths validated these theoretical predictions, with measured angular sizes closely matching calculated values across the encounter timeline. However, when participant response events were mapped against visual growth rates, no consistent threshold growth rate was identified that triggered either detection or maneuvering decisions. The occurrence of events at varying distances and times-to-collision corresponded to different growth rates across encounters, suggesting that absolute separation distance or other perceptual factors may be more influential than dynamic visual expansion in driving pilot responses. This finding was significant as it indicated that static separation standards may be more appropriate than dynamic, closure-rate-dependent thresholds for regulatory purposes.

A critical validation of the experimental design was confirmed through analysis of visual acquisition rates across the sequential presentation of encounters, which remained stable throughout the testing sessions. Detection rates fluctuated naturally between 90% and 100% across

the 32-encounter sequence, with no systematic increase that would indicate participants were learning to anticipate UAS appearance patterns or locations. This stability was particularly noteworthy given that participants experienced the same sequence of vertical separations and encounter angles, suggesting that each encounter was assessed independently based on visual information rather than predictive strategies. The maintenance of consistent response patterns throughout extended VR sessions also validated that fatigue effects were minimal and that the data collected from later encounters remained as reliable as from earlier encounters.

The convergence of multiple analytical approaches within the VR simulation framework provided strong evidence for reconsidering current well clear standards, particularly regarding horizontal separation requirements. The finding that, for 0 ft vertical separation, only 25% of pilots desired to maneuver at horizontal distances beyond 1,531 ft in the VR environment, combined with the median maneuver-desired distance of 1,285 ft, suggested that the current 2,000 ft horizontal standard may be conservative. These results were particularly compelling because they were derived under conditions of focused attention, where participants' primary task was visual acquisition and avoidance decision-making without the competing demands present in actual flight operations, which almost assuredly enhanced visual acquisition performance. The validation of the 250 ft vertical separation standard through empirical pilot response data, showing the 25% transition point at 281 ft, provided important support for existing regulatory frameworks.

2.1.2.3.2 Flight Test Results

The team executed a total of 75 live-flight encounters between MA and UAS across daytime (33 encounters) and nighttime (29 encounters) conditions. Operational challenges did necessitate adaptations during the daytime testing. Tests were executed at the Gorman Field test range, with data successfully captured from 31 daytime and 27 nighttime. Two unsuccessful encounters occurred during the daytime owing to encounter timing issues and two unsuccessful events occurred at nighttime due to GPS data collection failure. The effectiveness of a 400 ft vertical separation buffer was verified through post-flight analysis, confirming that no well clear violations occurred according to the (Weinert, Campbell, Vela, Schuldt, & Kurucar, 2018) criteria, thereby validating the safety protocols while enabling meaningful RoW impact assessment. The stark differences observed between daytime and nighttime results provided unexpected insights into the role of visual conspicuity and lighting in pilot threat perception, fundamentally challenging assumptions about visual acquisition and response patterns under varying visibility conditions.

2.1.2.3.2.1 Daytime Flight Test Results

The daytime flight tests revealed critical limitations in visual detection capabilities that necessitated adaptive modifications to the test protocol, ultimately providing valuable insights into the practical challenges of see-and-avoid principles. During the initial ten encounters with the DJI Matrice 300 moving along prescribed trajectories, the safety pilot was unable to visually acquire the unmanned aircraft in any instance, despite knowing the general direction and approximate timing of the approaching UA. This complete visual acquisition failure with a moving Group 2 UAS under optimal daylight conditions demonstrated the severe limitations of relying on visual acquisition for collision avoidance with small UA, even when pilots were specifically tasked with looking for conflicting traffic.

Following the recognition that moving encounters would not yield usable RoW impact data, the methodology was adapted to implement hovering encounters for the remaining 23 daytime tests, with pilots informed of the approximate hover location to facilitate detection. This modification enabled successful visual acquisition in 22 of 23 hovering encounters, though it was acknowledged that these detections were artificially enhanced by prior knowledge of the UAS position. The mean horizontal distance for visual acquisition under these assisted conditions was 2,183 ft with a median of 2,026 ft, substantially greater than the VR simulation results, likely reflecting the combination of prior knowledge and the stationary target presentation. Maneuver-desired decisions occurred at a mean distance of 1,494 ft with a median of 1,413 ft, showing reasonable alignment with VR findings despite the methodological differences. The progression from visual acquisition to maneuver initiation demonstrated a clear decision hierarchy, with the 50th percentile thresholds occurring at 2,026 ft for spotting, 1,413 ft for maneuver desired, and 752 ft for maneuver strongly desired, establishing distinct zones of increasing urgency in pilot response. It is noted that the 25th percentile for maneuver desired occurred at 1,712 ft.

2.1.2.3.2.2 Nighttime Flight Test Results

The nighttime flight tests produced dramatically different results relative to both daytime tests and VR simulations, with the enhanced visibility provided by aircraft lighting systems fundamentally altering the visual acquisition and response dynamics. The Boeing-Insitu ScanEagle UAS equipped with navigation lights and a high-intensity strobe was visible to the pilots throughout the entire test period, with visual acquisition occurring immediately upon initiating an encounter. This continuous visibility resulted in UAS spotted distances averaging 6,926 ft with a median of 6,548 ft, far exceeding any distances achieved in the VR environment (and corresponding roughly to the maximum encounter separation distance).

The distances at which pilots indicated a desire to maneuver during nighttime operations were much larger than those for daytime testing and VR simulations, with a mean of 5,248 ft and median of 5,119 ft, substantially exceeding both the current 2,000 ft horizontal. Even more striking were the maneuver-strongly-desired thresholds, which averaged 3,641 ft with a median of 3,782 ft, distances that exceeded the maximum visual acquisition ranges achieved during daytime operations. The 25th percentile for maneuver-desired responses occurred at 5,625 ft, suggesting that even the least conservative quartile of responses exceeded the 2,000 ft threshold by a significant margin. These large distances occurred, as indicated by the pilots, because at night it was much easier to determine that a conflict existed owing to the ScanEagle being larger, more visually conspicuous (with lighting), and having the appearance of an aircraft moving at ownship owing to the presence of the lights, including the red-green light pair.

The comparison between daytime and nighttime results reveals fundamental differences in how lighting conditions affected both detection capabilities and risk perception. While daytime visual acquisition was essentially impossible for moving aircraft without prior position knowledge, achieving a 0% detection rate for dynamic encounters, nighttime operations with properly illuminated aircraft achieved 100% detection rates with immediate visual acquisition upon initiating encounters. The horizontal separation thresholds for equivalent response levels showed dramatic variations between conditions, with the 25th percentile for maneuver-desired occurring at 1,712 ft during daytime versus 5,625 ft at night, a difference of nearly 4,000 ft that could not be explained solely on differences in visual acquisition capability. Based on these results, one could

argue for different well clear requirements for daytime versus nighttime. While the RoW impact data supports this, the caveat is that a Group 3 UAS was used in the nighttime testing and that likely resulted in larger values than would have occurred with a Group 1 or 2 UAS.

2.1.2.4 Task Conclusions

In this study, VR simulations and live flight test were used to understand dependence of RoW impacts on vertical and horizontal separation for MA encountering UA. Owing to challenges with visually acquiring small UAS, group 3 UAS were generally used, with group 2 UAS used when issues with one of the tests UAS arose. Owing to the lack of other pilot duties during VR tests and previous knowledge of UAS position during daytime tests, test results do not accurately represent visual acquisition capability. They do, however, provide information regarding RoW impacts, which was the primary objective.

The results suggest that the current “well clear” standard of 2000 ft × 250 ft could reasonably be reduced to 1500 ft × 250 ft. VR results showed that 25% of the pilots begin to express vertical RoW impacts at around 281 ft, which supports the existing 250 ft vertical standard. In both VR and daytime flight tests, about 25% of pilots said they wanted to maneuver at horizontal distances of 1531 ft (VR) and 1712 ft (daytime), which are both below the current 2000 ft requirement. These results are qualified by potential latency impacts, which result in the 25% value for daytime tests being ~1965 ft.¹ Thus, daytime results indicate that a significant fraction of pilots (25%-75%), if they could visually acquire a small UA, could feel discomfort with a 1500 ft horizontal well clear threshold, especially for encounters that have horizontal separations in the 1500-2000 ft range.

Pilots typically could not visually acquire moving UAS during the day, while illuminated aircraft at night were visually acquired 100% of the time. This reinforces the understanding that UAS that are illuminated at night are easy to visually acquire.

The results provided herein are conservative because Group 3 UAS were used to enable visual acquisition whereas the desire is to understand RoW impacts for MA encountering sUAS (Group 1 and 2 UAS). This provides further justification for a 1500 ft horizontal well clear threshold for Group 1 and 2 UAS.

Key takeaways are:

- Vertical separation RoW impact threshold established at 281 ft (based on 25% threshold)
- Based upon a 25% threshold, the horizontal well clear threshold for sUAS could be reduced from 2000 ft to 1500 ft
 - For daytime testing, including latency impacts suggests 2000 ft may be better. However, no maneuver-strongly-desired events happened at distances ≥ 1500 ft (maximum maneuver-strongly-desired distance is < 1000 ft).
 - VR simulations support a 1500 ft threshold even when including latency.
 - Nighttime results indicate RoW impacts at much larger distances owing to the increased perception of risk (larger aircraft, apparent conflict owing to lighting).

¹ Test pilots estimated latency associated with recording values (visual acquisition, maneuver desired, maneuver strongly desired) as being between 1-2 s. Use of 1.5 s and closure rates used in testing results in the increased value of 1965 ft.

- No visual acquisition for UAS in daytime without position cueing
- 100% nighttime visual acquisition with proper lighting (lights included a flashing strobe and a red-green light pair on the wings)
- High visual acquisition rate (98.4%) for VR simulations driven by size of UAS (Group 3) and lack of other pilot duties, with a 1285 ft median maneuver distance for co-altitude encounters
- Encounter angle (0° vs 315°) showed minimal impact on RoW thresholds
- No strong dependence upon closure rate was identified, through the spread of closure rates is limited
- Visual growth rate not identified as primary driver of pilot response decisions
- 400 ft vertical buffer validated as safe for RoW flight testing

Many opportunities to further explore RoW compliance exist. These include:

- Expand testing to include a range of background conditions (weather, surface conditions) to better understand impacts on visual acquisition.
- Expand testing to consider more aircraft shapes and sizes.
- Expand testing to examine different approaches for increasing visual conspicuity. This includes coloring, striping, use of illumination, etc.
- Execute tests using sUAS that maximize contrast in the hopes that such testing would provide useful information regarding RoW impacts.
- Expand encounter geometries beyond 0° and 315° , which can include encounters having horizontal accelerations (e.g., linear accelerations and decelerations, curved trajectories), climb and descent encounters (both ownship and intruder), and non-collision geometries. The opportunity here is limited by the ability to see out of the windscreen of the ownship aircraft.
- Include other pilot duties in testing. For the VR tests, the only real responsibilities that the “pilot” had were to see the intruder aircraft and press buttons when it was visually acquired and when a maneuver was desired. The lack of other duties likely resulted in the very high visual acquisition rate. In the flight tests, a safety pilot was in the aircraft. This individual also had the responsibilities of visually acquiring the intruder and indicating when that occurred and when maneuvers were desired. The lack of other duties for this pilot likely enabled visual acquisition. It is noted that Amerson et al. (2024) had a visual acquisition rate of ~ 0.45 when one MA overtook a UAS having a wingspan of 18 ft. In those tests, the pilot was responsible for flying the aircraft and for visually acquiring other aircraft.
- Establish an effort where data regarding actual pilot maneuvers based upon see and avoid are collected. Given the currently limited number of UAS operations, in the near term this would primarily provide information regarding MA-MA interactions.

Of these, the most impactful potential research areas are expansion to include more encounter geometries and inclusion of other pilot duties in testing. The latter has been considered (e.g., Amerson et al. 2024) whereas the former would enable a better understanding of RoW impacts.

2.1.3 UTM Services Field testing

2.1.3.1 Task Overview

This research task investigates the use of UTM systems to provide separation between manned aircraft and one or more sUAS. Extensive simulations and flight testing were performed to investigate how a UTM system can provide well clear separation. The UTM-based flight test encounters include sUAS separation from cooperative and non-cooperative manned aircraft. Manned aircraft position was provided to the UTM based on ADS-B detections, radar detections, and/or based on direct cellular communication from the manned aircraft. In all task flights, the sUAS maneuvered autonomously to provide such separation. UTM services were provided by Unifly and Canadian UAV Sparrowhawk radar was used in flights that use radar positions. The study investigates the minimum detection distances at which the manned intruder needs to be detected by the sUAS to allow for well clear separation. The latencies and message update rates experienced during UTM-based aircraft separation are analyzed. Simulated encounters involving a manned aircraft and more than one sUAS are also studied. The following is a concise summarized presentation of the research methods, approach, results, and conclusions for this research task. Further details can be found in the Task 4 Execution Report published on the ASSURE website.

2.1.3.2 Method and Approach

This study is built on two components: extensive simulations, and extensive flight tests. The goal of the simulations is to identify the minimum detection distances at which the sUAS needs to detect the manned intruder in order to be able to maneuver in time and remain well clear. The goal of the flight tests is to perform field testing of the UTM system and validate the simulation results. The following is a description of the methods and approaches used for simulation and flight testing.

2.1.3.2.1 The Morphing Potential Field Collision Avoidance Algorithm

In all simulation and flight test encounters, the sUAS autonomously maneuvered to remain well clear from the manned aircraft. The Morphing Potential Field (MPF) algorithm was used for autonomous avoidance (Stastny, Garcia, & Keshmiri, 2014). This is based on Khatib's research into obstacle avoidance in robotics (Khatib, 1985), similar multi-agent approaches such as Reynolds' ground-breaking work on local flocking behaviors (Reynolds, 1987), and Leonard and Fiorelli's work on coordinated control of groups (Leonard & Fiorelli, 2001). In these approaches, a potential field is computed which creates a repelling influence on navigation and guidance by creating a "cost" to enter an undesired volume of airspace, in particular as in Equation 2.4.

$$pf = A \cdot \exp \left\{ - \left(\frac{\| \vec{p}^{obj} - \vec{p}^o \|}{\sigma} \right)^2 \right\} \quad \text{Equation 2.4}$$

In the numerator, the argument of the exponent is the distance norm between the object to be avoided and the avoiding aircraft. Figure 2.4 shows a plot of a stationary potential field and a morphing potential field, described below.

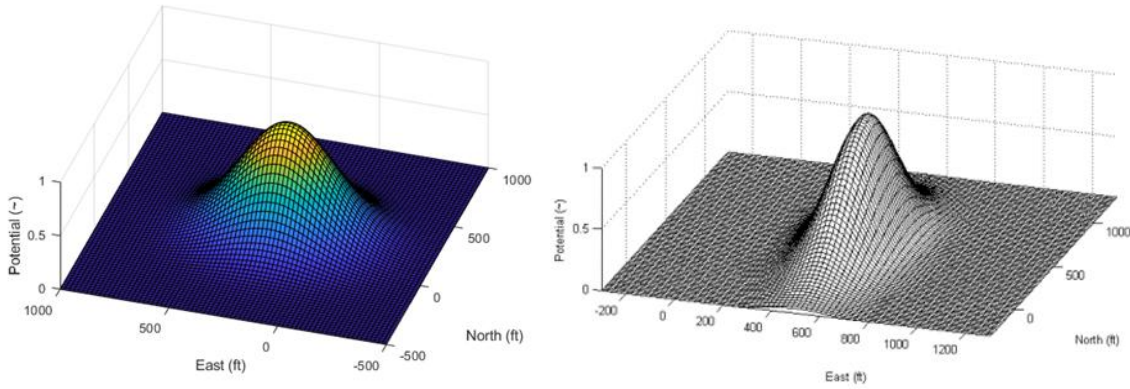


Figure 2.4: A stationary potential field (left) and a morphing potential field (right).

Considering the kinematic and physical constraints of aircraft flying at high speeds (e.g., minimum turning radii and limited deceleration capabilities), the aircraft must begin evasion of traffic somewhat further in advance than would be necessary for slower-moving vehicles (or a stationary object). Use of the generic potential formulation from Equation 2.4 in such an application is possible but would require significant enlargement in amplitude and/or choice of a larger avoidance radius. The resulting evasion path would be inefficient, with respect to time off the desired trajectory, and lead to unnecessary avoidance maneuvers in aircraft passing an object at a safe distance with a nonconflicting heading, thereby inhibiting operations with tight spatial constraints or in a congested urban area. To remedy these issues, a “morphing” factor Γ was integrated into the potential function, based on the angle of approach, the magnitude of the relative velocity between aircraft, and kinematic aircraft constraints.

This extension of the potential field (visualized in Figure 2.4) “repels” the avoiding aircraft from entering airspace, which might cause a right-of-way violation without the undesirable effects of amplitude or avoidance radius enlargement seen in the generic formulation. An additional reference shifting term \mathbf{S} has also been included in the distance norm as a means of further shaping the potential field to avoid unnecessary levels of cost beyond the avoided obstacle by shifting the potential function origin (point “c” in Figure 2.5) away from the centroid of the object. The resultant formulation is deemed a morphing potential function (Stastny, Garcia, & Keshmiri, 2014):

$$mpf = \exp \left\{ -\Gamma \left(\frac{\|\vec{p}^{obj} - \vec{p}^o - \vec{S}\|}{\sigma} \right)^2 \right\} \quad \text{Equation 2.5}$$

The values of Γ and \mathbf{S} have been selected based on hundreds of sUAS encounters in flight testing. Figure 2.5 shows the geometric meanings of the terms in parenthesis in Equation 2.5.

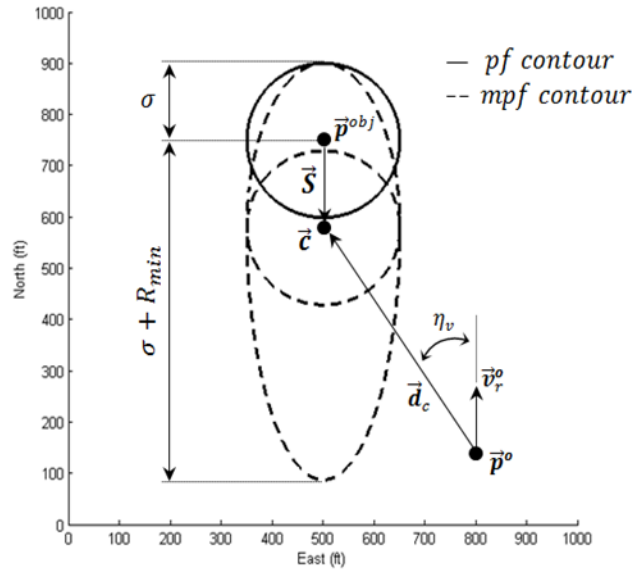


Figure 2.5: Morphing potential field geometry.

2.1.3.2.2 Aircraft Used in this Research Task

Three aircraft were used in this research task. They are presented below and in Figure 2.6.

- 1) The SkyHunter sUAS: is the sUAS used in this work. This UAS is outfitted with the KU Automated Flight System (AFS) which includes a Raspberry Pi 5 flight computer, Pixhawk Orange Cube+, flight sensors, and communication devices. The sUAS flies around 45 ft/s, weighs about 9 pounds, and has a wing span of 71 inches.
- 2) The Cessna 172: is an asset of the University of Kansas (KU) and was used for all manned flights in Lawrence, KS.
- 3) The Cessna L319: is an asset of Rasket Flight Research Laboratory at Mississippi State University (MSU). The aircraft was used for all manned flights with the Sparrowhawk radar in Starkville, Mississippi.

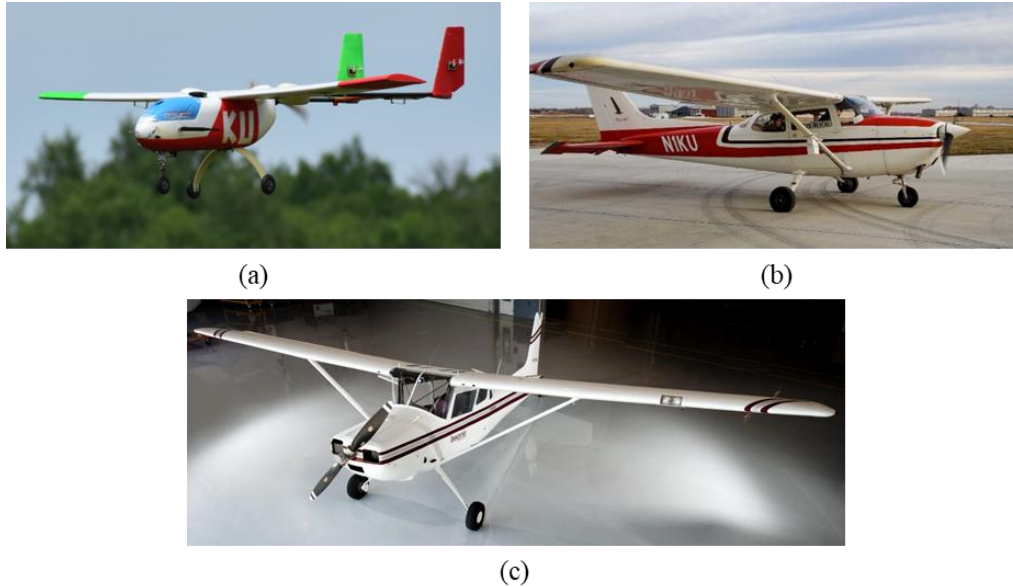


Figure 2.6: Aircraft used in this work: (a) SkyHunter sUAS, (b) Cessna 172, (c) Cessna L319.

2.1.3.2.3 Simulation Approach for sUAS-MA Encounters

Extensive simulations are conducted for sUAS-MA encounters to identify the minimum detection distance needed for a sUAS to stay well clear from a manned aircraft. In the encounters, there is a manned aircraft flying in a straight line, and it is considered to have right-of-way. It is referred to as the "intruder". Then, there is the "avoider" sUAS, which is set to fly in the same airspace. The simulation flight paths are designed such that the manned aircraft and the avoider sUAS would collide if they kept flying in a straight line. In the encounter, the sUAS performs avoidance maneuvers to remain well clear from the manned aircraft using the avoidance algorithm discussed in Section 2.1.3.2.1. The aim is for the sUAS to maintain the horizontal well clear separation from the manned aircraft.

The minimum detection distance needed to stay well clear from the manned aircraft is originally unknown. Therefore, the simulation is performed using an initial detection distance. Then, the simulation is repeated multiple times, where higher detection distances are tested in each simulation run. Using these simulation results, the minimum detection distance which allows for a well clear encounter is identified.

The above simulation procedure is followed for encounters where the manned aircraft approaches from different angles and at different approach speeds. The sUAS was always flying at 45 ft/s. Simulations were conducted for the manned aircraft approaching at speeds of 145, 170, and 195 ft/s and from relative approach angles ranging from 0 degrees (an overtaking scenario) to 180 degrees (a head-on scenario). Figure presents the heading angle definition for the intruder aircraft.

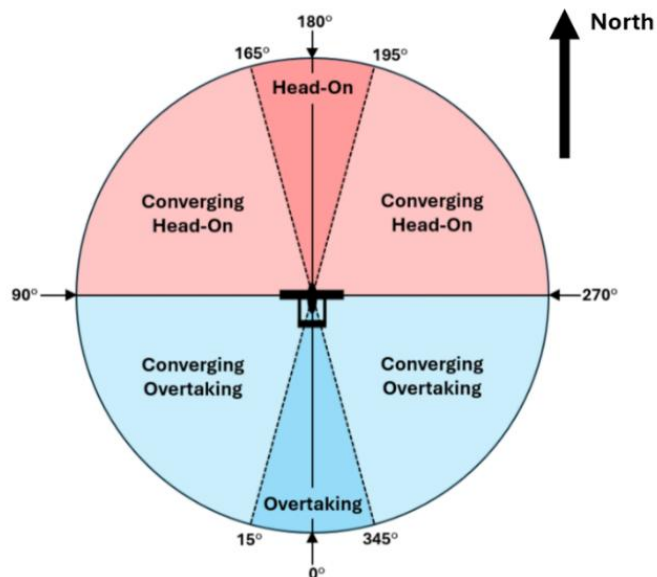


Figure 2.7: Intruder aircraft heading angle definition.

The above simulations were conducted for two horizontal well clear definitions: 2000 ft, which is the separation currently in use (ASTM F3442-25, 2025) and (Weinert, Campbell, Vela, Schuldt, & Kurucar, 2018), and 1500 ft. The simulation results are presented in Section 2.1.3.3.1.

2.1.3.2.4 Unifly UTM

UTM services were provided by Unifly, a European company providing flight planning, tracking, and alerting services within the U-Space system. Notably, the software system allows users to plan and manage sUAS operations. During the operation planning, an operation area is reserved and deconflicted with other potential operations or airspaces in real time. As such, the Unifly customer can plan and request authorization of flights (in case an authorization is needed) for the operation area.

The Unifly UTM system can determine the position and velocity of air traffic either directly via the Long-Term Evolution (LTE) network or from other service providers, as well as from broadcast signals from ADS-B or other tracking devices. Tracking information is used to provide subscribers with situational awareness of their sUAS and other air traffic (both unmanned and manned) as well as (collision and non-conformance) alerts about traffic, deviation from the operation area, and potential entry into no-fly zones. Such services may contribute to the overall DAA capabilities of an sUAS.

2.1.3.2.5 Flight Test Approach

Extensive flight testing was conducted for sUAS-manned aircraft encounters to test the use of the UTM system for aircraft separation and to validate the simulation results. The flight test encounters were designed to have similar trajectories as the simulated encounters. That is the sUAS and the manned aircraft were set to approach each other from different relative angles and relative speeds. The sUAS was set to autonomously maneuver to remain well clear from the manned aircraft.

The sUAS was allowed to detect the manned aircraft once the aircraft was within the detection distance specified by the flight test team for that encounter. This allows the team to evaluate if the specified detection distances were sufficient to maintain well clear separation or not. The team then compared the detection distances needed in the flight tests to the detection distances needed in the simulations.

In all sUAS-manned aircraft flight test encounters, the sUAS received the position of the manned aircraft from the Unifly UTM over cellular connection. The manned aircraft position was provided to the Unifly UTM in one of four ways:

- 1) Approach 1 (Figure 2.8): The manned aircraft broadcasts its location using ADS-B. A secondary ground station has an ADS-B receiver on the ground. The secondary ground station receives the ADS-B messages and forwards them to Unifly UTM using a cellular connection.
- 2) Approach 2 (Figure 2.9): The manned aircraft directly sends its location to the Unifly UTM using a cellular connection.
- 3) Approach 3 (Figure 2.10): A computer running a radar simulation is used to “detect” the location of the manned aircraft as if it were detected by a radar. Starting with the ADS-B location, delays and uncertainties are added to that location as if the aircraft is being detected by a rotating radar. These simulated radar detections are sent to Unifly UTM using a cellular connection.
- 4) Approach 4 (Figure 2.11): A real radar is used to detect the manned aircraft location. The real radar detections are then forwarded to Unifly using an internet connection. Flight testing using this approach was conducted in Starkville, Mississippi, using the Sparrowhawk radar available at MSU.

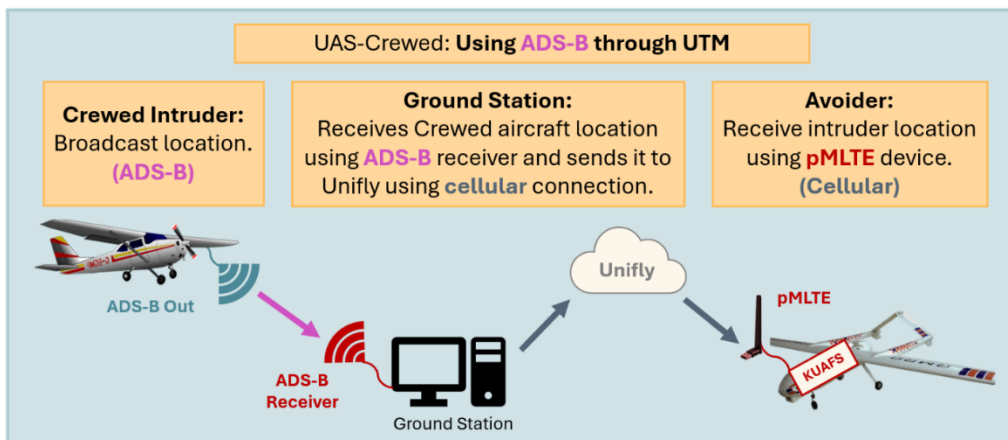


Figure 2.8:sUAS-Manned Aircraft Approach 1: ADS-B receives messages through Unifly

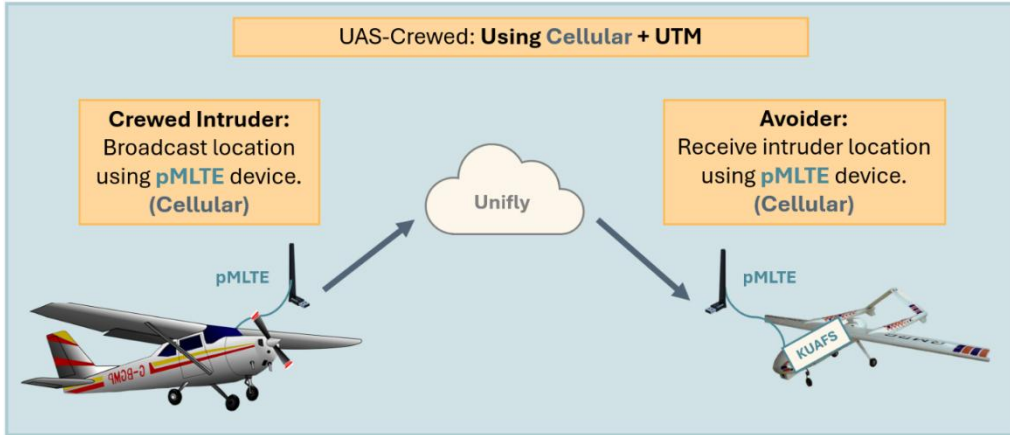


Figure 2.9: sUAS-Manned Aircraft Approach 2: Using Unify UTM.

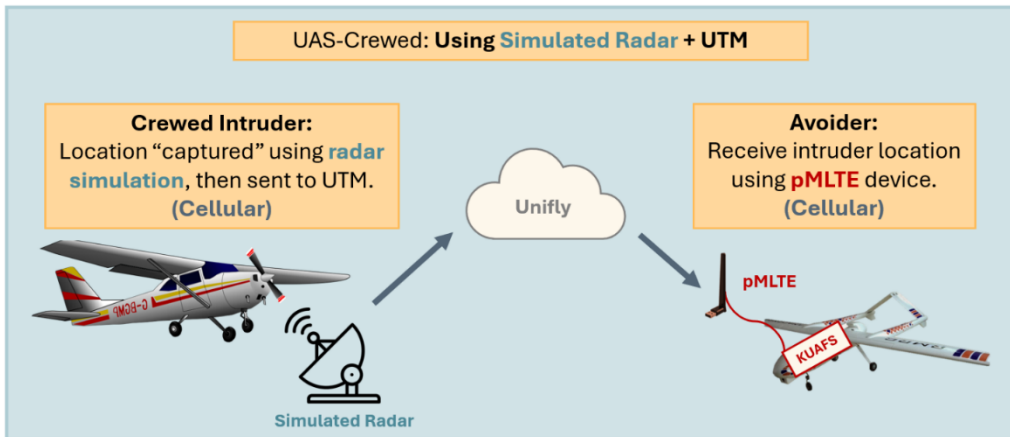


Figure 2.10: sUAS-Manned Aircraft Approach 3: Simulated radar data sent to Unify UTM.

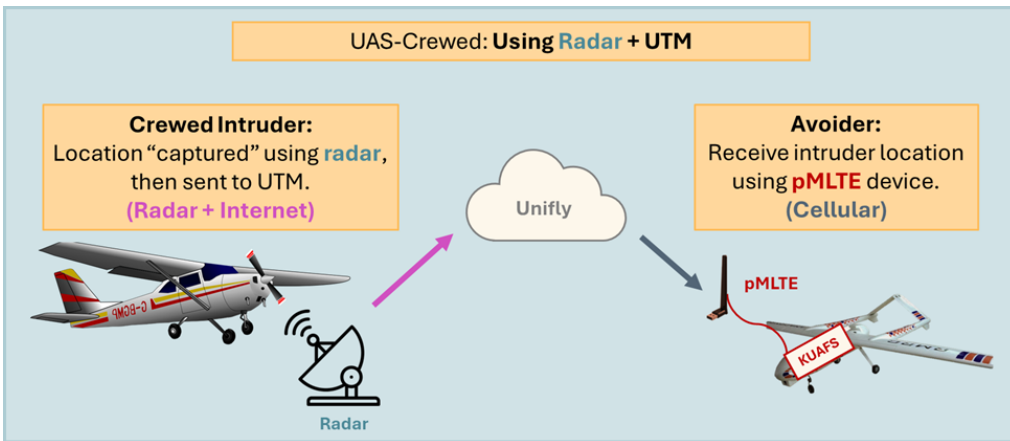


Figure 2.11: sUAS-Manned Aircraft Approach 4: Actual radar data sent to Unify UTM.

Flight testing using Approaches 1 to 3 were conducted in Lawrence, KS using the SkyHunter sUAS and the Cessna 172. Flight testing using the real radar (Approach 4) was conducted in Starkville, MS using the SkyHunter sUAS and the Cessna L319. The Canadian UAVs Sparrowhawk radar, owned by MSU, was used for detecting the Cessna L319 aircraft. Flight test encounters using the Sparrowhawk radar were conducted such that the Cessna L319 was a non-cooperative manned aircraft. That is, ADS-B messages from the Cessna L319 were not received by the SkyHunter sUAS, only radar detections of the Cessna L319 were received by the SkyHunter sUAS. The flight test results are presented in Section 2.1.3.3.1.3.

2.1.3.2.6 Analysis of Cellular Connectivity, Latencies, and Update Rates

Analysis was performed to evaluate the latencies and message update rates observed during flight testing with the UTM. The analysis was performed in several ways:

- 1) The latency between sending the manned aircraft position to the UTM system and receiving that message on the avoiding sUAS was calculated. This is the latency associated with the diagram in Figure 2.9
- 2) The latency between making a radar detection then receiving that radar detection from the UTM on the sUAS was calculated. This is the latency associated with the diagram in Figure 2.11.
- 3) The latency between sending manned aircraft positions to the UTM system and receiving these messages on a laptop on the ground was calculated. This is the latency associated with the diagram in Figure 2.12.

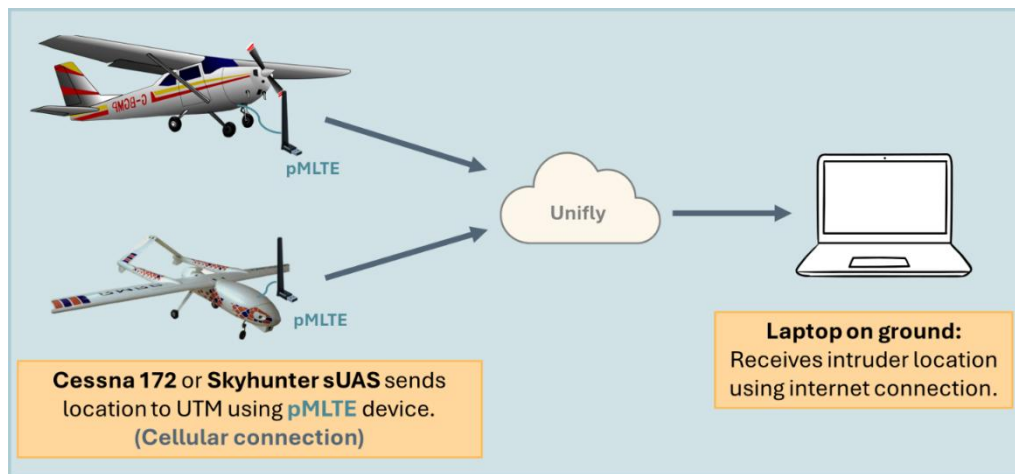


Figure 2.12: UTM messages received on the ground using a laptop.

The latencies identified using the first two ways, present latencies observed during flight operation from one aircraft to another. These latencies are impacted by both aircraft cellular connectivity. The latencies identified using the latter two ways (items 3 and 4 in the above list) focus on the manned aircraft or sUAS connectivity more separately. That is, the observed latency during a flight is not impacted by the receiving side's location – since the laptop is not moving.

The latencies were calculated as:

$$\text{Latency} = t_{\text{receive}} - t_{\text{send}} \quad \text{Equation 2.6}$$

Where $t_{receive}$ is the timestamp when the position was received on the receiving sUAS or laptop, and t_{send} is the timestamp when the position was sent by the manned aircraft, radar computer, or sUAS to the UTM system.

The Cessna 172 and SkyHunter sUAS were set to send messages to the UTM system at 1 Hz, i.e., the time period between sending messages is 1 second. The update period that was actually observed by the receiving laptop was calculated as:

$$\text{Update Period} = t_{receive_{k+1}} - t_{receive_k} \quad \text{Equation 2.7}$$

Where $t_{receive_{k+1}}$ and $t_{receive_k}$ are the timestamps when the position messages were received for two consecutive data points (e.g., data point at time steps $k+1$ and k).

The results of the analysis of cellular connectivity, latencies, update periods are presented in Section 2.1.3.3.2.7.

2.1.3.2.7 Encounters With More Than One sUAS

This research task also investigated the effect of increased sUAS traffic density on maintaining well clear between sUAS and a manned aircraft. Two scenarios were investigated:

- 1) Corridor Scenario: A scenario involving two sUAS flying in trail formation in a “corridor” with an intruder aircraft flying in a straight flight path to intercept the formation.
- 2) Surveying Scenario: a surveying scenario in which a manned aircraft intercepts two sUAS flying in a laterally offset/trail formation, both following a rectangular flight pattern.

In these scenarios, the two sUAS were set to autonomously avoid the manned aircraft and each other. The goal was for the sUAS to maintain a 2000 ft horizontal well clear dimension from the manned aircraft, and a 500 ft horizontal well clear dimension from the other sUAS.

2.1.3.2.7.1 Corridor Scenarios

For the corridor scenarios, a similar simulation procedure was conducted as described for the single sUAS encountering a manned aircraft in Section 2.1.3.2.3. The goal of the simulations was to identify the minimum detection distance at which the sUAS need to see other intruders (the manned aircraft and the other sUAS) to be able to maneuver in time and remain well clear. Figure 2.13 presents the corridor encounters geometry. In all encounters the sUAS were flying at 45 ft/s. The following encounter parameters were varied:

- 1) Manned intruder speed. Simulations were conducted for a manned intruder approaching at 145, 170, and 195 ft/s.
- 2) Manned intruder approach angle. Simulations were conducted for a manned intruder approaching from 0 degrees to 180 degrees relative headings at increments of 15 degrees.
- 3) The trailing separation between the sUAS flying in the corridor was varied. Three separations were used: 1000, 1500, and 2000 ft.
- 4) The point at which the manned aircraft would cross the path of the sUAS formation was varied. Three interception ratios were used: 0, 0.25 and 0.5.

The interception ratio defines where the manned aircraft would cross the path of the sUAS formation. As presented in Figure 2.13,

- An interception ratio of 0 means: direct intersection with the leading sUAS.

- An interception ratio of 0.25 means: intersection one quarter of the way between the two sUAS.
- An interception ratio of 0.5 means: intersection midway between the two sUAS.
- An interception ratio of 1 means: direct intersection with the trailing sUAS.

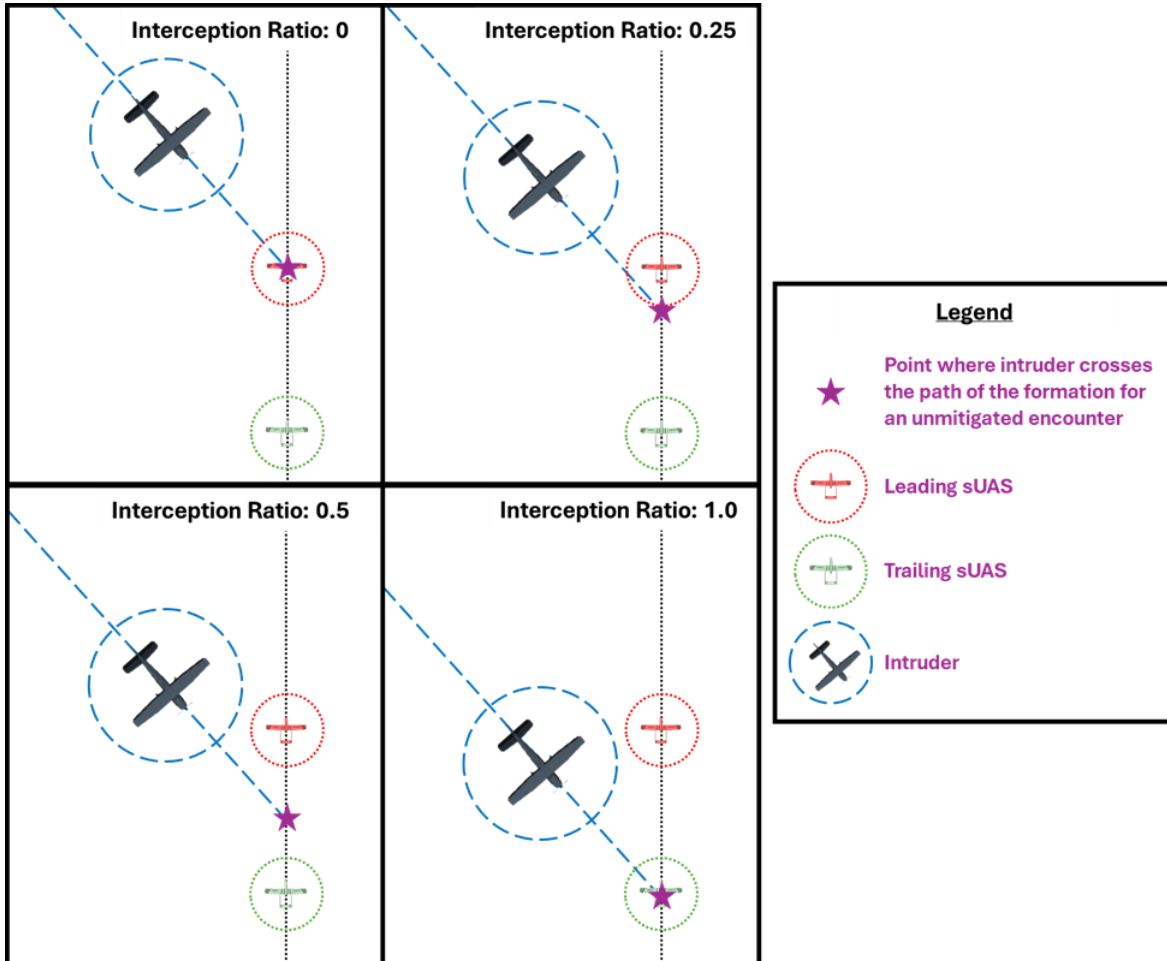


Figure 2.13: Diagram of corridor scenario for trailing sUAS with manned intruder interception ratios.

The minimum detection distance needed to allow the sUAS to stay well clear from the manned aircraft and the other sUAS during the encounter is originally unknown. Therefore, the simulation is initially performed using a user defined starting detection distance. Then, the simulation is repeated multiple times, where higher detection distances are tested in each simulation run. Using these simulation results, the minimum detection distance which allows for a well clear encounter between all aircraft is identified.

The simulation results are briefly discussed in Section **Error! Reference source not found.**

2.1.3.2.8 Surveying Scenarios

A second multi-sUAS scenario was tested. The scenario consists of two sUAS flying in a surveying formation. A manned aircraft approaches the two sUAS and passes through the rectangular survey path. The sUAS need to maneuver to remain well clear from the manned aircraft and from each

other. There are many variations that can be designed for this surveying scenario. The research task presented simulation results for three surveying scenario encounters. The simulation results are presented in the more extended project report (Task 4 Execution Report) published on the ASSURE website.

2.1.3.3 Results and Discussion

2.1.3.3.1 Simulation Results

2.1.3.3.1.1 2000-ft Horizontal Well Clear

Based on the simulation approach presented in Section 2.1.3.2.3, the minimum detection distances at which the sUAS needs to detect the manned aircraft intruder are presented in Figure 2.14. These results are for a 2000 ft horizontal well clear dimension. Results are presented in Figure 2.14 for manned aircraft flying at 145, 170, and 195 ft/s.

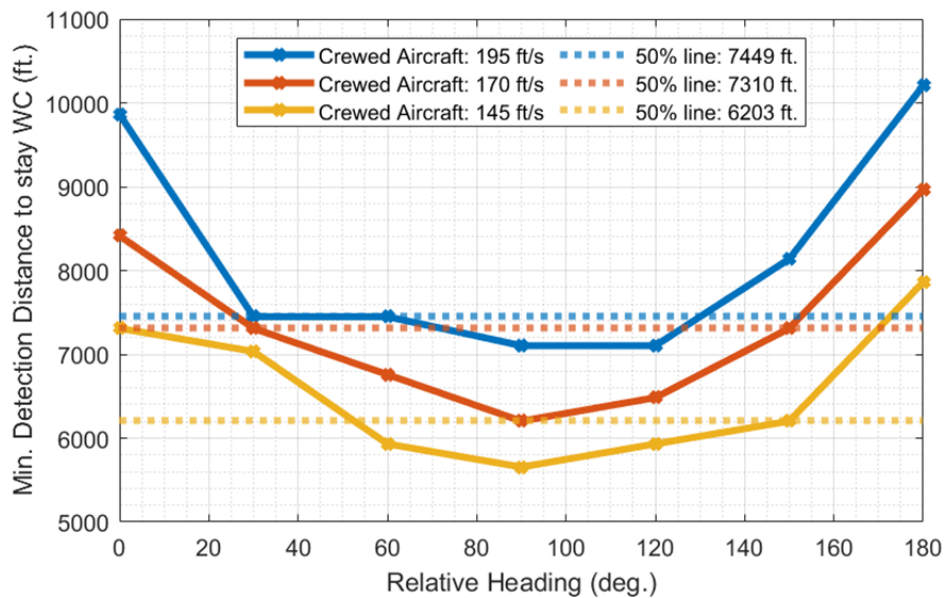


Figure 2.14: Simulated sUAS-manned aircraft encounters: minimum detection distance at different relative encounter angles and three Cessna airspeeds. Results are for a 2000 ft horizontal well clear volume. Broken lines show the detection distances allowing 50% of the sUAS-manned aircraft simulated encounters to be well clear.

As expected, larger detection distances are needed when the manned aircraft is approaching at higher flight speeds. The head-on (around 180 degrees) and overtaking (around 0 degrees) encounters required higher detection distances compared to the other approach angles. Head-on encounters have higher approach speeds, so a higher detection distance is needed to allow enough time for maneuvering to remain well clear. Overtaking encounters, though they start off having the lowest approach speeds, required high detection distances because the sUAS starts off right in front of the approaching manned aircraft. The sUAS needs a large enough detection distance to maneuver out of the 2000 ft well clear radius while having a much lower flight speed (45 ft/s) than the approaching manned aircraft. It is important to not also that the detection distances obtained are dependent on the avoidance algorithm used and the sUAS maneuvering capabilities. If different avoidance algorithms are used or the sUAS has different maneuvering capabilities, the required detection distances would be different.

ASTM DAA requirements do not require the sUAS to remain well clear from the manned aircraft for 100% of the encounters (ASTM F3442-25, 2025). Instead, the ASTM standard requires that the LoWC Risk Ratio be 0.50 or less for non-cooperative intruders, and 0.40 or less for ADS-B equipped intruders. In this work, a first order approach is used to find the acceptable detection distance. The minimum detection distances needed for each encounter to be well clear is first identified. Then, the detection distance which allows 50% of the encounters to be well clear is identified. Table 2-2 summarizes the minimum required distances which allow 100% and 50% of the encounters to be well clear for three manned aircraft flight speeds.

Table 2-2: Minimum detection distances which allow 100% and 50% of the sUAS-Manned aircraft encounters to be well clear, based on simulation. Results are for a 2000 ft horizontal well clear radius.

Manned aircraft speed (ft/s)	Minimum required detection distance (ft)	
	For 100% of Encounters WC	For 50% of Encounters WC
145	7862	6203
170	8965	7310
195	10207	7449

2.1.3.3.1.2 2000 ft vs 1500 ft Horizontal Well Clear

Comparison between the detection distances needed to maintain horizontal well clear definitions of 2000 ft and 1500 ft is conducted. Figure 2.15 presents the results for a manned aircraft flight speed of 145 ft/s. Similar trends were observed for the higher manned aircraft speeds (170 and 195 ft/s). Table 2-3 summarizes the detection distances needed for 50% and 100% of the encounters to be well clear.

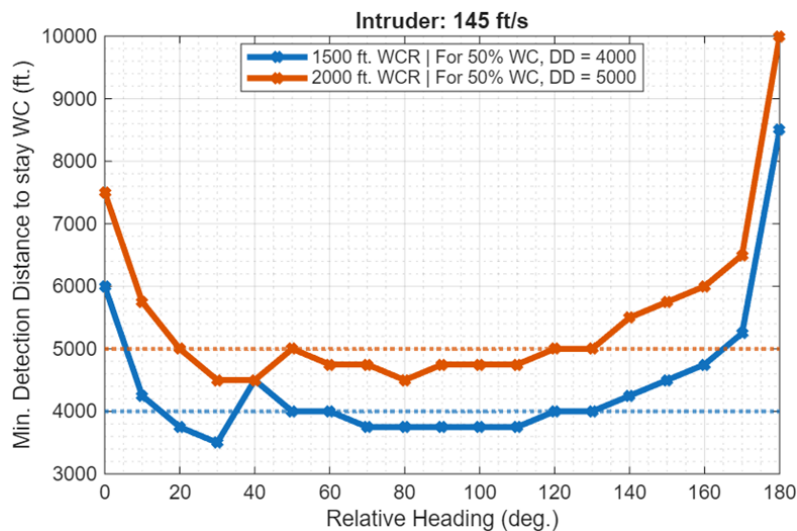


Figure 2.15: Minimum required detection distances to maintain 1500 and 2000 ft horizontal well clear separation between sUAS and manned aircraft. Manned intruder's speed is 145 ft/s.

Table 2-3: Minimum detection distances which allow 100% and 50% of the sUAS-manned aircraft encounters to be well clear, based on simulation. Results are for two horizontal well clear

dimensions: 1500 ft and 2000 ft. Avoidance algorithm is set to have σ = horizontal well clear radius + 50.

Intruder Speed	145 ft/s		170 ft/s		190 ft/s	
	50%	100%	50%	100%	50%	100%
1500 ft WC	4000	8500	4500	10000	5250	11500
2000 ft WC	5000	10000	5750	12000	6500	13750

As expected, the detection distances needed for a 1500 ft well clear separation are lower than the detection distances needed for a 2000 ft separation. Based on the simulations, the 1500 ft horizontal well clear separation required 1000 to 2250 ft smaller detection distances than the 2000 ft horizontal well clear separation, as seen in Table 2-3.

2.1.3.3.1.3 Multi- sUAS vs MA Simulation Results

The main observation from the corridor flight scenarios is that higher detection distances were needed in these multi-sUAS encounters than the encounters with only one sUAS. For 50% of the corridor encounters to be well clear, the needed detection distances ranged between 10,125 and 14,500 feet – much larger than the (up to 7449 feet) detection distances needed when only one sUAS is in the encounter. The Task 4 execution report contains the extended results

2.1.3.3.2 Flight Test Results

Several flight tests were conducted of sUAS-manned aircraft encounters. The goals of conducting the flight test encounters were:

- 1) Evaluating the potential of using UTM for sUAS-manned aircraft separation.
- 2) Comparing the flight test results with the simulation results.

In all encounters, the goal was to maintain 2000 ft horizontal separation between the aircraft. If the two aircraft maintained at least 2000 ft separation, the encounter was a well clear encounter. If the two aircraft got closer than 2000 ft to each other, the encounter was a well clear violation. In all flight test cases, a vertical separation was maintained between aircraft.

Much more details are presented in the Task 4 Execution Report published on the ASSURE website. The following is a concise summary.

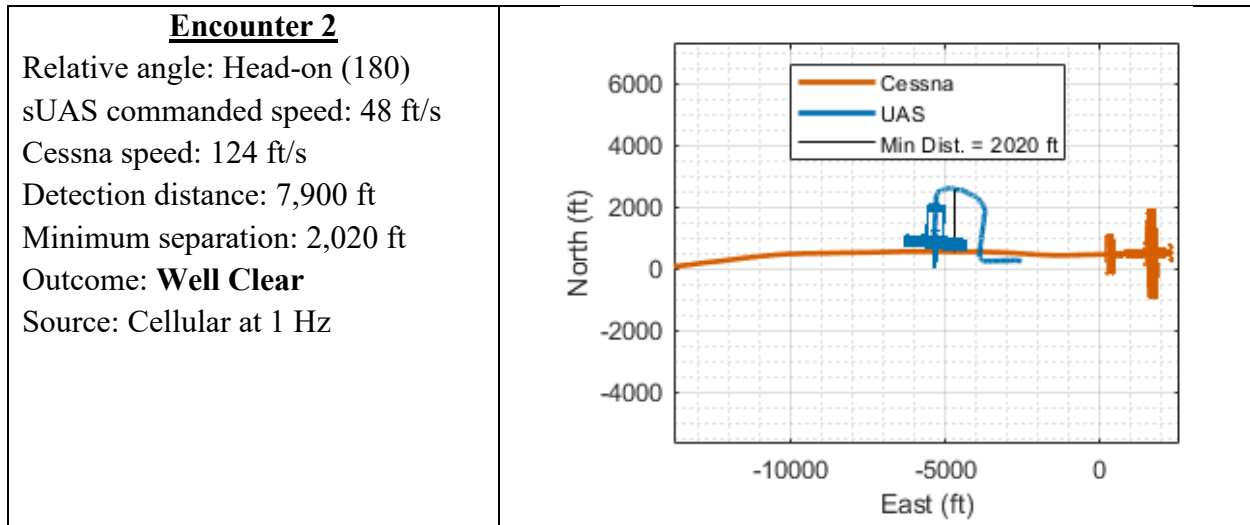
In Lawrence, KS, encounters were performed at four relative heading angles: Head-on (180-degrees), 90-degrees, 30-degrees, and overtaking (0-degrees). Flight test encounters were also performed using a real radar in Starkville, MS. The flight test results are presented in the following subsections.

2.1.3.3.2.1 Head-On Flight Test Encounters

Eight head-on flight test encounters were conducted. As a sample, Table 2-4 **Error! Reference source not found.** presents the flight trajectory and encounter details for one of the head-on encounters.

Table 2-4: Sample head-on flight test encounter.

Encounter Parameters	Flight Trajectories
----------------------	---------------------



The eight encounters are summarized in Table 2-5. The table presents the sUAS and manned aircraft flight speeds during the encounter, the detection distance at which the sUAS was allowed to see the manned intruder, and the minimum separation observed between the two aircraft during the encounter. If the minimum observed separation was greater than 2000 ft, the encounter was labeled as WC, if the minimum separation was less than 2000 ft, the encounter was labeled as a WC violation. Table 2-5 also identifies the manned aircraft information source.

Table 2-5: Summary of sUAS-manned aircraft head-on flight test encounters.

#	sUAS (ft/s)	Cessna (ft/s)	Detection Distance (ft)	Information Source	Minimum Separation (ft)	Status
1	48	126	10,000	Cellular (Figure 2.9)	2077	WC
2	48	124	7,900	Cellular (Figure 2.9)	2020	WC
3	48	118	5,000	Cellular (Figure 2.9)	1844	WC violation
4	48	123	10,000	Simulated radar (Figure 2.10)	2045	WC
5	48	148	14,000	Simulated radar (Figure 2.10)	2128	WC
6	48	156	12,000	Cellular (Figure 2.9)	2091	WC
7	52	134	12,000	ADS-B (Figure 2.8)	2103	WC
8	50	135	12,000	ADS-B + Simulated radar (Figure 2.8+Figure 2.9)	2088	WC

From these encounters, the following conclusions can be made:

1. Using UTM for sUAS-manned aircraft separation is possible. This was demonstrated in multiple head-on encounters in which well clear separation was maintained. The encounters were conducted at different sUAS-manned aircraft relative speeds.

2. Using UTM for sUAS-manned aircraft separation is possible through multiple approaches. The encounters demonstrated separation using:
 - a. ADS-B data sent to the UTM system.
 - b. Manned aircraft location sent to the UTM system using cellular connection.
 - c. Simulated radar detections sent to the UTM system.
3. For the head-on encounters, the minimum required detection distance identified in flight testing (7,900 ft for a relative encounter speed of 172 ft/s) is similar to the minimum detection distance identified in simulation (7,862 ft for a relative encounter speed of 190 ft/s).

2.1.3.3.2.2 90-degree Flight Test Encounters

Three 90-degree flight test encounters were conducted. These encounters are summarized in Table 2-6. From these encounters, the following conclusions can be made:

1. The results again demonstrate that using UTM for sUAS-manned aircraft separation is possible, as shown in Encounter 11.
2. For a 90-degree encounter with the sUAS flying at 50 ft/s and the Cessna flying around 150 ft/s, the minimum detection distance which allowed a well clear encounter was 14,000 ft.
3. The minimum detection distance of 14,000 ft identified in flight test does not agree with simulation results. The minimum detection distances identified in simulated 90-degree encounters with similar flight speeds were much lower (5,655 to 6,203 ft.) as presented in the extended Task 4 Execution Report.

Table 2-6: Summary of sUAS-manned aircraft 90-degree flight test encounters.

#	sUAS (ft/s)	Cessna (ft/s)	Detection Distance (ft)	Information Source	Minimum Separation (ft)	Status
9	50	146	11,000	Cellular (Figure 2.9)	1931	WC violation
10	50	150	12,000	Cellular (Figure 2.9)	1962	WC violation
11	50	159	14,000	Simulated radar (Figure 2.10)	2246	WC

2.1.3.3.2.3 30-Degree Flight Test Encounters

Three 30-degree flight test encounters were conducted. These encounters are summarized in Table 2-7. **Error! Reference source not found.** From these encounters, the following conclusions can be made:

1. The results again demonstrate that using UTM for sUAS-manned aircraft separation is possible, as shown in Encounters 13 and 14.
2. For a 30-degree encounter with the sUAS flying at ~50 ft/s and the Cessna flying around ~150 ft/s, the minimum detection distance which allowed a well clear encounter was 12,000 ft.

- The minimum detection distance of 12,000 ft identified in the flight test does not agree with simulation results. The minimum detection distance identified in simulated 30-degree encounters with similar flight speeds was much lower (7034 ft.), as presented in the extended Task 4 Execution Report.
- For a given detection distance, the sUAS may or may not maintain the desired separation from manned aircraft based on the used avoidance algorithm (or based on the human sUAS pilot avoidance maneuvers). This is observed by comparing Encounters 12 and 14.

Table 2-7: Summary of sUAS-manned aircraft 30-degree flight test encounters.

#	sUAS (ft/s)	Cessna (ft/s)	Detection Distance (ft)	Information Source	Minimum Separation (ft)	Status
12	48	142	12,000	Cellular (Figure 2.9)	1,871	WC violative
13	52	154	13,000	ADS-B (Figure 2.8)	2,007	WC
14	52	154	12,000 <i>*Used higher MPF strength ($\sigma = 2400$)</i>	ADS-B (Figure 2.8)	2,195	WC

2.1.3.3.2.4 Overtaking Flight Test Encounters

Two overtaking flight test encounters were conducted. These encounters are summarized in Table 2-8. From these encounters, the following conclusions can be made:

- The results again demonstrate that using UTM for sUAS-manned aircraft separation is possible.
- For an overtaking encounter with the sUAS flying at ~50 ft/s and the Cessna flying around ~155 ft/s, the minimum detection distance which allowed a well clear encounter was 12,000 ft.
- The minimum detection distance identified in simulated overtaking encounters with similar flight speeds was much lower (7310 ft.). Further flight testing is needed to verify if a detection distance lower than 12,000 ft is sufficient.

Table 2-8: Summary of sUAS-manned aircraft overtaking flight test encounters.

#	sUAS (ft/s)	Cessna (ft/s)	Detection Distance (ft)	Information Source	Minimum Separation (ft)	Status
15	50	155	12,000	Cellular (Figure 2.9)	2,021	WC
16	52	156	12,000	ADS-B (Figure 2.8)	2,019	WC

2.1.3.3.2.5 Flight Test Encounters with Real Radar Detections

sUAS-manned aircraft flight testing was conducted with the Sparrowhawk radar capturing the location of the manned aircraft and sending it to the Unifly UTM system for aircraft separation (approach in Figure 2.11). The flight testing was conducted in Starkville, Mississippi, using the Sparrowhawk radar owned and operated by MSU. Sending radar detections to a UTM system is relevant in situations where a non-cooperative manned aircraft is in the airspace, and the UTM system is used to help a sUAS maintain separation from that manned aircraft.

An overtaking flight test encounter was conducted using this approach. The encounter flight trajectories are presented in Table 2-9. In this encounter, the commanded sUAS speed was 58 ft/s, and the manned Cessna L319 aircraft was flying at an average speed of 137 ft/s. In this scenario, a detection distance of 14,000 ft was used. A *well clear encounter* was observed based on the detected radar locations, with the minimum aircraft separation being 2,012 ft.

Table 2-9: Head-on sUAS-manned aircraft encounters using real radar data sent to Unifly

Encounter Parameters	Flight Trajectories
<p style="text-align: center;"><u>Encounter 17</u></p> <p>Relative angle: Overtaking (0) sUAS commanded speed: 58 ft/s Cessna speed: 137 ft/s Detection distance: 14,000 ft Minimum separation:</p> <ul style="list-style-type: none"> • 2,012 ft (based on radar) • 2,339 ft (based on ADS-B) <p>Outcome: Well Clear Source: Real Radar Sigma: 2400 (higher MPF strength)</p>	

It is important to compare the aircraft position obtained from the radar with the ADS-B position of the aircraft. *An offset is seen in the radar data, where the radar data is shifted more North compared to the ADS-B data (See Table 2-9 and Figure 2.16). The difference between radar and ADS-B data is presented in Figure 2.17 where the errors have magnitudes around 500 ft and higher.* The observed position errors are a result of at least two factors: (1) uncertainties in radar measurements, and (2) delays in receiving the radar detections. (Note that better setup/calibration of the radar may have allowed for smaller position errors.)

It is important to account for such position errors if radar data were to be used for aircraft separation. Serendipitously, in the above encounter, the manned aircraft was detected by radar to be about 500 feet closer to the sUAS than actual, making the avoidance “easier.” Unfortunately, due to the possibility that the radar “puts” the intruder aircraft further from the sUAS than actual, say by 500 feet, to maintain an actual 2000-foot separation, the avoidance algorithm needs to account for the position errors. One way to do that is to attempt to execute a larger, say a 2500-foot, separation maneuver when radar data is used to mitigate the possible position errors.

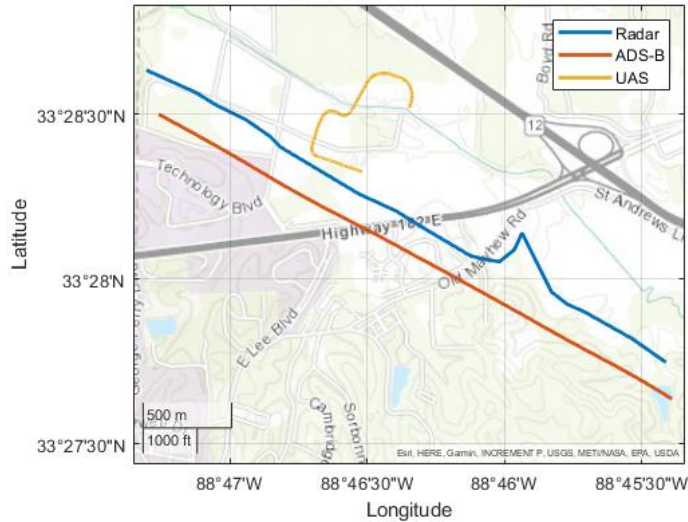


Figure 2.16: Comparison between Cessna L319 trajectories as obtained from radar detections and from the aircraft flight logs.

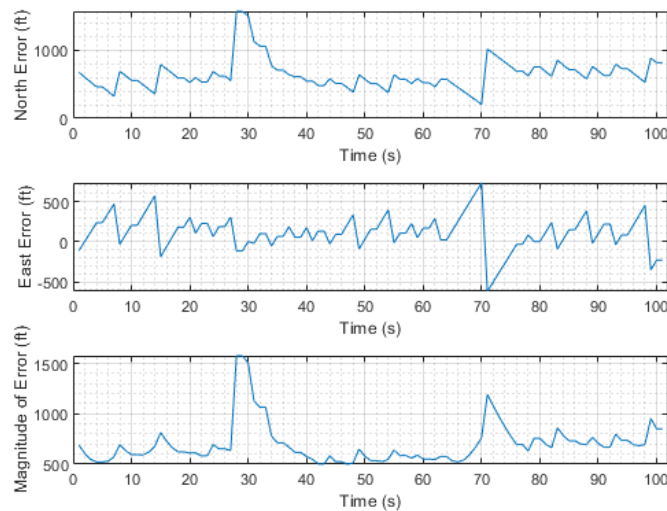


Figure 2.17: Error between detected radar positions and ADS-B positions: North error, East error, and magnitude of error. Errors are presented for the duration of Encounter 17.

2.1.3.3.2.6 Comparison of Flight Test Results with Simulation Results

One of the goals of the flight test encounters was to validate the simulated encounters outputs. This subsection presents a summarized comparison of the flight test results and simulation results. In sections 2.1.3.3.2.1 to 2.1.3.3.2.4, the flight test encounters were discussed for relative encounter heading angles of 180-degree (head-on), 90-degree, 30-degree, and 0-degree overtaking). Table 2-10 compares the minimum detection distances needed for well clear encounters as evaluated from simulation, and as evaluated from flight tests.

Table 2-10: Summarized comparison of simulation and flight test detection distances.

Relative Heading	Flight Test Cessna Speed	Minimum Detection Distance from Simulation (ft)	Minimum Detection Distance from Flight Test (ft)	Comparison Outcome
Head-on (180)	124	7862	7900	Agreement
30-degree	154	7034	13000	Higher detection distance needed in flight test
90-degree	160	5655	11000	Higher detection distance needed in flight test
Overtaking (0)	155	7310	12000	Higher detection distance needed in flight test

The results in Table 2-10 show that for the head-on encounter, the detection distance needed in flight test was similar to the detection distance needed in simulation. This validates the simulation results. However, for the 30-degree, 90-degree and overtaking encounters, considerably higher detection distances were needed in the flight tests (compared to simulation) in order to allow for well clear encounters. For example, simulation indicated that the 30-degree encounter would require 7034 ft detection distance, while flight test required a 13000 ft detection distance.

Some of this behavior is because flight test trajectories meant to mirror those simulations are difficult to achieve in flight test due to encounter set-up inaccuracies, GPS latencies and position biases, and the presence of ambient winds. For example, timing the flight test encounters to mirror the initial encounter starting positions used in simulation was difficult. In flight test the aircraft can easily be further ahead or behind than the desired starting location. Also, flight test encounters require much more time and effort for data collection compared to simulation. Therefore, in some cases, smaller detection distances may have allowed for well clear encounters. However, it was not feasible to test these smaller detection distances in flight.

2.1.3.3.2.7 Cellular Connectivity Analysis

Analysis was performed to evaluate the latencies and message update rates observed during flight testing with the UTM. Expanded presentation of the results is in the Task 4 Execution Report published on the ASSURE website. The following is a summary.

2.1.3.3.2.8 Latency in Transmitting MA Position Through UTM

This subsection presents the latency between sending the manned aircraft position to the UTM system and receiving that message on the avoiding sUAS. This is the latency associated with the diagram in Figure 2.18.

A summary of the latency statistics for each of the ten flights is presented in Table 2-11. For most flights (9 out of 10), the average latency was between 0.38 to 0.55 seconds, and the percentage of messages having a latency less than 1 second was more than 93%. The last flight had higher latencies, with the average latency being 1.45 seconds, and all messages having latencies higher than 1 second. Yet, in this last flight, 99.7% of the messages had a latency of less than 2 seconds.

Table 2-11: Summary of latency statistics for the ten sUAS-manned aircraft flight tests.

Flight	Latency Statistics				
	Average (s)	Standard Deviation (s)	Minimum (s)	Maximum (s)	% less than 1 second
1	0.55	0.48	0.30	8.12	94.5
2	0.55	0.60	0.29	7.78	93.5
3	0.50	0.51	0.29	5.20	96.3
4	0.43	0.41	0.28	7.50	96.2
5	0.48	0.79	0.28	23.03	96.3
6	0.55	0.82	0.28	11.95	94.3
7	0.49	0.78	0.31	22.26	95.4
8	0.42	0.31	0.19	5.00	97.5
9	0.38	0.12	0.30	2.67	99.8
10	1.45	0.09	1.30	2.92	0

2.1.3.3.2.9 Latency in Transmitting Radar Detections Through UTM

This section presents the latency between making a radar detection and receiving that radar detection from the UTM on the sUAS. This latency includes the time to make a radar detection, the time to send the information to the UTM, and the time until the information arrives at the sUAS. This is the latency associated with the diagram in Figure 2.11. The latencies observed in one of the flight encounters using radar data are presented in the following figure. Two additional encounters had similar trends in the latencies (as presented in the Task 4 Execution Report). The minimum observed latency is around 4.8 seconds. The latency plots show a repeating trend where latency appears to linearly increase with time and then drop suddenly. This trend is observed because the same radar message is received multiple times until a new radar detection is made. The latencies need to be appropriately accounted for. One way to account for the latencies is to require an increase in the detection distances. On the other hand, if the DAA system required performance is limited, in that it cannot support the required minimum detection distance, the WC volume could be increased.

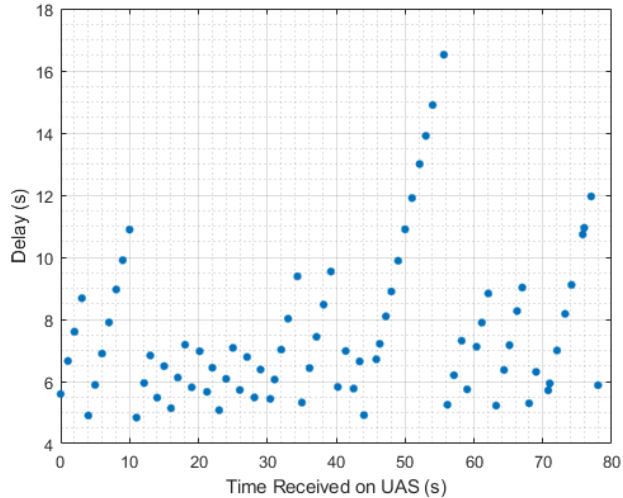


Figure 2.18: Latency in obtaining radar detection using the UTM system, as observed during the duration of Encounter 17.

2.1.3.3.2.10 Analysis of Cellular Connectivity for Manned Aircraft

4,867 data points were collected in Lawrence, KS with the manned aircraft sending its position using cellular connection directly to the UTM system using the approach in Figure . This position information was received using the laptop computer. The Cessna was set to send its position at 1 Hz, thus the data is equivalent to 4,867 seconds of flight or 81.1 minutes of flight.

This data was used to analyze the reliability of the cellular connection on the manned aircraft. The data was also used to investigate the presence of cellular drop out locations, or if there is a correlation between cellular connectivity and manned aircraft flight altitude, ground speed, or orientation changes.

Much more details are discussed in the Task 4 Execution Report. The following table summarizes the latencies and update rates observed in this flight data collection.

Table 2-12: Statistics of the observed latencies and update periods for the Cessna 172 flight data. 4,867 data points were collected (~81.1 minutes of flight).

Variable	Min.	Max.	Average	Standard Deviation	90 th Percentile	95 th Percentile	99 th Percentile
Latency (s)	0.13	22.71	0.40	0.57	0.70	0.82	2.41
Update period (s)	0.29	23.46	1.08	0.58	1.23	1.44	3.31

Generally, the cellular connectivity worked well during the Cessna 172 flight tests. It was possible to conduct manned aircraft and sUAS separation through the UTM based on cellular connectivity. In most flights, the observed latencies were mostly low. In most flights, the update period of the received data averaged around 1 second, which is the set update period in the system (i.e., 1 Hz). No tangible correlations were calculated between latencies and update rates against altitude,

ground speed, heading, and heading rate. No geographic latitude and longitude locations were identified as having poor connectivity. (Except for one potential location in Lawrence, KS). In some cases, turning flight may be associated with decreased connectivity. It is important to note that the latencies identified in this subsection (Section 2.1.3.3.2.10) have some errors in their magnitude due to the clock synchronization errors, as discussed in Task 4 Execution Report.

2.1.3.4 Task Conclusions

Horizontal separation services provided to a sUAS by a UTM system for an autonomous sUAS have been shown to be feasible to maintain either a 2000-foot or 1500-foot separation distance between sUAS and manned aircraft at a success rate of 50% IF the UTM system AND the information services that it relies upon meet the following requirements:

- The manned aircraft can be detected by the UTM system at the *minimum required detection distance* determined by simulation and validated by flight test.
 - Minimum required detection distances have been determined through simulation for a range of manned aircraft speeds, and encounter angles for encounters in which a mid-air collision would occur if no mitigation occurred. Flight tests of sUAS encountering manned aircraft have been conducted to provide a comparison with simulations. While some encounters studied in simulation and subsequently flown in flight test show good agreement with simulation, some encounters required up to twice the detection distance to avoid a well-clear violation. Some of this behavior is due to the fact that flight test trajectories meant to mirror those simulations are difficult to achieve in flight test due to encounter set-up inaccuracies, GPS latencies and position biases, and the presence of ambient winds.
- The manned aircraft position information used by the UTM system from ADS-B or radar must have a position error which is not large with respect to the required separation distance.
 - For flight tests using an available, but likely not well-registered, marine radar, position errors of 500 feet and higher were observed, which could cause well clear violations to occur at a rate larger than the 50% rate unless the avoidance maneuver algorithm is adjusted to incorporate such position errors. In particular, the avoidance algorithm should avoid as if the required separation distance is increased from the mandated distance—for a 500 ft position error, the sUAS would avoid as if the required WC distance is 2500 ft, without the requirement to change the mandated 2000 ft distance. This way the ownship can mitigate the possible position errors while attempting to maintain the desired horizontal well clear separation distance from the othership.
- The UTM system must have reliable communication services in the operational area such that any “drop-outs” in service, in conjunction with the closing speed of the encounter is not large with respect to the minimum required detection range.
 - In flight tests with the Unifly UTM system, communication latencies were typically under 1 second. However, there were some much larger latencies, which have not been explained yet and can be a subject of further investigation.
 - Note: For sUAS under the command of a human pilot, the latencies of detection and maneuver may be somewhat different.

In the flight tests conducted in this work, the cellular connectivity onboard the manned aircraft and the sUAS were found to be reliable. It was possible to conduct sUAS separation from manned aircraft based on data sent to and received from the UTM system using cellular connectivity.

Encounters with higher traffic densities (i.e., encounters with more than two aircraft) required higher detection distances in order to maintain well clear separation between all aircraft involved. This is a factor to be considered by DAA systems designers, manufacturers, and operators.

2.2 sUAS-sUAS Separation and Enabling Technologies

2.2.1 UTM Services Field Testing

2.2.1.1 Task Overview

This task investigates the use of UTM systems to provide separation between sUAS. This section is part of the same research task in Section 2.1.3. Section 2.1.3 focused on sUAS-manned aircraft separation. This section focuses on sUAS-sUAS separation. Extensive simulations were performed to investigate the minimum detection distances at which a sUAS needs to detect another sUAS to remain well clear. Flight testing was performed to test UTM-based sUAS separation. Flight test data was collected with the sUAS sending its position to the UTM system directly over cellular connection and using Network RID. In all simulated and flight test encounters, the avoider sUAS maneuvered autonomously to maintain separation from the intruder sUAS. UTM services were provided by Unifly. The latencies and message update rates experienced during flight are analyzed. Currently, there is no agreed upon well clear separation volume for sUAS-sUAS encounters. Six well clear definitions were investigated using simulation. Simulated encounters involving more than two sUAS are also studied. The following is a concise summarized presentation of the research methods, approach, results, and conclusions for this research task. Further details can be found in the Task 4 Execution Report published on the ASSURE website.

2.2.1.2 Method and Approach

This study is built on two components: extensive simulations, followed by flight testing. The goal of the simulations is to identify the minimum detection distances at which the sUAS needs to detect other sUAS in order to be able to maneuver in time and remain well clear. The goal of flight testing is to perform field testing of the UTM system and validate the simulation results. The following is a presentation of the methods and approaches used for simulation and flight testing. Much of the methods and approaches are as described in Section 2.1.3.2 for the sUAS-manned aircraft study.

- In all simulation and flight test encounters, the sUAS autonomously maneuvered to remain well clear from the manned aircraft. The avoidance algorithm used for autonomous avoidance was described in Section 2.1.3.2.1.
- The sUAS used in this work is the SkyHunter sUAS described in Section 2.1.3.2.2.
- The Unifly UTM system used in this work is described in Section 2.1.3.2.4.

2.2.1.2.1 Simulation Approach for sUAS-sUAS Encounters

Extensive simulations are conducted for sUAS-sUAS encounters to identify the minimum detection distance needed for a sUAS to stay well clear from another sUAS. In the encounters, there is a sUAS flying in a straight line, and it is considered to have right-of-way. It is referred to as the "intruder" sUAS. Then, there is the "avoider" sUAS, which is set to fly in the same airspace.

The simulation flight paths are designed such that the intruder and avoider sUAS would collide if they kept flying in a straight line. In the encounter, the avoider sUAS performs avoidance maneuvers to remain well clear from the intruder sUAS using the avoidance algorithm discussed in Section 2.1.3.2.1. The aim is for the sUAS to maintain the horizontal well clear separation from the sUAS. Currently, there is no agreed upon well clear separation volume for sUAS-sUAS separation. In this work, six horizontal well clear candidates were investigated: 100, 200, 300, 400, 500 and 600 ft.

The minimum detection distance needed to stay well clear from the intruder sUAS is originally unknown. Therefore, the simulation is performed using an initial detection distance. Then, the simulation is repeated multiple times, where higher detection distances are tested in each simulation run. Using these simulation results, the minimum detection distance which allows for a well clear encounter is identified.

The above simulation procedure is followed for encounters where the intruder sUAS approaches from different angles and at different approach speeds. The avoider sUAS was always flying at 45 ft/s. Simulations were conducted for the intruder sUAS approaching at speeds of 45, 60, and 90 ft/s and from relative approach angles ranging from 0 degrees (an overtaking scenario) to 180 degrees (a head-on scenario). Figure 2.7 in Section 2.1.3.2.3 presented the heading angle definition for the intruder aircraft.

The simulation results are presented in Section 2.2.1.3.1.

2.2.1.2.2 Flight Test Approach

Flight testing was conducted for sUAS-sUAS encounters to test the use of the UTM system for aircraft separation and to validate the simulation results. The flight test encounters were designed to have similar trajectories as the simulated encounters. That is the avoider and intruder sUAS were set to approach each other and the avoider sUAS was set to autonomously maneuver in order to remain well clear from the intruder sUAS. In flight testing, the 500 ft. horizontal well clear definition was used.

The avoider sUAS was allowed to detect the intruder sUAS once it was within the detection distance specified by the flight test team for that encounter. This allows the team to evaluate if the specified detection distance was sufficient to maintain well clear separation or not. The team then compared the detection distances needed in flight testing to the detection distances needed in the simulations.

Flight testing of sUAS-sUAS encounters was conducted using two approaches:

- 1) Approach 1 (Figure 2.19): The intruder sUAS directly sent its location to the Unifly UTM using cellular connection. Then, the avoider sUAS received the position of the intruder sUAS from the Unifly UTM over cellular connection. Two encounters were conducted using this approach.
- 2) Approach 2 (Figure 2.20): The intruder sUAS sent its location to the avoider sUAS over 900 Mhz communication. Two encounters were conducted using this approach.

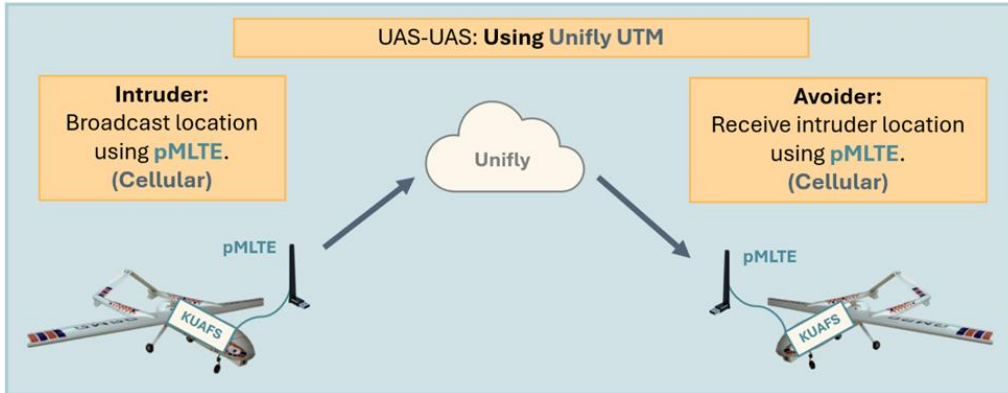


Figure 2.19: sUAS-sUAS Approach 1: Using Unify UTM.

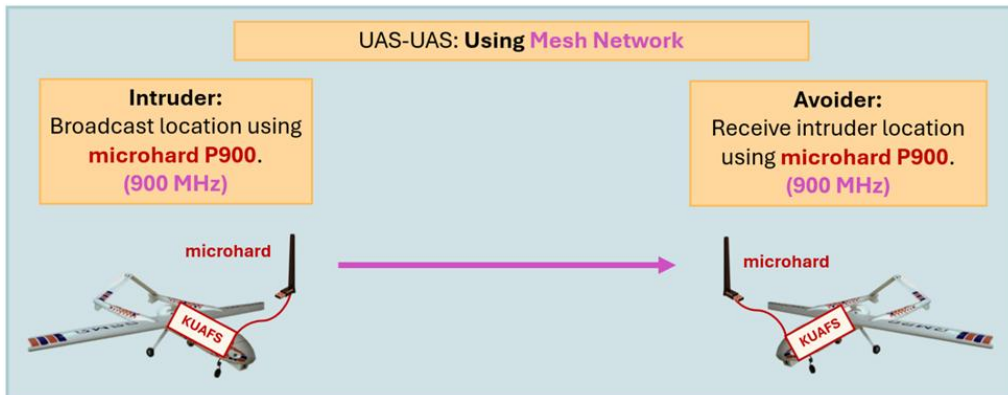


Figure 2.20: sUAS-sUAS Approach 2: Using 900 MHz communication.

Flight testing using Approaches 1 to 2 were conducted in Lawrence, KS using the SkyHunter sUAS. The flight test results are presented in Section 2.2.1.3.2.

Flight test data was also collected using a third approach, presented in Figure 2. In the third approach, a Dronetag Mini device attached to the intruder sUAS sent network RID data to the Dronetag online cloud using cellular connection. Then, the RID data was forwarded to the Unify UTM system. A laptop on the ground received the intruder sUAS information from Unify using an internet connection. No encounters were conducted using this approach. However, flight test data was collected from this approach and analysis of the communication latency was conducted.

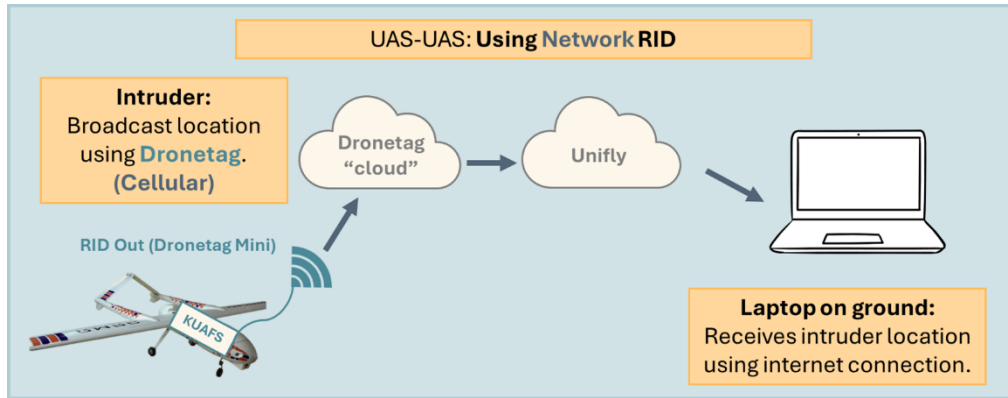


Figure 2.:sUAS Approach 3: Using network RID through Unify UTM.

2.2.1.2.3 Analysis of Cellular Connectivity, Latencies, and Update Rates

Analysis was performed to evaluate the latencies and message update rates observed during flight testing with the UTM. The analysis was performed in several ways:

- 1) The latency between sending the intruder sUAS position to the UTM system and receiving that message on the avoiding sUAS was calculated. This is the latency associated with the diagram in Figure 2.19.
- 2) The latency between sending the intruder sUAS network RID data to the UTM system then receiving that message on the ground by a Laptop was calculated. This is the latency associated with the diagram in Figure 2.
- 3) The latency between sending the sUAS positions to the UTM system and receiving these messages on a laptop on the ground was calculated. This is the latency associated with the diagram in Figure 2.12.

The latencies identified using the first way, present latencies observed during flight operation from one aircraft to another. These latencies are impacted by both aircraft cellular connectivity. The latencies identified using the second and third ways (items 2 and 3 in the above list) focus on the sUAS connectivity more separately. That is, the observed latency during a flight is not impacted by the receiving side's location – since the laptop is not moving.

The latencies and update periods are calculated using Equation 2.6 and Equation 2.7 as described in Section 2.1.3.2.6. The results of the analysis of cellular connectivity, latencies, update periods are presented in Section 2.2.1.3.2.2.

2.2.1.2.4 Encounters With More Than Two sUAS

Similar to Section 2.1.3.2.7, this research task also looked into the effect of increased sUAS traffic density on maintaining well clear encounters between sUAS when there are more than two aircraft in the encounters. Two scenarios were investigated:

- 1) Corridor Scenario: A scenario involving two sUAS flying in trail formation in a “corridor” with an intruder sUAS flying in a straight flight path to intercept the formation.
- 2) Surveying Scenario: a surveying scenario in which an intruder sUAS intercepts two sUAS flying in a laterally offset/trail formation following a rectangular flight pattern.

In these scenarios, the two sUAS (in corridor/surveying flight paths) were set to autonomously avoid the third intruding sUAS and each other. The goal was for the two avoiding sUAS to maintain a 500 ft horizontal well clear dimension from each other and the third sUAS. The intruding sUAS did not conduct any avoidance maneuvers.

The corridor scenario is as described in Section 2.1.3.2.7.1. However, the differences here are that:

- 1) The manned aircraft is replaced with a sUAS which does not conduct any avoidance maneuvers.
- 2) Simulations were conducted with the third sUAS intruder approaching at 45, 60, and 90 ft/s. (The two avoiding sUAS were always flying at 45 ft/s.)

The corridor scenario simulation results are presented in Section 2.2.1.3.2.6.

The surveying scenario is as described in Section 2.1.3.2.8. However, in this section, the intruder is a third sUAS, not a manned aircraft. The third intruding sUAS does not conduct any avoidance maneuvers. The simulation results are presented in the more extended project report (Task 4 Execution Report) published on the ASSURE website.

2.2.1.3 Results and Discussion

2.2.1.3.1 Simulation Results

2.2.1.3.1.1 500 ft sUAS-sUAS Horizontal Well Clear

Based on the simulation approach presented in Section 2.2.1.2.1, the minimum detection distances at which the avoider sUAS needs to detect the intruder sUAS are presented in Figure 2.21. These results are for a 500 ft horizontal well clear dimension. Results are presented for intruder sUAS flying at 45, 60, and 90 ft/s.

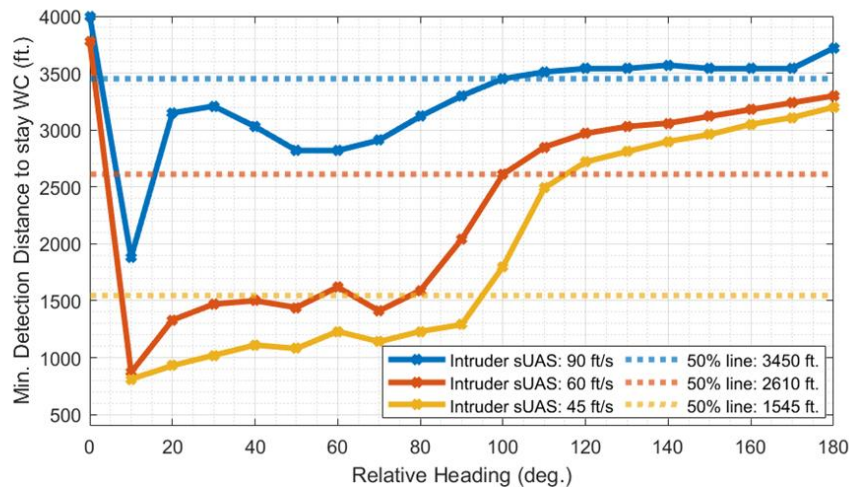


Figure 2.21: Simulated sUAS-sUAS encounters: minimum detection distance at different relative encounter angles and three intruder sUAS airspeeds. Results are for a 500 ft horizontal well clear volume. Broken lines show the detection distances allowing 50% of the sUAS-sUAS encounters to be well clear.

Table 2-13: Minimum detection distances which allow 100% and 50% of the sUAS-sUAS encounters to be well clear, based on simulation. Results are for a 500 ft horizontal well clear radius.

Intruder sUAS speed (ft/s)	Minimum required detection distance (ft)	
	For 100% WC encounters	For 50% WC encounters
45	3200	1545
60	3780	2610
90	4000	3450

2.2.1.3.1.2 Six sUAS-sUAS Horizontal Well Clear Dimensions

Six sUAS-sUAS horizontal well clear separations were studied: 100, 200, 300, 400, 500, and 600 ft. The detection distances needed to maintain these six well clear separations were obtained for encounters with different relative speeds and encounter angles. The detection distances needed are identified in the following figures and in Table 2-14.

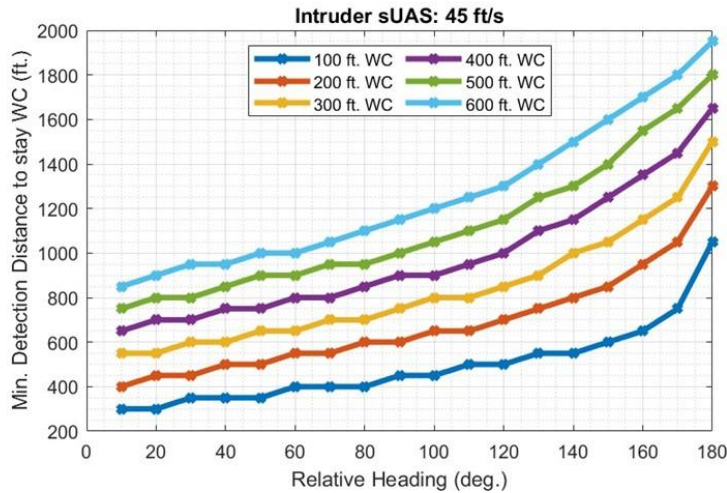


Figure 2.22: Minimum required detection distances to maintain the six studied sUAS-sUAS horizontal well clear separations. sUAS intruder's speed is 45 ft/s.

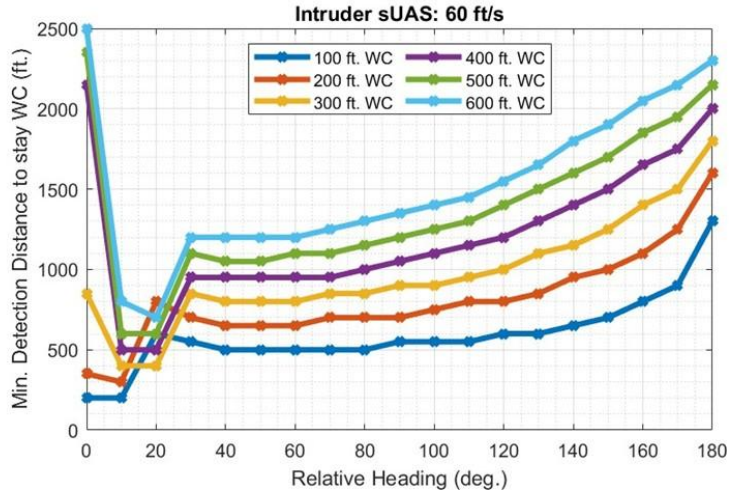


Figure 2.23: Minimum required detection distances to maintain the six studied sUAS-sUAS horizontal well clear separations. sUAS intruder’s speed is 60 ft/s.

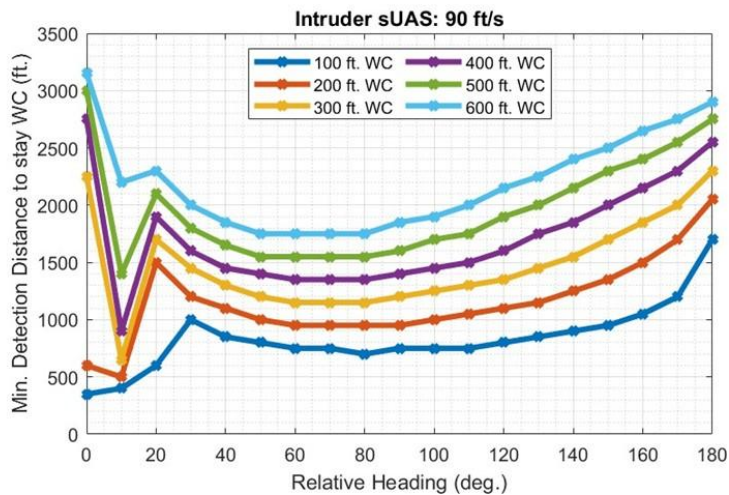


Figure 2.24: Minimum required detection distances to maintain the six studied sUAS-sUAS horizontal well clear separations. sUAS intruder’s speed is 90 ft/s.

In this section, the avoidance algorithm was encouraged to avoid the horizontal well clear distance with some margin. That is, instead of setting σ equal to the well clear distance, it was set to be the well clear distance plus 50. This results in a little more repulsion from the intruder and encourages smaller detection distances. This, along with other avoidance algorithm updates that were done over time causes the results in this section (Section 2.2.1.3.1.2) to be different from the results in the previous section (Section 2.2.1.3.1.1). The simulations in the previous section used σ equal to the well clear distance.

Table 2-14: Minimum detection distances which allow 100% and 50% of the sUAS-sUAS encounters to be well clear, based on simulation. Results are for six horizontal well clear separations. Avoidance algorithm is set to have $\sigma = \text{horizontal well clear radius} + 50$.

Intruder Speed	45 ft/s		60 ft/s		90 ft/s	
	50%	100%	50%	100%	50%	100%
100 ft WC	450	1050	550	1300	800	1700
200 ft WC	625	1300	750	1600	1100	2050
300 ft WC	775	1500	900	1800	1350	2300
400 ft WC	900	1650	1100	2150	1600	2750
500 ft WC	1025	1800	1250	2350	1800	3000
600 ft WC	1175	1950	1400	2500	2150	3150

The results show that, to remain well clear, larger detection distances are required for (1) head-on and overtaking encounters, (2) sUAS intruders flying at higher speeds, and (3) larger horizontal well clear radii.

Testing of multiple RID devices was performed as described in Section 2.2.2. The results from these RID tests are combined with the detection distances presented in this section to evaluate the horizontal well clear radius that can be supported by RID communication. Further discussion is presented in Section 2.2.2.

2.2.1.3.2 Flight Test Results

Flight tests were conducted of sUAS-sUAS encounters. The goals of conducting the flight test encounters were:

- 1) Evaluating the potential of using UTM for sUAS-sUAS separation.
- 2) Comparing the flight test results with the simulation results.

In all encounters, the goal was to maintain a 500 ft horizontal separation between the sUAS. If the two sUAS maintained at least 500 ft separation, the encounter was a well clear encounter. If the two aircraft got closer than 500 ft to each other, the encounter was a well clear violation. In all flight test cases, a vertical separation was maintained between aircraft.

More details are presented in the Task 4 Execution Report published on the ASSURE website.

2.2.1.3.2.1 Head-On Flight Test Encounters

Four sUAS-sUAS head-on encounters were conducted. The first two encounters were conducted using the Unifly UTM for sUAS-sUAS separation. The second two encounters were conducted using 900 MHz communication (which is the baseline approach used in previous KU flight tests). These encounters are summarized in Table 2-15 **Error! Reference source not found.** From these encounters, the following conclusions can be made:

1. Using UTM for sUAS-sUAS separation is possible, as demonstrated in the first encounter.
2. sUAS flying at 48-60 ft/s were able to maintain well clear separation with a detection distance of 3,450 ft for head-on encounters. This agrees with the detection distances identified through simulation results (3200-3300 ft). However, the strength of the

avoidance algorithm in the flight tests had to be increased to maintain separation while using this detection distance.

Table 2-15: Summary of sUAS-sUAS head-on flight test encounters

#	Avoider sUAS (ft/s)	Intruder sUAS (ft/s)	Detection Distance (ft)	Sigma	Information Source	Minimum Separation (ft)	Status
1	50	48	3,450	650	Cellular (Figure 2.19)	583	WC
2	50	51	4,500	500	Cellular (Figure 2.19)	446	WCV
3	50	54	3,450	500	900 MHz Comms. (Figure 2.20)	227	WCV
4	50	57	3,450	750	900 MHz Comms. (Figure 2.20)	700	WC

2.2.1.3.2.2 Cellular Connectivity Analysis

Analysis was performed to evaluate the latencies and message update rates observed during flight testing with the UTM. Expanded presentation of the results is in the Task 4 Execution Report published on the ASSURE website. The following is a summary.

2.2.1.3.2.3 Latency in Transmitting sUAS Position Through UTM to the sUAS

This subsection presents the latency between sending the intruder sUAS position to the UTM system and receiving that message on the avoiding sUAS (method in Figure 2.19). Figure 2.25 presents the latencies observed during the flight test containing sUAS-sUAS Encounters 1 and 2 discussed in Section 2.2.1.3.2.1. As presented in the figure, the average latency was 0.36 seconds, and the standard deviation was 0.2 seconds.

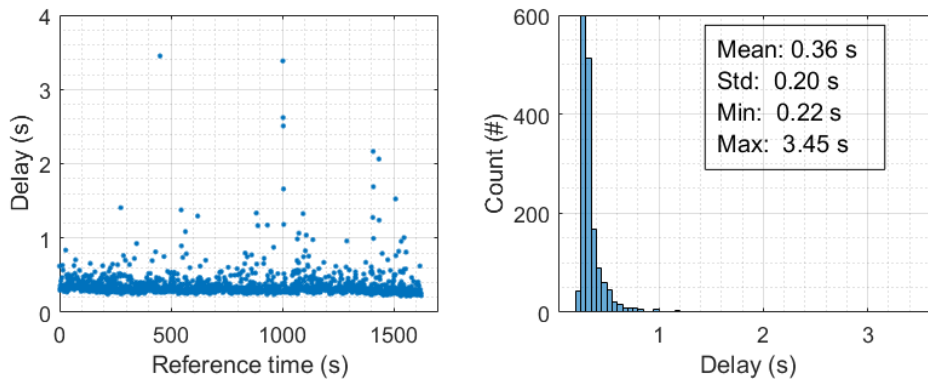


Figure 2.25: Observed UTM communication latencies in the flight containing sUAS-sUAS Encounters 1 and 2. The left plot shows the observed latency over the duration of the flight. The right plot shows the same data using a histogram plot.

2.2.1.3.2.4 Latency in Transmitting Network RID Position Through UTM to Ground Laptop

This subsection presents the latency between sending sUAS network RID position to the UTM system and receiving that message on a laptop on the ground (method in Figure 2). Table 2-16 presents the latencies observed in two flights using this method.

Table 2-16: Statistics of latencies observed with network RID data forwarded to Unify.

Flight	Latency for network RID (Figure 2)	
	Average (s)	Standard Deviation (s)
1 st flight	3.31	1.17
2 nd flight	3.89	3.23

2.2.1.3.2.5 Analysis of cellular Connectivity for sUAS

13,488 data points were collected in Lawrence, KS with sUAS sending their position using cellular connection directly to the UTM system using the approach in Figure 2.19. This position information was received using the laptop computer. The sUAS were set to send their position at 1 Hz, thus the data is equivalent to 13,488 seconds of flight or 224.8 minutes of flight.

Additionally, 1980 data points were collected in Starkville, MS with sUAS sending their position using cellular connection directly to the UTM system using the approach in Figure 2.19. This position information was received using the laptop computer. The sUAS were set to send their position at 1 Hz, thus the data is equivalent to 1980 seconds of flight or 33 minutes of flight.

This data was used to analyze the reliability of the cellular connection on the sUAS in Lawrence, KS and Starkville, MS. The data was also used to investigate the presence of cellular drop out locations, or if there is a correlation between cellular connectivity and manned aircraft flight altitude, ground speed, or orientation changes.

Much more details are discussed in the Task 4 Execution Report. Table 2-17 and Table 2-18 summarize the latencies and update rates observed in the Lawrence, KS and Starkville, MS flight data, respectively.

Table 2-17: Statistics of the observed latencies and update periods for the sUAS flight data at Lawrence, KS. 13,488 data points were collected (~224.8 minutes of flight).

Variable	Min.	Max.	Average	Standard Deviation	90 th Percentile	95 th Percentile	99 th Percentile
Latency (s)	0.06	22.01	0.69	0.44	1.15	1.26	1.57
Update period (s)	0.07	50.42	1.01	0.60	1.19	1.28	1.60

Table 2-18: Statistics of the observed latencies and update periods for the sUAS flight data at Starkville, MS. 1980 data points were collected (~33 minutes of flight).

Variable	Min.	Max.	Average	Standard Deviation	90 th	95 th	99 th
----------	------	------	---------	--------------------	------------------	------------------	------------------

				Deviation	Percentile	Percentile	Percentile
Latency (s)	0.26	1.99	0.64	0.28	1.00	1.10	1.35
Update period (s)	0.16	2.23	1.00	0.17	1.18	1.28	1.54

Generally, the cellular connectivity worked well during the sUAS flight tests. It was possible to conduct sUAS separation (from manned aircraft and other sUAS) through the UTM based on cellular connectivity. In most flights, the observed latencies were mostly low. In most flights, the update period of the received data averaged around 1 second, which is the set update period in the system (i.e., 1 Hz). No tangible correlations were calculated between latencies and update rates against altitude, ground speed, heading, and heading rate. No geographic latitude and longitude locations were identified as having poor connectivity for the sUAS data. In some cases, turning flight may be associated with decreased connectivity. It is important to note that the latencies identified in this subsection (Section 2.2.1.3.2.5) have some errors in their magnitude due to the clock synchronization errors, as discussed in Task 4 Execution Report.

2.2.1.3.2.6 Multi-sUAS vs sUAS Simulation Results

The main observation from the corridor flight scenarios is that higher detection distances were needed in these multi-sUAS encounters than the encounters with only one avoider sUAS. For 50% of the corridor encounters to be well clear, up to 4,800 feet detection distances were needed – larger than the (up to 3450 feet) detection distances needed when only one avoider sUAS was in the encounter. The Task 4 execution report contains the extended results.

2.2.1.4 Task Conclusions

Horizontal separation services provided to a sUAS by a UTM system for an autonomous sUAS avoiding another sUAS have been shown to be feasible to maintain separation distances ranging from 100 feet to 600 feet at a success rate of 50% IF the UTM system AND the information services that it relies upon meet the following requirements:

- The sUAS can be detected by the UTM system at the ***minimum required detection distance*** determined by simulation and validated by flight test.
 - Minimum required detection distances have been determined through simulation for a range of othership sUAS speeds, and encounter angles for encounters in which a mid-air collision would occur if no mitigation was attempted. A small number of flight tests of sUAS encountering another sUAS head-on have been conducted to provide a comparison with simulations with a 500-foot well-clear distance goal. Using the Unifly UTM system, in the two encounters flown, one resulted in a well clear encounter and the other had a small, 50-foot well clear violation. In these flight tests, the UTM used “self-reported” GPS position information from both sUAS via cellular links. Alternatives to obtain othership position might be from an RID broadcast (which was attempted) or from on-board/airborne radar on the ownship (which was not available). In two head-on encounters with the KU “mesh network” used for self-reported GPS position, one resulted in a well clear encounter while the other had a well clear violation. The same, onboard avoidance algorithm was used in the encounters using mesh network and Unifly.

- The position knowledge bias is small with respect to the desired separation distance.
 - In all flight tests conducted, the position knowledge bias was small because both sUAS self-reported GPS position. As such, the GPS biases were likely very similar, and, as they approached one another, became essentially the same.
- The UTM system must have reliable communication services in the operational area such that any “drop-outs” in service, in conjunction with the closing speed of the encounter is not large with respect to the minimum required detection range.
 - In flight tests with the Unifly UTM system, communication latencies were typically under 1 second.
 - Note: For sUAS under the command of a human pilot, the latencies of detection and maneuver may be somewhat different.

In the flight tests conducted in this work, the cellular connectivity onboard the sUAS were found to be reliable in both flight test locations (Lawrence, KS and Starkville, MS). It was possible to conduct sUAS separation from other aircraft (sUAS and manned aircraft) based on data sent to and received from the UTM system using cellular connectivity.

Encounters with higher traffic densities (i.e., encounters with more than two aircraft) required higher detection distances in order to maintain well clear separation between all aircraft involved. This is a factor to be considered by DAA systems designers, manufacturers, and operators.

2.2.2 Remote ID Field Testing

2.2.2.1 Task Overview

This research task evaluates the feasibility of using RID as an enabling data source for DAA decision-making in BVLOS sUAS operations. The task aims to answer the following research question:

What should the separation and performance requirements be for BVLOS sUAS to remain separated from other sUAS that broadcast their RID?

To support this objective, the task focuses on assessing whether current commercial off-the-shelf (COST) and onboard RID solutions, particularly those operating at the minimum ASTM broadcast requirements, can support sUAS-sUAS avoidance to maintain safe separation. The ASTM minimum standard represents the lowest capability legally compliant aircraft may exhibit in the NAS. Establishing the level of RID performance that can be achieved to maintain safe separation between sUAS helps determine whether the current ASTM RID specification is sufficient, or whether higher update rates and transmission power are needed to support safe separation.

The evaluation considers a set of candidate sUAS Horizontal “well clear” separation distances (referred to as sHWC) ranging from 100 ft to 600 ft, representing proposed horizontal “well-clear” dimensions applicable to multirotor and small fixed-wing classes. Since there is no current standard established for sUAS-sUAS separation, the candidate separation thresholds were adopted from the sUAS community idea sharing and discussion as well as previous ASSURE projects and FAA policies (A47, 2023) (FAA, 8040.6A, 2023), which considered traditional UAS well-clear frameworks, reduced collision severity for uncrewed encounters, and aircraft size-based collision geometry scaling.

This research task does not seek to demonstrate that any specific horizontal separation ensures safety. The goal is to assess whether currently fielded RID systems, operating at ASTM minimum update rates and transmission power, can reliably meet the communication and accuracy performance needed to support DAA within these candidates “well-clear” horizontal dimensions.

The study conducted both stationary and dynamic flight tests using multiple RID COST modules and standard RID systems across Bluetooth and Wi-Fi RID protocols. Each RID system was evaluated at the edge of the proposed sHWC distances to characterize position accuracy and the performance difference between static and flight scenarios.

This task employs the Minimum Detection Distances (MDD) derived from the encounter simulations described in section 2.2.1 of this report. The simulations incorporated avoidance logic and aircraft dynamics to determine the minimum range required for the ownship sUAS to execute an avoidance maneuver and remain “well clear”. The resulting MDD values are used in this task to guide field range checks and ensure the RID system was evaluated against the separations needed for both baseline and enhanced avoidance algorithms in head-on (0°) and overtaking (180°) encounter geometries.

The MDDs obtained from the encounter simulations served as reference thresholds against which RID performance was evaluated. The flight testing characterized RID performance at increasing horizontal separation distances to determine whether ASTM compliant RID systems can reliably provide the detection ranges needed to maintain safe separation. The findings indicate whether ASTM’s current minimum RID requirements are sufficient to maintain “well-clear” at candidate separation distances, and where performance limitations suggest the need for increased transmission rates, higher radiated power, or additional DAA sensing capabilities.

2.2.2.2 Method and Approach

This section describes the approach and methodology used to evaluate whether RID performance is sufficient to support safe horizontal separation for sUAS-sUAS encounters. The approach combined RID accuracy testing at candidate sHWC distances with range testing informed by simulation-derived MDDs. The testing followed two main paths:

- Accuracy-focused boundary testing: assessing whether RID data remains reliable and accurate when aircraft are operating near the proposed sHWC distances. This represents the “can RID support decision-making at different horizontal well clear separation distances?” question.
- Simulation-driven MDD range evaluation: evaluating whether RID performance allows detection early enough to support automated maneuvering to remain well-clear, using encounter simulation MDD outputs. This represents the “can RID support timely detection for avoidance?” question.

Testing was conducted using ASTM F3411-22a compliant RID systems at their minimum broadcast rate and power, to determine whether minimum-standard RID performance is sufficient or whether increased transmission performance may be needed. These minimums require a dynamic broadcast rate of ≥ 1 Hz and a static broadcast rate of approximately 0.33 Hz, with minimum transmit power levels of approximately +11 dBm for 2.4 GHz Wi-Fi/Bluetooth and +3 dBm for 5 GHz Wi-Fi.

Table 2-19 shows the six candidate horizontal “well-clear” separation distances, characterized by sHWC and aligned with aircraft class and size.

Table 2-19: Proposed Well -Clear Volumes for sUAS-vs-sUAS

sHWC (ft)	Comment
600	13' Fixed Wing
500	13' Fixed Wing
400	13' Fixed Wing
150	Quadcopter
100	Quadcopter
50	Quadcopter

Each sHWC was tested with a “wagon wheel” shaped flight path, matching the horizontal component being evaluated. Exploration of the vertical component of “well-clear” is not included in this task.

Figure 2.26 shows the testing matrix that was used for flight testing. The altitude was set at 300 ft AGL to provide proper clearance above the ground and allow additional vertical space to maneuver if necessary. The receiver is represented by the dot in the middle of the testing zone with each concentric ring representing the horizontal distances in Table 2-19. Each horizontal separation distance evaluated along with an additional “declaration distance”, which provides the additional buffer for the ownship to initiate an avoidance maneuver and remain well clear. These declaration distances were taken directly from the simulation results and used to structure the flight-test evaluation.

The remainder of this section describes the flight test campaigns and equipment used to evaluate RID performance at these sHWC distances and to assess communication performance against the simulation-derived MDDs.

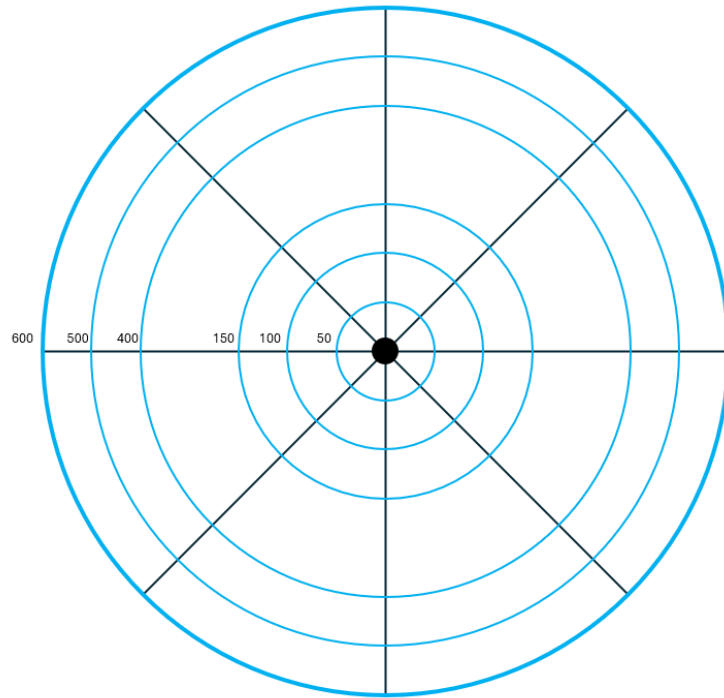


Figure 2.26: Simplified testing matrix for evaluating RID performance

2.2.2.2.1 *Flight Test Setup for RID Accuracy*

This part of the flight test evaluates RID performance at the edge of proposed sHWC. The intent of this test series was not to prove that any specific sHWC is “the right one,” but to observe how real RID broadcasts perform, in data correctness, when aircraft are separated by the distances proposed for sUAS-to-sUAS encounters.

Two flight profiles were designed to represent distinct boundary-encounter conditions:

1- Static hover profile:

The aircraft hovers at the target sHWC for 60 seconds while broadcasting RID messages. The ground receiver continuously logged packet the hovering time. Each test run was repeated 3 times across different periods of the campaign to capture environmental and temporal variation in signal performance.

2- Dynamic out and back profile:

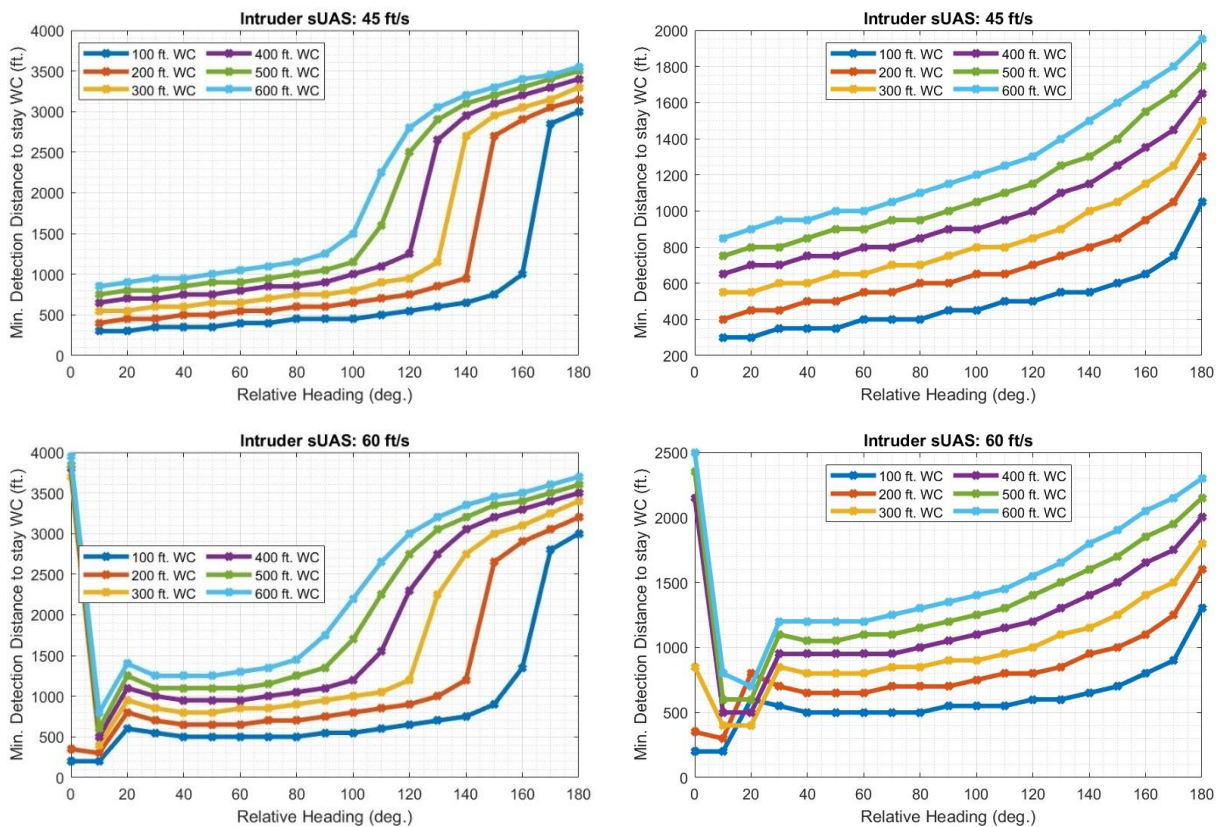
In the dynamic configuration, the aircraft flew from directly above the RID receiver out to the designated horizontal distance and then back to the receiver location, maintaining a constant ground speed. The test was repeated at 25%, 50%, 75%, and 100% of the aircraft’s maximum speed, for each aircraft and for each RID device.

The results from these tests quantify how the positional accuracy (the difference between RID-reported and ground-truth GNSS positions at matched timestamps, vary across horizontal separation distances, flight speeds, and RID module types. These metrics are important in determining whether the current RID systems can reliably support horizontal well-clear maintenance in sUAS operations.

2.2.2.2.2 Flight Test Setup for RID Performance at Minimum Detection Distances

This part of the flight test campaign aimed to evaluate RID communication performance at the MDDs derived from the encounter simulation runs. These simulations modeled sUAS-sUAS encounters using the proposed sHWC distances as reference separation thresholds. The MDD represents the minimum range at which an intruder aircraft must be detected for an avoidance algorithm to execute a timely maneuver and maintain the required horizontal separation distance.

A series of Monte Carlo encounter simulations were conducted for the proposed sHWC distances using two relative encounter geometries: overtaking (0°) and head-on (180°). In each simulation, the ownship maintained a constant velocity of 45 ft/s, while the intruder operated at 45, 60, or 90 ft/s. The encounters were configured such that, without avoidance, the two aircraft would collide. The avoidance logic was then activated at varying detection distances to determine the minimum detection range required to maintain well clear separation. Two avoidance algorithm tunings were assessed: base tuning ($\sigma = \text{sHWC}$) and stronger tuning ($\sigma = \text{sHWC} + 50 \text{ ft}$). The resulting MDDs, are consolidated in Figure 2.27 for base (left) and stronger (right) avoidance tunings across intruder speeds.



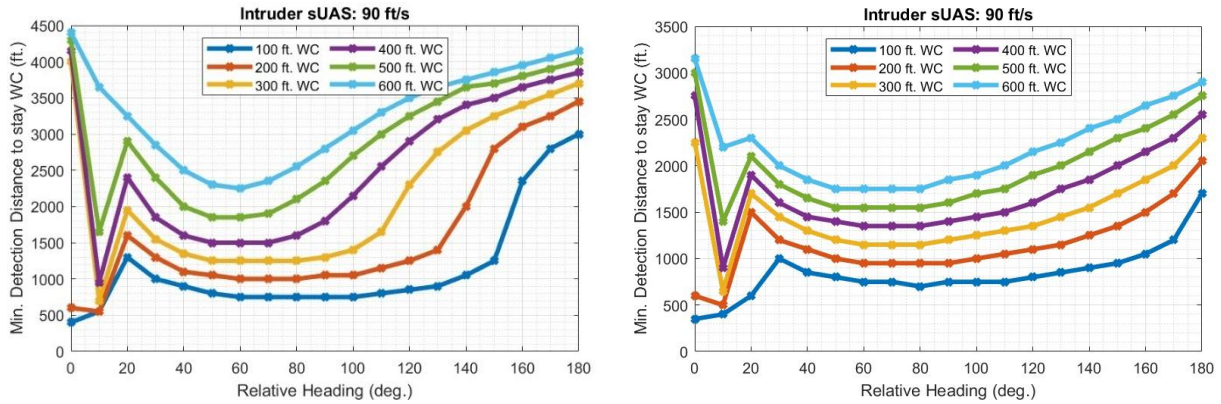


Figure 2.27: Simulated sUAS-sUAS encounters- minimum required detection distances to remain well clear across sHWC distances, and relative encounter angles. Left column: basic avoidance tuning ($\sigma = \text{sHWC}$), right column stronger avoidance tuning ($\sigma = \text{sHWC} + 50\text{ft}$). Rows show intruder speeds of 45 ft/s, 60 ft/s, and 90 ft/s.

As mentioned earlier in 2.1.3.3.1, the ASTM standard F3442-25 for DAA systems performance requirements (ASTM F3442-25, 2025) states that a DAA system for non-cooperative encounters is considered acceptable if its loss of well clear loss ratio is less than or equal to 0.5, implying that not all encounters must remain well clear as long as the ratio stays within the allowable threshold. Thus, two sets of MDD values are derived from the simulation result:

- 50% WC MDDs: distances at which half of encounters remain well clear, consistent with the ASTM LR = 0.5 acceptance criterion, reported in Table 2-20.
- 100% WC MDDs: distances ensuring all simulated encounters remain well clear, summarized in Table 2-21.

Table 2-20: Minimum Detection Distances which allow 50% of the sUAS-sUAS encounters to be well clear, based on simulation across sHWC distances, intruder speeds and avoidance algorithm tuning.

Intruder speed:	45 ft/s		60 ft/s		90 ft/s	
Avoidance algorithm:	Basic	Stronger	Basic	Stronger	Basic	Stronger
sHWC (ft)	Minimum required detection distance (ft)					
100	450	450	550	550	750	800
200	600	625	750	750	1050	1100
300	750	775	950	900	1300	1350
400	900	900	1100	1100	1800	1600
500	1050	1025	1350	1250	2350	1800
600	1250	1175	1750	1400	2800	2150

Table 2-21: Minimum Detection Distances which allow 100% of the sUAS-sUAS encounters to be well clear, based on simulation across sHWC, intruder speeds and avoidance algorithm tuning.

Intruder speed:	45 ft/s		60 ft/s		90 ft/s	
Avoidance algorithm:	Basic	Stronger	Basic	Stronger	Basic	Stronger
sHWC (ft)	Minimum required detection distance (ft)					
100	3000	1050	3000	1300	3000	1700
200	3150	1300	3200	1600	3450	2050
300	3300	1500	3700	1800	4000	2300
400	3400	1650	3800	2000	4150	2550
500	3500	1800	3850	2150	4300	2750
600	3550	1950	4000	2300	4400	2900

The same two flight-test profiles described in the accuracy evaluation (the static hover and dynamic out and back test), are employed in this MDD test. While the accuracy tests focused on broadcast behavior at the edge of the sHWC, this test extended the operation ranges to capture the full detection distances reported in Table 2-20 and Table 2-21.

In the static hover tests, the aircraft maintained a stationary position at predetermined horizontal distances from the ground-based RID receiver, ranging from 500 ft to 4000 ft in 500-ft increments. Each hover lasted approximately 60 seconds. These test points were selected so that the measured ranges collectively covered all simulated MDDs across both avoidance algorithms, all intruder speeds, and all sHWC distances.

For the dynamic out-and-back flights, the aircraft departed from the receiver location, flew out to 5000 ft, and returned along the same trajectory while broadcasting RID messages at a constant speed of 18 m/s (≈ 60 ft/s). This test setup replicated the relative motion conditions used in the encounter simulations for the 60 ft/s intruder case, providing data on how range and continuity are affected by movement and increasing separation. Although the 90 ft/s case was also modeled, it was not flown due to aircraft performance limitations, the maximum speed of the tested aircraft is 66 ft/s.

2.2.2.2.3 Test Aircraft and RID Systems

This subsection describes the aircraft platforms, RID broadcast modules, and receiver equipment used in the flight test campaign. While some devices were initially evaluated (e.g., an onboard receiver module), only those systems that produced usable data are reported in the results.

- Aircraft Platforms:
 - *DJI Mavic 2 Zoom*: a compact quadcopter (~ 2 lb) flown during shorter-range and static test profiles. It incorporates a built-in Wi-Fi RID broadcast at ~ 1 Hz; transmit power was not specified by the manufacturer and could not be accessed

- *DJI Mavic 2 Enterprise Zoom*: used as a baseline quadcopter platform (no built-in RID), to allow direct comparison of external modules under identical flight profiles.
- *DJI Matrice 600*: a heavy-lift hexacopter (~11.05 lb) used as a surrogate for larger fixed-wing sUAS. It was used in the longer-range dynamic tests to capture extended separation behavior.

All aircraft flew within their manufacturer-prescribed flight envelopes and used the same airfield, altitude (300 ft AGL), and line-of-sight control that were used for the well-clear boundary and MDD tests.

- RID Broadcast Modules:
 - *Standard Built-in RID (Mavic 2 Zoom)*: broadcasts over Wi-Fi at ~1 Hz dynamic rate; exact broadcast power is not explicitly published in the product documentation; however, the technical specification sheet lists an EIRP of ≤ 26 dBm in the 2.400–2.4835 GHz band.
 - *DroneTag Mini*: a Bluetooth-only RID module mounted externally; transmit power = +8 dBm, broadcast rate (static/dynamic) = 1 Hz. Manufacturer documentation indicates configurable broadcast power and rate, but no adjustments were successfully made for this campaign.
 - *Drone Beacon (DB120)*: a dual-mode module supporting Wi-Fi Beacon and Bluetooth Low-Energy transmissions. Transmit power = +18 dBm and broadcast rates were Wi-Fi ~1 Hz and BLE ~3 Hz (as configured).

For context, ASTM F3411-22a establishes minimum Remote ID broadcast performance requirements, including:

- Dynamic broadcast rate ≥ 1 Hz.
- Static broadcast rate ≥ 0.33 Hz.
- Minimum transmit power of approximately +11 dBm for 2.4 GHz Wi-Fi/Bluetooth and +3 dBm for 5 GHz Wi-Fi.

All three tested modules operated at or above the ASTM-required broadcast rate, and two of the three (the Mavic 2 Zoom's built-in RID and the DB120) transmitted at power levels significantly above the ASTM minimum.

- RID receiver systems:
 - *DroneScout DS230*: primary ground-based receiver supporting Bluetooth (legacy & Long Range) and Wi-Fi Beacon/NaN protocols across 2.4 GHz and 5 GHz. It features 5 dBi omnidirectional antennas (N-type connectors), PoE power (802.3af/at), and an environmental enclosure rated IP67. The manufacturer specifies a practical detection area of ~80 km² (~5 km radius) in open space. The receiver outputs real-time data via MQTT and supports integration with the DroneScout Dashboard application for laptop visualization and logging.
 - *DroneScout DS100 (Onboard relay receiver)*: initially mounted on the aircraft as an onboard receiver/relay system using the DroneScout Pro mobile app (iOS/Android) and smartphones (iPhone + Samsung Galaxy S20). During pre-flight tests the DS100 module was powered on and broadcast; however, no RID packets

were received or relayed by this system, across all tested configurations. As a result, no data from the DS100 system is included in the analysis.

2.2.2.3 Results and Discussion

This section summarizes the results from the flight test campaigns conducted to evaluate RID system performance under real operational conditions. The analysis focuses on the ability of different RID modules and communication protocols to maintain reliable broadcast and reception across the tested separation distances. Metrics include message reception continuity, positional accuracy, and broadcast update consistency are discussed to assess how RID behavior aligns with the performance needed to support well clear maintenance in sUAS encounters.

2.2.2.3.1 RID Accuracy Results

A series of flight tests were conducted using the tested aircraft and RID modules to evaluate broadcast performance at various horizontal separation distances that encompass the sHWC boundary, under both stationary and dynamic speed profiles. The data collected was analyzed to assess the accuracy of the transmitted position information from each RID system. The results of these flight scenarios are presented and discussed below, and a summary of the key findings is provided in the task conclusion section.

The stationary flight tests were conducted at fixed horizontal distances from the RID receiver, with each aircraft hovering for approximately 60 seconds while continuously broadcasting RID messages. The position accuracy results presented in Table 2-22 and

Table 2-23: Mean and standard deviation of horizontal position error (in feet) for different aircraft – RID (BLE) module configurations across varying distances.

Aircraft	Mavic 2 Enterprise				DJI Matrice 600			
	DB120 BLE		Dronetag BLE		DB120 BLE		Dronetag BLE	
Horizontal distance (ft)	Mean (ft)	Std (ft)	Mean (ft)	Std (ft)	Mean (ft)	Std (ft)	Mean (ft)	Std (ft)
100	13.58	0.97	7.086	2.94	NA	NA	NA	NA
200	14.50	0.98	9.33	3.44	22.11	3.96	40.66	29.08
300	14.34	1.08	8.66	2.40	19.55	0.95	55.94	12.05
400	14.06	0.65	8.07	3.28	17.03	5.30	31.40	11.36
500	NA	NA	NA	NA	18.37	1.83	46.01	5.28

600	NA	NA	NA	NA	15.71	1.34	57.98	12.23
------------	----	----	----	----	-------	------	--------------	-------

quantify the position difference between the broadcast RID data and the ground-truth GPS data recorded onboard the aircraft.

The Mavic 2 Zoom demonstrated exceptionally high positional accuracy, with mean errors below 0.05 ft and minimal variation across all tested distances. This near-perfect agreement is expected, as both the broadcasted RID data and flight logs are generated from the same onboard GPS source. For the Mavic 2 Enterprise, the DB120 Wi-Fi module shows the lowest positional error among external modules, with consistently small standard deviations. The slightly higher mean error compared to the Mavic 2 Zoom reflects the use of separate GPS systems between the RID module and the aircraft’s internal navigation unit. The DB120 BLE module showed larger errors, averaging around 14 ft, but remained consistent across distances, as indicated by its low standard deviation (less than 1 ft). For the DJI Matrice 600, the results revealed the largest errors and variability, particularly when using the Dronetag BLE module, where position error reached up to 60 ft with standard deviations exceeding 30 ft. This inconsistency is likely due to the aircraft’s larger frame and complex structure, which have introduced signal interference or reduced GPS accuracy depending on the RID module placement. Overall, all tested systems achieved acceptable positional accuracy within the small-UAS horizontal separation ranges, with smaller multirotor platforms exhibiting superior consistency compared to the larger Matrice platform.

Table 2-22: Mean and standard deviation of horizontal position error (in feet) for different aircraft – RID (WiFi) module configurations across varying distances.

Aircraft	Mavic 2 Zoom		Mavic 2 Enterprise		DJI Matrice 600	
RID Module	Standard WiFi		DB120 WiFi		DB120 WiFi	
Horizontal distance (ft)	Mean (ft)	Std (ft)	Mean (ft)	Std (ft)	Mean (ft)	Std (ft)
100	0.03	0.02	4.95	1.02	NA	NA
200	0.03	0.02	5.75	2.09	20.11	11.20
300	0.04	0.02	6.27	0.59	14.40	3.42

400	0.04	0.03	6.85	1.09	7.79	4.14
500	NA	NA	NA	NA	10.15	4.23
600	NA	NA	NA	NA	9.02	4.81

Table 2-23: Mean and standard deviation of horizontal position error (in feet) for different aircraft – RID (BLE) module configurations across varying distances.

Aircraft	Mavic 2 Enterprise				DJI Matrice 600			
	DB120 BLE		Dronetag BLE		DB120 BLE		Dronetag BLE	
	Mean (ft)	Std (ft)	Mean (ft)	Std (ft)	Mean (ft)	Std (ft)	Mean (ft)	Std (ft)
100	13.58	0.97	7.086	2.94	NA	NA	NA	NA
200	14.50	0.98	9.33	3.44	22.11	3.96	40.66	29.08
300	14.34	1.08	8.66	2.40	19.55	0.95	55.94	12.05
400	14.06	0.65	8.07	3.28	17.03	5.30	31.40	11.36
500	NA	NA	NA	NA	18.37	1.83	46.01	5.28
600	NA	NA	NA	NA	15.71	1.34	57.98	12.23

Dynamic tests were

flight

conducted to evaluate RID performance while the aircraft was in motion, following a straight outbound–inbound flight path extending to 600 ft from the RID receiver. Each aircraft flew at constant speeds of 5, 10, 15, and 20 m/s (20 m/s speed point was not included for DJI Matrice 600, its maximum speed around 18 m/s), while continuously broadcasting RID messages. The horizontal position accuracy results in Table 2-24 and Table 2-25 were computed by comparing the latitude and longitude broadcasted by the RID modules with the aircraft flight log data at identical timestamps. However, unlike the stationary tests, motion introduces a temporal offset between broadcast and log recordings due to transmission delay and GPS update latency, which naturally increases the apparent position error.

The Mavic 2 Zoom, using its standard Wi-Fi RID, maintained the smallest mean positional errors among all systems across speed profiles, with values increasing gradually from approximately 2 ft at 5 m/s to 7.5 ft at 20 m/s. The Mavic 2 Enterprise displayed a similar trend, with the DB120 Wi-Fi module producing the most consistent results (mean errors below 25 ft). The DB120 BLE module also performed reasonably well, maintaining similar error magnitudes, though slightly higher and more variable than the Wi-Fi configuration.

Further inspection of the broadcast data revealed that for the DB120 BLE, although the nominal broadcast rate is 3 Hz, many packets transmitted within the same one-second interval contained identical position values, resulting in repeated rather than updated positional information. This duplication reduced the effective update frequency of position data and contributed to moderate increases in positional error. In theory, a 3 Hz broadcast rate with truly updated packets could improve positional accuracy; however, this benefit was not realized in the observed data because of repeated broadcasts.

For the Dronetag BLE, an additional behavior was observed where identical position values were broadcast across multiple successive seconds (up to 4–5 s) while the aircraft was in motion. This extended duplication caused more pronounced horizontal position errors, particularly at higher speeds where the aircraft traveled significant distances before transmitting a new position update.

The DJI Matrice 600 results were broadly consistent with those of the Mavic 2 Enterprise, showing moderate increases in mean position error with speed, but without extreme increases in the position errors. The variation among its RID configurations followed similar patterns, Wi-Fi modules providing slightly smaller errors than BLE modules, though the overall accuracy remained comparable to that of the smaller platforms.

In summary, while all configurations exhibited increasing positional error with speed, the results demonstrate that both Wi-Fi and BLE RID modules maintained practical positional accuracy within the short-range flight test envelope. Observed differences were primarily attributed to packet update behavior and data duplication rather than inherent differences in radio protocol, except for the Dronetag BLE, which consistently showed prolonged repetition of identical position data over several seconds, leading to notably higher positional errors at all speed points.

Table 2-24: Mean and standard deviation of horizontal position error (in feet) for different aircraft – RID (WiFi) module configurations across varying speeds.

Aircraft	Mavic 2 Zoom		Mavic 2 Enterprise		DJI Matrice 600	
RID Module	Standard WiFi		DB120 WiFi		DB120 WiFi	
Speed (m/s)	Mean (ft)	Std (ft)	Mean (ft)	Std (ft)	Mean (ft)	Std (ft)
5	2.02	2.45	11.15	3.21	12.97	3.72
10	4.51	4.19	14.16	4.73	26.25	8.95
15	5.76	6.16	17.94	5.93	28.66	13.50

20	7.52	7.78	23.69	6.94	NA	NA
-----------	-------------	-------------	--------------	-------------	----	----

Table 2-25: Mean and standard deviation of horizontal position error (in feet) for different aircraft – RID (BLE) module configurations across varying speeds.

Aircraft	Mavic 2 Enterprise				DJI Matrice 600			
	DB120 BLE		Dronetag BLE		DB120 BLE		Dronetag BLE	
Speed (m/s)	Mean (ft)	Std (ft)	Mean (ft)	Std (ft)	Mean (ft)	Std (ft)	Mean (ft)	Std (ft)
5	11.48	2.98	45.15	32.6	11.56	7.26	62.17	43.69
10	18.67	7.52	84.59	71.8	13.70	6.63	76.89	50.43
15	25.37	13.15	154.7	143.5	29.22	19.5	120.9	129.0
20	30.04	15.18	256.2	209.9	NA	NA	NA	NA

2.2.2.3.2 RID Detection Range Results

This part of the results presents and discusses the performance of the RID modules at horizontal distances that cover the MDD ranges resulted the encounter simulation. The results are based on two flight test profiles, a) stationary test, where the aircraft hovered at fixed horizontal separation distances ranging from 500 ft to 4000 ft in 500-ft increments, b) dynamic test, where the aircraft flew outbound from the receiver to a 5000-ft horizontal distance at a constant speed of 18 m/s, the same speed used in the simulation scenario for the intruder model, and then returned along the same path.

Both test profiles were performed using two aircraft:

- The Mavic 2 Zoom, equipped with the standard built-in Wi-Fi RID module.
- The Mavic 2 Enterprise, used to evaluate three external RID modules: DB120 (Wi-Fi), DB120 (BLE), and Dronetag (BLE).

Table 2-26 presents the hovering duration at each distance and the corresponding number of RID packets received. The packet reception rate (in Hz) was calculated as the ratio of the total received packets to the hovering time, as shown in Figure 2.28. The standard RID on the Mavic

2 Zoom demonstrated consistent performance across all tested distances, maintaining a reception rate above 0.8 Hz up to 3000 ft and decreasing slightly to 0.6 Hz at 4000 ft. Given that the broadcast rate of the standard RID is 1 Hz, this indicates that the receiver successfully detected more than 60% of the transmitted packets even at the farthest distance. Thus, the standard RID can be considered detectable with a probability greater than 0.6 at 4000 ft.

For the Wi-Fi-based DB120 module, broadcast at 1 Hz, the reception rate remained relatively low but stable, approximately 0.3 Hz across all distances, indicating a consistent, though less frequent, detection capability. This suggests that the DB120 (Wi-Fi) module provides longer detection range but with a low probability of packet reception. In the case of the DB120 (BLE), which broadcasts at a higher rate of 3 Hz, the reception rate exceeded 1.5 Hz up to 2000 ft but declined to 0.5 Hz at 2500 ft and dropped to zero beyond that distance. This pattern indicates that while the higher broadcast rate improves detection at shorter ranges, it does not extend the effective detection distance. The maximum detection range for the DB120 (BLE) was therefore around 2500 ft, with an estimated detection probability of 0.5.

The Dronetag (BLE) module exhibited the shortest effective detection range, maintaining a reception rate of 0.6 Hz at 500 ft and decreasing to 0.2 Hz at 1000 ft, with no packets received beyond that point. This behavior highlights the limited detection capability of the Dronetag BLE system, constrained to about 1000 ft with a detection probability near 0.2.

In this analysis, the detection probability was computed as the ratio of the observed reception rate to the known broadcast rate of each RID module, representing the proportion of successfully received packets relative to those transmitted.

Table 2-26: Hover time and total number of received RID packets for each aircraft–RID module configuration across horizontal separation distances.

Aircraft	Mavic 2 Zoom		Mavic 2 Enterprise					
	Standard WiFi		DB120 WiFi		DB120 BLE		Dronetag BLE	
RID Module								
Horizontal distance (ft)	Time (s)	Num pkt	Time (s)	Num pkt	Time (s)	Num pkt	Time (s)	Num pkt
500	63	69	70	23	70	143	61	33
1000	63	51	65	18	66	121	62	12
1500	61	52	62	6	70	130	60	0
2000	62	48	62	17	66	104	64	0
2500	69	52	64	17	70	35	60	0
3000	64	54	78	23	60	0	60	0
3500	64	46	61	16	60	0	60	0
4000	83	54	62	5	60	0	60	0

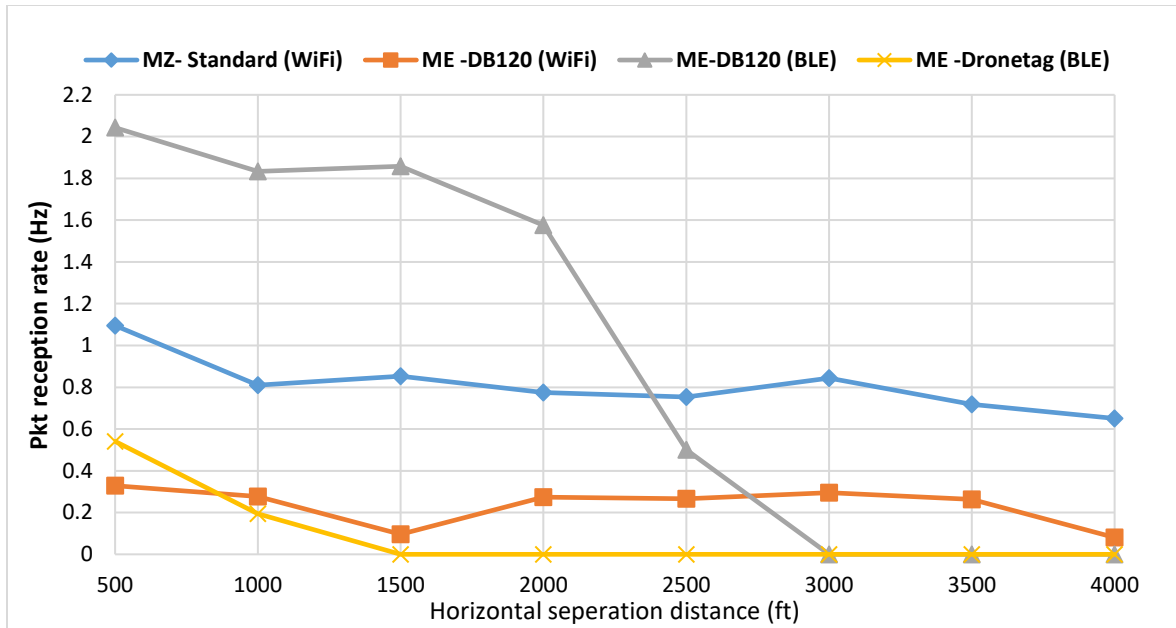


Figure 2.28: Packet reception rate (Hz) versus horizontal distance for all RID module configurations.

Upon examining the received packets in more detail, repeated position reports were observed, indicating that the modules transmitted duplicate packets across consecutive seconds without updating their positional data. To quantify this effect, duplicate packets were removed, and the RID update rate, representing the true frequency of new position reports, was computed.

Table 2-27 contains the hovering time and the number of updated RID packets, those that are not duplicates, for each RID module and Figure 2.29 presents the update rate, calculated as the number of updated packets divided by the hovering time. From the tables and figures, the standard Wi-Fi RID on the Mavic 2 Zoom shows a slight decrease in update rate compared to its reception rate. Fewer than five duplicate packets were observed at each distance, implying that the RID module was broadcasting new positional information approximately in each packet. For the DB120 (Wi-Fi) module, no duplicate packets were identified; all received packets carried updated position data. This indicates that the module maintained steady positional reporting throughout the hovering tests, with each transmission reflecting a new location.

In contrast, the DB120 (BLE) module produced a high number of duplicate packets, more than two-thirds of all received packets. Given its 3 Hz broadcast rate, this module was expected to transmit three dynamic RID packets per second, each containing updated position information. However, many of these packets were redundant, leading to an effective update rate below 1 Hz. Although the higher broadcast rate contributed to a stronger detection probability at shorter ranges, it did not improve positional update performance.

The Dronetag (BLE) module also exhibited a considerable number of duplicate packets, more than ten duplicates or roughly one-third of all received packets at each distance. This outcome reflects the module's limited performance both in detection range and in position update frequency, resulting in fewer unique position reports and overall reduced reliability compared to the other modules.

Table 2-27: Hover time and number of unique (non-duplicate) RID packets for each aircraft–RID module configuration across horizontal separation distances

Aircraft	Mavic 2 Zoom		Mavic 2 Enterprise					
	Standard WiFi		DB120 WiFi		DB120 BLE		Dronetag BLE	
Horizontal distance (ft)	Time (s)	Num pkt	Time (s)	Num pkt	Time (s)	Num pkt	Time (s)	Num pkt
500	63	58	70	23	70	65	61	22
1000	63	48	65	18	66	55	62	10
1500	61	49	62	6	70	44	60	0
2000	62	48	62	17	66	46	64	0
2500	69	52	64	17	70	22	60	0
3000	64	52	78	23	60	0	60	0
3500	64	44	61	16	60	0	60	0
4000	83	51	62	5	60	0	60	0

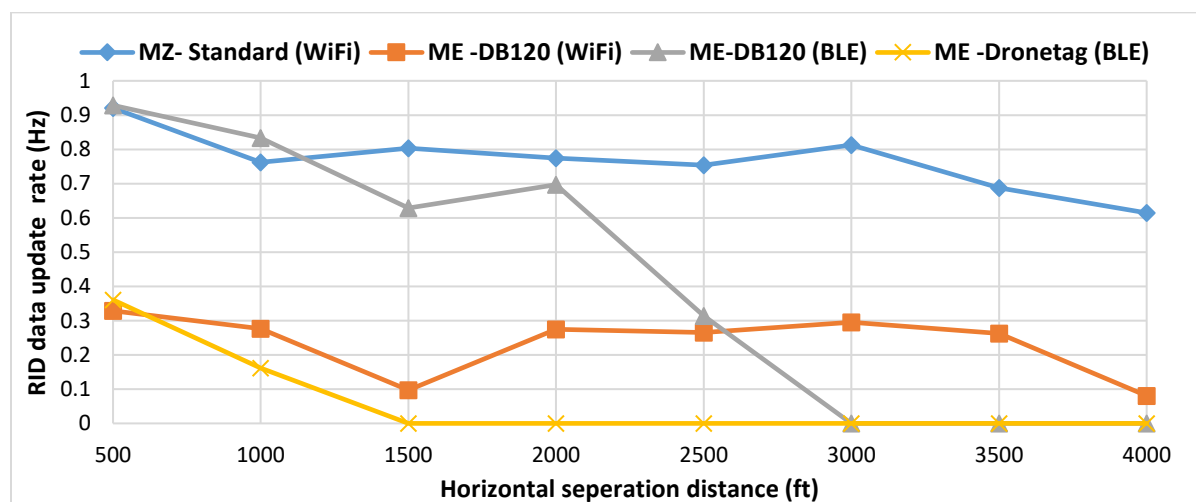


Figure 2.29: RID packet update rate (Hz) versus horizontal distance for all RID modules.

The dynamic profile tests include two parts, inbound and outbound direction, where inbound the intruder aircraft flies away from the RID receiver location, while inbound direction the intruder flies toward the RID receiver. In the analysis the focus is only on the inbound flight profile, which represents more realistic encounter scenario. When the aircraft flies away from the ownship, it poses no immediate risk, where the inbound trajectory is more critical from timely detection and situational awareness.

During the inbound flight, the aircraft flew from 5000 ft toward the receiver, and the distance was divided into 500 ft segments (5000, 4000, 3500, 3000, 2500, 2000, 1500, 1000, 500 ft). For each segment, the travel time and the number of received RID packets were recorded and shown in Table 2-28 and the packet reception rate (Hz) was computed and illustrated in Figure 2.30 Figure .

The Wi-Fi modules, both the standard RID on the Mavic 2 Zoom and the DB120, showed stable reception rates in the range of 0.9 to 1 Hz, consistent with their 1 Hz broadcast rate. Detection remained reliable up to 2500 ft for both modules. Beyond that point, the DB120 Wi-Fi exhibited a noticeable decline in signal quality, although it remained detectable through the remainder of the inbound flight. In contrast, the standard Wi-Fi RID maintained a strong reception rate close to 1 Hz up to 4000 ft, with degradation only at 5000 ft, yet still at a detectable level.

In contrast to the Wi-Fi performance, the Bluetooth modules exhibited noticeably weaker results. Although the DB120 BLE broadcasts at 3 Hz, higher than the Wi-Fi modules, its advantage was only evident at short ranges: packet reception exceeded 2 Hz up to 2000 ft. Beyond 2500 ft, the signal quality degrades rapidly, and no packets were received. The Dronetag BLE module showed the poorest performance overall. Packet reception was sporadic and unstable even at shorter ranges and was only intermittently detectable up to 2000 ft, after which the signal was completely lost.

Table 2-28: Inbound flight results showing segment travel time and number of received RID packets.

Aircraft	Mavic 2 Zoom		Mavic 2 Enterprise					
RID Module	Standard WiFi		DB120 WiFi		DB120 BLE		Dronetag BLE	
Horizontal distance (ft)	Time (s)	Num pkt	Time (s)	Num pkt	Time (s)	Num pkt	Time (s)	Num pkt
500	8	8	8	8	8	18	8	10
1000	8	7	8	7	7	15	8	0
1500	8	7	9	9	8	8	8	3
2000	7	7	7	6	7	4	8	4
2500	8	8	7	7	7	0	8	1
3000	7	7	8	4	8	0	8	0
3500	9	9	8	1	7	0	8	0
4000	8	8	8	1	7	0	8	0
5000	16	5	16	1	16	2	17	0

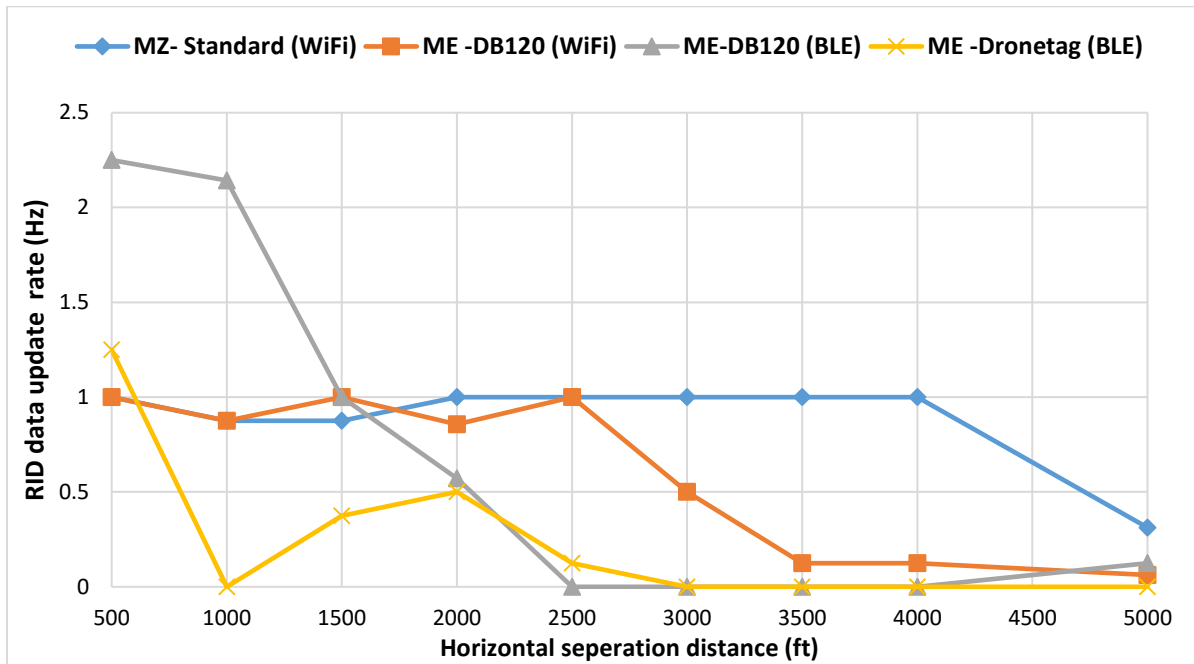


Figure 2.30: Packet reception rate versus horizontal distances during the inbound flight profile.

After examining the total packet reception rate, further analysis of the RID packet update rate was conducted, which was computed as the number of unique RID packets (i.e., packets reporting a new position rather than duplicating the previous one) divided by the time spent traveling each distance segment.

A comparison between the received-packet rate and the update-packet rate reveals a clear distinction between Wi-Fi and Bluetooth RID modules. For both Wi-Fi modules, the Standard Wi-Fi RID and the DB120 Wi-Fi, the update rate was effectively identical to the received rate across all distance segments, indicating that every received packet corresponded to a new positional update rather than a repeated message. This behavior is evident in Table 2.2929 **Error! Reference source not found.** which lists the number of unique packets at each horizontal separation: the counts match the total number of packets received for both Wi-Fi systems at all distances. In contrast, the Bluetooth-based modules exhibited substantial packet duplication, leading to update rates that were consistently lower than their received-packet rates. The DB120 BLE produced significantly fewer unique packets than total received packets at short ranges, and no position updates beyond 2500 ft, while the Dronetag BLE showed minimal unique packets even at short distances, with no updated packets detected beyond 2000 ft. These results indicate that, unlike Wi-Fi modules, Bluetooth RID devices did not maintain continuous positional refresh and therefore provided limited situational awareness in fast-closing encounter scenarios.

Table 2.2929: Inbound flight results showing segment travel time and number of received RID packets

Aircraft	Mavic 2 Zoom	Mavic 2 Enterprise		
RID Module	Standard WiFi	DB120 WiFi	DB120 BLE	Dronetag BLE

Horizontal distance (ft)	Time (s)	Num pkt						
500	8	8	8	8	8	8	8	5
1000	8	7	8	7	7	6	8	0
1500	8	7	9	9	8	7	8	3
2000	7	7	7	6	7	4	8	4
2500	8	8	7	7	7	0	8	1
3000	7	7	8	4	8	0	8	0
3500	9	9	8	1	7	0	8	0
4000	8	8	8	1	7	0	8	0
5000	16	5	16	1	16	2	17	0

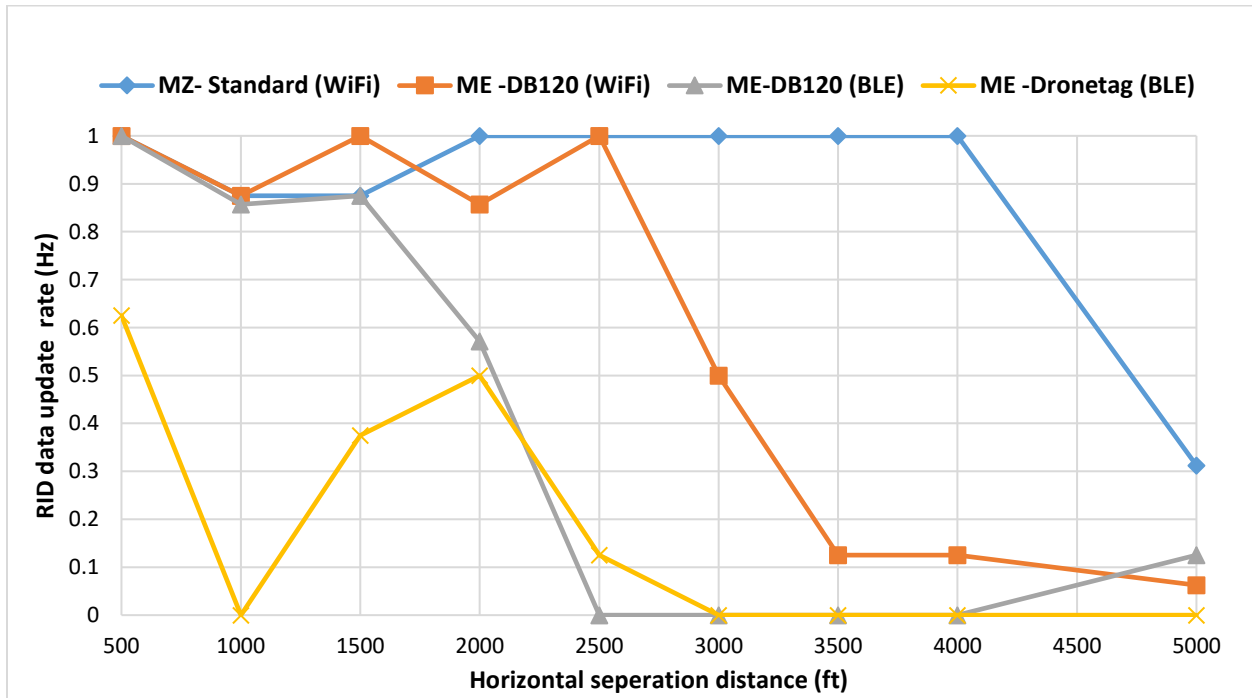


Figure 2.31: RID packet update rate versus horizontal distances during the inbound flight profile.

2.2.2.3.3 sUAS-sUAS horizontal well clear separation: A brief assessment

Error! Reference source not found. attempts to provide a concise comparison between the RID communication capabilities and the detection distances needed to allow well clear separation between sUAS. The top part of **Error! Reference source not found.** replicates the detection distances needed to allow WC separation between sUAS for six horizontal well clear definitions. The detection distances needed for 50% and 100% of the encounters to be well clear at three

different intruder speeds are presented. These detection distances are obtained as discussed in Section 2.2.1.3.1.2 and using the avoidance algorithm tuning discussed in that section (i.e., σ is set equal to the well clear distance plus 50).

The bottom part of **Error! Reference source not found.** lists the four RID equipment tested in this work. The first column of the bottom part of the table lists the maximum communication range at which each of the RID equipment showed at least 0.8 Hz data update rate. These values are obtained from Figure 2.31 in section 2.2.2.3.2. (Note: the RID standards use 1 Hz message update rate. The analysis in Table 2-30 allowed this update rate to be relaxed a little bit to 0.8 Hz.).

The right six columns of the bottom part of **Error! Reference source not found.** identify the maximum horizontal well clear definition that can be supported by each RID device (for the three different intruder sUAS speeds and the two percentages of well clear encounters). For example, for Standard WiFi, the table lists that the device allowed up to 4000 ft communication at 0.8 Hz. This 4000 ft communication range is compared to the detection ranges presented in the top part of the table. It was observed that the 4000 ft communication range supported up to 600 ft horizontal well clear separation for all columns in **Error! Reference source not found.**. The same process is repeated for each RID equipment.

Table 2-30: sUAS-sUAS horizontal well clear separation: A brief assessment

Intruder Speed →	45 ft/s		60 ft/s		90 ft/s	
Percentage of encounters being WC →	50%	100%	50%	100%	50%	100%
100 ft WC	450	1050	550	1300	800	1700
200 ft WC	625	1300	750	1600	1100	2050
300 ft WC	775	1500	900	1800	1350	2300
400 ft WC	900	1650	1100	2150	1600	2750
500 ft WC	1025	1800	1250	2350	1800	3000
600 ft WC	1175	1950	1400	2500	2150	3150
RID Equipment (Max. 0.8 Hz comms. range)	Maximum WC volume that can be supported (ft)					
Standard WiFi (up to 4000 ft)	600	600	600	600	600	600
DB120 WiFi (up to 2500 ft)	600	600	600	600	600	300
DB120 BLE (up to 1500 ft)	600	300	600	100	300	None
Dronetag BLE (up to 500 ft)	100	None	None	None	None	None

2.2.2.4 Task Conclusions

The results of this task directly address the primary research question: What horizontal separation requirement is needed for BVLOS sUAS to remain well clear from another sUAS that broadcasts its RID, given the actual broadcast performance of current RID systems?

Based on the measured broadcast and position-update performance of the evaluated RID systems, maintaining WC separation between two sUAS at horizontal ranges of 100–600 ft is feasible, but the success level depends strongly on the type of RID module and the avoidance algorithm used as follow:

- Using the stronger avoidance algorithm, WC was maintained at least 50% of the time across the entire 100–600 ft separation envelope when either the standard Wi-Fi RID system or the out-module Wi-Fi RID system was used, also when using the DB 120 BLE module.
- When only the basic avoidance algorithm is used, the performance differs by system type:
 - The Wi-Fi-based RID systems meet the 50% WC requirement across the full 100–600 ft separation band for all intruder speeds, demonstrating enough detection and positional fidelity for basic avoidance logic.
 - In contrast, the BLE module supports WC only in the 100–300 ft range when paired with the basic avoidance algorithm, and its performance deteriorates at 400 - 600 ft ranges, where it can no longer reliably sustain WC without enhanced avoidance logic.
- With respect to 100% WC maintenance, the standard Wi-Fi RID system achieves full WC performance across 100–600 ft under both the basic and the stronger avoidance algorithms and for all intruder speeds.
- The out-module Wi-Fi RID system can maintain 100% WC across 100–600 ft, but only when the stronger avoidance algorithm is used; under the basic algorithm its performance is insufficient to maintain WC at all separation distances.
- The BLE RID module can maintain 100% WC only across 100–300 ft, and only when paired with the stronger avoidance algorithm; with the basic algorithm it cannot meet the 100% WC requirement over any full separation range.

In addition, these results provide insights toward the secondary research question: Do the current ASTM RID broadcast minimum performance requirements meet the performance necessary for sUAS-to-sUAS DAA?

- The RID configurations that successfully supported both 100% WC and 50% WC across the 100–600 ft horizontal separation region were the standard RID Wi-Fi module and the Wi-Fi RID out module. Both operated at the ASTM-compliant 1 Hz broadcast rate, but importantly, both transmitted at broadcast power levels noticeably above the ASTM minimum, which specifies approximately +11 dBm for 2.4 GHz Wi-Fi/Bluetooth and +3 dBm for 5 GHz Wi-Fi. In comparison, the standard RID transmitted at +26 dBm and the OEM Wi-Fi RID at +18 dBm.
- Both operated at the ASTM-compliant 1 Hz broadcast rate, but importantly, both transmitted at broadcast power levels noticeably above the ASTM minimum, which specifies approximately +11 dBm for 2.4 GHz Wi-Fi/Bluetooth and +3 dBm for 5 GHz Wi-Fi. In comparison, the standard RID transmitted at +26 dBm and the OEM Wi-Fi RID at +18 dBm.
- The Bluetooth -based modules, the distinctions were more pronounced. The DB120 BLE, operating at 3 Hz and +18 dBm, enabled 50% WC performance across 100–600 ft, and 100% WC performance across 100–400 ft, but it was unable to sustain 100% WC performance across the full WC envelope. Meanwhile, the Bluetooth module configured at 1 Hz and +8 dBm, though technically operating near the ASTM minimum, performed substantially below the other devices and only achieved 50% WC in the limited 100–200 ft separation range.

- The results do not yet allow a definitive assessment of whether the ASTM minimum broadcast requirements are sufficient for sUAS-to-sUAS DAA across all operational conditions. The RID modules used in this study did not allow full control over rate and power configurations. Therefore, additional testing with configurable RID systems where broadcast rate and power can be systematically varied and evaluated across different hardware platforms is required to fully determine the RID performance envelope needed to reliably support sUAS-to-sUAS DAA.

All results reported in this section were obtained under semi-controlled flight-test conditions. The campaigns were executed in an open rural environment with a clear line-of-sight between the aircraft and the ground-based RID receiver, minimal RF activity in the surrounding area, and no intentional physical obstructions. The use of a stationary ground receiver ensured that variations in packet reception and update rate were driven by the RID modules and aircraft dynamics rather than by receiver motion. Throughout testing, each RID device operated as installed on the aircraft without external amplifiers or antennas, reflecting its native broadcast capability. The controlled setting therefore enabled direct observation of module-level performance characteristics under clean channel conditions, without the influence of urban congestion or indoor attenuation.

3 CONCLUSIONS AND RECOMMENDATIONS

The ASSURE A68 project was initiated to assess the current sUAS WC separation criteria, defined in ASTM F3442/F3442M-23 as a 2,000-ft horizontal and 250-ft vertical volume. These criteria were originally developed using unmitigated encounter analysis, simplified assumptions, and limited operational data. As sUAS operations expand into BVLOS missions, low-altitude environments, and UTM ecosystems, a more rigorous assessment is needed.

A68 conducted a multi-faceted evaluation of WC that included:

1. Large-scale encounter model simulations to characterize MAC risk under alternative WC volumes,
2. Right of Way quantification through flight testing and VR experiments,
3. RID field evaluations to assess surveillance accuracy and update rates for sUAS-sUAS separation, and
4. UTM field testing to assess network-supported separation services, surveillance limitations, and multi-aircraft management.

This project offers the most complete evaluation to date of whether the existing ASTM F3442/F3442M-23 WC criteria remain appropriate for current NAS-representative sUAS operations. The following sections summarize the project-level conclusions by directly addressing the research questions established at project outset. The findings inform recommended updates to WC separation distances, highlight conditions under which surveillance performance constrain safety, and identify operational factors that must be considered when defining WC for both sUAS-manned aircraft and sUAS-sUAS interactions.

3.1 sUAS-MA Separation

This section outlines the project’s research questions for sUAS-MA interactions and addresses them based on the tasks’ main takeaways and the team’s reasoning and expertise:

1. *How do different DAA Well-Clear requirements (WCRs) impact collisions likelihood for UAS equipped with DAA?*

Across more than three million Monte-Carlo simulations, the project revealed that:

- Moderate reduction to the horizontal WC distance from 2000 ft to 1500 ft results in:
 - Only small increases in NMAC Risk Ratio (NMAC-RR) and LoWC Ratio (LoWCR),
 - Mid-Air Collision (MAC) probabilities remain comparable to the current ASTM standards when adequate surveillance performance is available, and
 - Safety metrics remain within ASTM thresholds for cooperative encounter models
 - For non-cooperative encounters, a 1500 ft horizontal WC remains viable only when sensor performance (range, track quality, coverage) is sufficient.
- ➔ Collision Likelihood remains within ASTM safety thresholds for a 1500 ft horizontal WC, for both cooperative and non-cooperative cases, under adequate and reliable sensor performance.

2. *Concerning the proposed ASTM criteria (2000' horizontal, 250' vertical), is the vertical distance sufficient? Can the horizontal distance be reduced? Are the proposed distances sized correctly to 1) not interfere with manned operations while also balancing 2) the industry desire to reduce surveillance range if it is safe to do so? Are different well clear distances recommended based on the equipage of the crewed aircraft?*

- Vertical separation (250 ft):
 - RoW VR simulations for a larger Group 3 UAS identify a vertical RoW impact at ~281ft (the distance at which 25% of the pilots begin to express a desire to maneuver and hence, feel their RoW is impacted). This supports retaining 250 ft as an adequate vertical WC separation for smaller (Group 1 and 2) UAS.
- ➔ Yes, the vertical distance is sufficient and no reduction in the vertical WC separation is recommended based on the results obtained from the VR test.

- Horizontal Separation (2000 ft):

Evidence from all tasks converges around 1500 ft as the minimum safe candidate for reducing WC horizontal separation:

- From RoW testing and based upon a 25% maneuver-desired threshold, the horizontal well clear threshold for sUAS could be reduced from 2000 ft to 1500 ft, further supported by the use of a larger Group 3 UAS in these tests:
 - For daytime testing, including latency impacts suggests 2000 ft may be better. However, no maneuver-strongly-desired events happened at distances ≥ 1500 ft (maximum maneuver-strongly-desired distance is < 1000 ft).
 - VR simulations support a 1500 ft threshold even when including latency.

- Nighttime results indicate RoW impacts at much larger distances owing to the increased perception of risk (larger aircraft, apparent conflict owing to lighting).
 - UTM based horizontal separation services maintained WC only when the system could detect the manned aircraft at or beyond the minimum required detection distances identified in simulation and verified in flight tests.
 - In the simulation, a 1500 ft horizontal well clear separation required 1000 to 2250 ft smaller detection distances than the 2000 ft horizontal well clear separation
 - In several real-world encounters, maintaining WC required up to twice the modeled detection distance, due to setup inaccuracies, GPS biases, and wind effects—indicating that detection range performance is the limiting factor in safely reducing WC distance.
 - Position errors from radar or ADS-B feeds must remain small relative to the WC boundary. Large (~500-ft) radar errors observed in testing could produce WC violations unless operators used a larger commanded separation to compensate.
- ➔ Although 1500 ft separation appears safe across most scenarios, *the controlling variable is surveillance performance*. The 1500-ft reduced horizontal separation inherently reduces the required surveillance range, thereby aligning with industry’s desire to reduce sensor and integration burdens. However, the WC reduction is safe only when the surveillance/UTM system reliably meets specific minimum detection distance thresholds. If sensors or UTM information services cannot consistently meet these thresholds, then a reduced 1500-ft WC would not be reasonable.

To maintain the highest levels of safety, the recommendation is to maintain the larger 2000’ horizontal dimension, unless it poses a significant operational efficiency burdens where a reduction to 1,500 ft may be appropriate. In such a case, it is essential to define the minimum detection range at which the surveillance sensor can *reliably* detect the intruder at the reduced WC boundary.

- Should WC differ based on MA equipage?

It is important to remember that WC is fundamentally an expression of risk. From Part 91, it is a human-perceived expression of RoW impact that inherently includes risk in that a pilot determines that aircraft are too close (if a RoW impact occurs). The subjective nature of this risk expression driven by human judgement can be removed through efforts such as the simulation efforts executed in this project.

- From a technical-design perspective to maneuver as to not interfere, WC may vary based on MA equipage:
 - Since sensor tracking range is not a limiting factor for avoiding cooperative traffic, reducing cooperative WC from 2000 ft to 1500 ft would not benefit sensor design and integration as it would for non-cooperative sensors that track non-cooperative aircraft. To maintain the highest levels of safety with minimal impact on operational efficiency, the recommendation is to retain the 2,000-ft well-clear distance for cooperative encounters. Cooperative aircraft also tend to operate at higher speeds,

which provides an additional rationale for maintaining a larger standoff distance when this does not create significant operational burdens. For non-cooperative encounters, allowing a reduction to 1,500- ft may be reasonable, provided it is accompanied by clearly defined minimum surveillance performance requirements

3. *What factors should be considered when assessing and validating proposed WCRs? Which factors are most important?*

Assessment and validation of proposed WCRs should be consistent with them fundamentally being an expression of risk. To do this, as indicated in the response to the previous question, that risk can be evaluated in two complementary ways: through human-based assessments of right-of-way impact—since WC originates from pilot perceptions of when aircraft are “too close”—and through objective encounter simulations that quantify MAC and NMAC probability and both approaches were used in this project

- Pilot RoW behavior
 - Maneuver-desired thresholds
 - Visual acquisition probability
- Encounter geometry
 - Head-on vs overtaking
 - Closure rate
- UAS category and size, which influence visual acquisition
- Operational context
 - Day vs night
 - High traffic density
 - BVLOS conditions
 - Environmental winds
- Maneuvering Variables (UA)
 - Speed
 - Turn rate
 - Algorithm for determining maneuvers

These factors are generally identified owing to their impact on human perception of risk/RoW impact, with the latter (maneuver variables) capturing variables that impact closest point of approach values owing to the maneuver characteristics of the UAS (mitigated risk evaluation). It is noted that environmental winds is listed because these can significantly impact the ability of a UAS to increase separation relative to an MA (mitigated risk evaluation).

Additional variables that impact performance relative to WC include:

- Surveillance performance
 - Detection range
 - Track accuracy
 - Latency
 - Coverage continuity
- DAA systems capability
 - Alert timing
 - Avoidance effectiveness

- Sensor biases and navigation uncertainty
- Environmental conditions
 - Clutter
 - Environmental winds

Most influential Factors:

- The main safety factor to consider with any WC volume is the effect on MAC risk. That is the ultimate safety goal. Therefore, any proposed WC volume should include evaluations of MAC and NMAC risk ratio effects.
- The WC volume should also be evaluated for RoW impact thresholds (what pilots perceive as unsafe), so that sUAS operations do not interfere with other operations that have the RoW. This does have the challenge of including subjectivity.
- From the above list, highly influential factors include:
 - UAS category and size (from RoW testing)
 - Operational context—night vs. day (from RoW testing)
- While Monte Carlo simulations included encounter geometries from all approach angles, encounter geometry, from the standpoint of horizontal collision vs. not, is likely to have an important impact on RoW. This was not evaluated in this project.

4. *What data elements are needed for information that is presented to a remote pilot to be useable for decision making when a pilot maneuvers to remain well clear?*

Evaluation of RoW impacts within this effort did not include maneuvering of UAS. To evaluate RoW impacts, aircraft were flown along linear trajectories that produced decreasing horizontal separations with a vertical offset for safety. Thus, remote pilots did not have to evaluate potential conflicts and execute maneuvers. However, previous research has considered the major steps associated with DAA. For instance, Askelson et al. (2017) decomposed DAA into four steps: Detect, Track, Evaluate, and Maneuver. Assuming BVLOS conditions, a remote pilot can play a role in the Track, Evaluate, and Maneuver steps. However, many effective techniques exist for establishing tracks and, thus, a pilot is most likely to play a key role in the Evaluate and Maneuver steps.² To properly perform those steps, the pilot needs to determine if a conflict exists (Evaluate) and, if so, do something about it (Maneuver). To properly evaluate if a conflict exists, information regarding the relative positions of ownship and intruders and information regarding where these aircraft are headed is required. This information can be provided in a variety of ways, including two-dimensional plan views and three-dimensional perspective views. To the team’s knowledge, a comprehensive study of all approaches to presenting this information has not been executed. However, both experience and approaches used by Air Traffic Control (ATC) indicate that two-dimensional displays that clearly indicate aircraft identity (e.g., ownship vs. intruder), aircraft headings/expected tracks, and aircraft altitudes can be very effective. In addition, those who have created such displays have provided recommended maneuver directions, as not all maneuvers are

² An exception could be highly cluttered environments where automated methods struggle to successfully remove clutter. In that case, a human could be more effective at visually estimating aircraft tracks.

created equally (e.g., Theisen et al. 2017). This can be effective in maximizing aircraft separation.

5. *What is the performance of on-board pilots to remain well clear of other aircraft that have the right-of-way?*

The right-of-way task results indicate that:

- Daytime visual acquisition of sUAS was extremely low (~0%) without position cueing
 - Nighttime visual acquisition was 100% with proper lighting (flashing strobe and a red-green light pair on the wings)
 - VR simulations showed a 98.4% detection rate supported by the use of a larger Group 3 UAS and the lack of additional pilot duties
 - Median maneuver distance for VR co-altitude encounters was ~1285 ft
 - No strong dependence on closure rate or encounter angle (0° vs 315°)
- Onboard pilot performance is highly dependent on visibility and aircraft size. For small UAS, relying on pilot visual acquisition alone is often insufficient, as visual acquisition of such aircraft is very difficult (Snyder, et al., 2024). DAA or cooperative surveillance is essential.

6. *The BVLOS ARC report recommends that non-cooperative aircraft below 500' AGL give way to BVLOS drones. How well can an onboard pilot using see-and-avoid do this for different manned low altitude operations? What are estimated probability of visual acquisition at range and example closest points of approach when trying to give way to a small or medium drone? Do lights or paint schemes help at all during the day?*

- Visual acquisition
 - Daytime: Almost 0% for sUAS unless given a position cue.
 - Nighttime: 100% with lighting for the sUAS used in tests.
 - High visual acquisition rate (98.4%) for VR simulations driven by size of UAS (Group 3) and lack of additional pilot duties
- CPA observations
 - Maneuver-strongly-desired distances were always < 1000 ft.
 - No strong RoW-impact events beyond 1500 ft.
 - These values are not CPA values, however, and indicate RoW impacts in daytime testing.
- Effects of lighting/conspicuity
 - Lighting dramatically increases detectability at night.
 - Daytime detection remains extremely poor even with lighting or paint—visual contrast is insufficient for small UAS.
- Visual acquisition as a function of range
 - VR tests at 0 ft vertical separation had a mean visual acquisition distance of ~1497 ft.
 - A group 3 UAS was used in VR tests.
 - No other pilot duties were present in VR tests.
 - Above factors indicate that an onboard pilot would, on average, visually acquire a small UAS at distances < ~1500 ft, which is the recommended WC boundary based upon

simulation and RoW impact results. Thus, the closest points of approach would generally be within the WC boundary. This is exacerbated by the likelihood that an onboard pilot typically would not visually acquire a small UAS.

→ Applying see-and-avoid below 500 ft AGL is unreliable for sUAS during daytime and cannot be depended upon as a primary WC mitigation.

In addition to the findings that directly address A68 research questions, several insights emerged from the UTM Services Filed Testing task that further inform how future refinements to WC criteria and DAA systems requirements. These results highlight that horizontal separation services provided to a sUAS by a UTM system for an autonomous sUAS have been shown to be feasible to maintain either a 2000 ft or 1500 ft separation distance between sUAS and manned aircraft at a 50% WC ratio IF the UTM system AND the information services that it relies upon meet the following requirements:

- The manned aircraft can be detected by the UTM system at the *minimum required detection distance* determined by simulation and validated by flight test.
- The manned aircraft position information used by the UTM system from ADS-B or radar must have a position error which is not large with respect to the required separation distance.
- The UTM system must have reliable communication services in the operational area such that any “drop-outs” in service, in conjunction with the closing speed of the encounter, do not lead to large position errors relative to the desired separation distance.

In the flight tests conducted in this task, the cellular connectivity onboard the manned aircraft and the sUAS were found to be reliable. It was possible to conduct sUAS separation from manned aircraft based on data sent to and received from the UTM system using cellular connectivity.

Encounters with higher traffic densities (i.e., encounters with more than two aircraft) required larger detection distances in order to maintain well clear separation between all aircraft involved. This is a factor to be considered by DAA systems designers, manufacturers, and operators.

For sUAS depending on a UTM system to provide separation services the following is strongly recommended:

- Regulators and standard bodies should consider focusing on providing the minimum required detection distances to sUAS DAA system designers and producers to allow them to give UTM systems the ability to provide reliable traffic alerting services while also supporting industry’s desire to reduce surveillance range where operationally justified.
 - The minimum required detection distances developed in this study apply to the range of speeds of fixed wing sUAS systems currently deployed. For multirotor systems that cannot fly as fast, the detection distances will actually be larger because, for head-on and overtaking encounters, slower sUAS cannot “get out of the way” fast enough to avoid a well clear violation.
 - The avoidance algorithm used in this study is, however, not the only one available, so other algorithms will likely require slightly different minimum required detection distances. Obviously, ACAS/sXu uses viable algorithms that separate air traffic; but, the biggest difference is that the MPF-based algorithm used in this study has the characteristic that the sUAS is provided with guidance to *return to the flight*

path in the mission before the encounter occurred. This is a capability that has value for operators controlling package delivery and for future corridor flight in the evolving UAM/AAM environment.

- Consider providing required minimum performance metrics to radar service providers to give UTM systems the ability to provide reliable traffic position information in their traffic alerting services.

3.2 sUAS-sUAS Separation

The results of this part of the project provide a unified answer to the research question:

What separation and performance requirements are needed for BVLOS sUAS to remain safely separated from other sUAS that broadcast their RID, or through UTM-provided separation services?

Flight test and simulation results indicate that, based on the broadcast performance of current RID systems, horizontal separation in the range of 100–300 ft is feasible for achieving a 50% WC ratio between small quadcopter-class sUAS, while horizontal separation in the range of 400–600 ft is feasible for achieving a 50% WC ratio for larger multirotor and fixed-wing sUAS. Accordingly, when two sUAS rely solely on RID broadcasts for cooperative detect-and-avoid, a horizontal separation envelope of 100–600 ft, scaled with aircraft size, was shown to be achievable at the 50% WC success level under the tested conditions.

Horizontal separation services provided to a sUAS by a UTM system for an autonomous sUAS avoiding another sUAS have been shown to be feasible to maintain separation distances ranging from 100 feet to 600 feet at a success rate of 50% IF the UTM system AND the information services that it relies upon meet the following requirements:

- The sUAS can be detected by the UTM system at the ***minimum required detection distance*** determined by simulation and validated by flight test.
- The position knowledge bias is small with respect to the desired separation distance.
- The UTM system must have reliable communication services in the operational area such that any “drop-outs” in service, in conjunction with the closing speed of the encounter do not lead to large position errors relative to the desired separation distance.
 - In the flight tests conducted in this work, the cellular connectivity onboard the sUAS were found to be reliable in both flight test locations (Lawrence, KS and Starkville, MS). It was possible to conduct sUAS separation from other aircraft (sUAS and manned aircraft) based on data sent to and received from the UTM system using cellular connectivity.

Based on the results, the team recommends the following:

- Regulators and industry standard bodies should consider focusing on defining the required minimum performance metrics for a new class of “UTM-enabling” RID broadcast devices
- Regulators and industry standard bodies should consider providing the required minimum performance metrics to RID broadcast receiver manufacturers to give UTM systems the ability to provide reliable alerting services.

- The RID range and drop-out studies detailed in this report support the notion that RID broadcasts with adequate range and reliability have the potential to be used for sUAS vs sUAS encounters.
- Conduct additional testing using RID devices with configurable broadcast parameters. The systems evaluated in this task did not allow full control of broadcast rate or power, limiting the ability to determine the exact thresholds necessary for consistent WC. Future flight test campaigns should use RID modules where broadcast power and broadcast rate can be systematically varied to identify the minimum performance envelope that still supports safe BVLOS separation.
- Validate performance across diverse operational environments. All findings in this report were obtained under rural, low-interference, line-of-sight conditions with a stationary ground receiver. To support nationwide BVLOS deployment, further work is needed in urban, suburban, and obstructed environments, and with receivers located onboard aircraft, where motion, radio frequency (RF) congestion, multipath, and obstruction will introduce real-world degradation.
- Support development of standardized flight-test methodologies for RID performance. A unified test protocol will help regulators and manufacturers assess and certify RID performance consistently across vendors. This includes standardized measurements of detection probability vs. distance, packet update rate, latency, range, and positional error.
- Encourage greater transparency from RID manufacturers. Significant discrepancies were observed between commercially advertised specifications and observed field performance. RID vendors should publish validated broadcast-range data, update-rate behavior during motion, and expected packet detection probabilities vs. distance, ideally using standardized tests.

4 REFERENCES

- Abreu, A. D., Arboleda, G., Olivares, G., Gomez, L., Singh, D., Bruner, T., . . . Weinert, A. (2023). *A47_A11L.UAS.89 – sUAS Mid-Air Collision (MAC)*. ASSURE.
- Amerson, D., Ryker, K., White, C., Bassou, R., Goodin, C., Dabbiru, L., . . . Dayarathna, V. (2023). *ASSURE A23 – Validation of low altitude detect and avoid standards: Final report*. Raspet Flight Research Laboratory, Mississippi State University; U.S. Department of Transportation Federal Aviation Administration.
- Amerson, D., Ryker, K., White, C., Goodin, C., Dabbiru, L., Babski-Reeves, K., . . . Sah, R. (2024). *A65 – Detect and Avoid Risk Ratio Validation Final Report*. USDOT FAA (ASSURE). Retrieved from https://www.assureuas.org/wp-content/uploads/2022/02/A65-Final-Report_v7.pdf
- ASTM. (2020). *Standard Specification for Detect and Avoid System Performance Requirements (ASTM F3442/F3442M-20)*. West Conshohocken: ASTM International.
- ASTM. (2023). *Standard Specification for Detect and Avoid System Performance Requirements (ASTM F3442/F3442M-23)*. Retrieved from https://doi.org/10.1520/F3442_F3442M-20
- ASTM. (2025). *Standard Specification for Detect and Avoid System Performance Requirements (ASTM F3442-25)*. Retrieved from <https://doi.org/10.1520/F3442-25>
- De Abreu, A., Arboleda, G., Olivares, G., Gomez, L., Singh, D., Bruner, T., . . . Wallace, R. (2023). *sUAS Mid Air Collision Likelihood - Final Report (Final Report A47, Issue A11L.UAS.87-002)*. Retrieved from <https://www.assureuas.com/projects/suas-mid-air-collision-likelihood/>
- Espindle, L., Griffith, J., & Kuchar, J. (2009). *Safety Analysis of Upgrading to TCAS Version 7.1 Using the 2008 U.S. Correlated Encounter Model (Project Report ATC-349)*. MIT Lincoln Laboratory.
- FAA. (2023, 9 1). *Order 8040.6A: Unmanned Aircraft Systems (UAS) Safety Risk Management (SRM) Policy*. U.S. Department of Transportation, Federal Aviation Administration. Retrieved from https://www.faa.gov/regulations_policies/orders_notices/index.cfm/go/document.information/documentl...
- FAA. (2025). Part 107.37—Small Unmanned Aircraft Systems—Operation Near Aircraft: Right-of-Way Rules. Retrieved 9 3, 2025, from <https://www.ecfr.gov/current/title-14/chapter-I/subchapter-F/part-107/subpart-B/section-107.37>
- FAA. (2025). Part 91.113—General Operating and Flight Rules—Right-of-Way Rules: Except Water Operations. Retrieved 9 3, 2025, from <https://www.ecfr.gov/current/title-14/chapter-I/subchapter-F/part-91#91.113>
- Hendrickson, A. (2015). *A candidate approach for deriving top-level sense and avoid (SAA) system requirements (Part 1)*. U.S. Army Aviation and Missile Research, Development, and Engineering Center.

- Hudson, T., Lin, M., Cohen, J., Gottschalk, S., & Manocha, D. (2000). V-COLLIDE: Accelerated Collision Detection for VRML. *Association for Computing Machinery, Monterey, California, USA*.
- ICAO, I. C. (2008). *WP/4 – DAA performance metrics*. International Civil Aviation Organization (ICAO).
- Khatib, O. (1985). Real-time obstacle avoidance for manipulators and mobile robots. *1985 IEEE International Conference on Robotics and Automation Proceedings, 2*, pp. 500-505. Retrieved from <https://doi.org/10.1109/ROBOT.1985.1087247>
- Leonard, N., & Fiorelli, E. (2001). Virtual leaders, artificial potentials and coordinated control of groups. *Proceedings of the 40th IEEE Conference on Decision and Control, 3*, pp. 2968-2973. Retrieved from <https://doi.org/10.1109/CDC.2001.980728>
- Muñoz, C., Narkawicz, A., Hagen, G., Upchurch, J., Dutle, A., Consiglio, M., & Chamberlain, J. (2015). DAIDALUS: Detect and Avoid Alerting Logic for Unmanned Systems. *IEEE/AIAA 34th Digital Avionics Systems Conference (DASC), Prague, Czech Republic*. Retrieved from <https://doi.org/10.1109/DASC.2015.7311421>
- NTSB. (1987). *Aircraft Accident Report: Midair Collision of Aeronaves De Mexico S.A. McDonnell Douglas DC-9-32 XA-JED and Piper PA-28-181 N4891F*.
- Reynolds, C. (1987). Flocks, herds and schools: A distributed behavioral model. *SIGGRAPH Computer Graphics, 21(4)*, 25-34. Retrieved from <https://doi.org/10.1145/37402.37406>
- RTCA. (2005). *Safety Analysis of Proposed Change to TCAS RA Reversal Logic (DO-298)*.
- RTCA. (2022). *Minimum Operational Performance Standards for Airborne Collision Avoidance System sXu (ACAS sXu) (DO-396)*.
- SC-228. (2021). *Minimum Operational Performance Standards (MOPS) for Detect and Avoid (DAA) Systems (DO-365B)*.
- Serres, C., Gill, B., Reheis, P., Edwards, M., Guendel, R., Weinert, A., . . . Klaus, R. (2020). mit-ll/degas-core: Initial Release (v1.0). Retrieved from <https://doi.org/10.5281/zenodo.4323620>
- Snyder, P., Kaabouch, N., Vidhyadharan Nair, S., Vacek, J., Pothana, P., Ullrich, M., . . . Keshmin, S. (2024). *A54-A11L.UAS.97: Propose UAS Right-of-Way Rules for Unmanned Aircraft Systems (UAS) Operations and Safety*. USDOT FFAA (ASSURE).
- Stastny, T., Garcia, G., & Keshmiri, S. (2014). Collision and Obstacle Avoidance in Unmanned Aerial Systems Using Morphing Potential Field Navigation and Nonlinear Model Predictive Control. *Journal of Dynamic Systems, Measurement, and Control, 137*, 014503. Retrieved from <https://doi.org/10.1115/1.4028034>
- Underhill, N., & Weinert, A. (2021). Applicability and Surrogacy of Uncorrelated Airspace Encounter Models at Low Altitudes. *Journal of Air Transportation, 1-5*. Retrieved from <https://doi.org/10.2514/1.D0254>

- Wallace, R., Loffi, J., Vance, S., Jacob, J., Dunlap, J., & Mitchell, T. (2018). Pilot visual detection of small unmanned aircraft systems (sUAS) equipped with strobe lighting. *Journal of Aviation Technology and Engineering*, 57-66.
- Weinert, A. (2021). Airspace-Encounter-Models/em-pairing-geospatial: October 2021 - Version 2.0.0 (v2.0.0). Retrieved from <https://doi.org/10.5281/zenodo.3978267>
- Weinert, A., Campbell, S., Vela, A., Schuldt, D., & Kurucar, J. (2018). Well-Clear Recommendation for Small Unmanned Aircraft Systems Based on Unmitigated Collision Risk. *Journal of Air Transportation*, 26(3), 113-122. Retrieved from <https://doi.org/10.2514/1.D0091>
- Weinert, A., Kochenderfer, M., Edwards, M., Gill, B., Guendel, R., Serres, C., & Underhill, N. (2021). Airspace-Encounter-Models/em-model-manned-bayes: October 2021 (v2.1.0). Retrieved from <https://doi.org/10.5281/zenodo.5544340>
- Weinert, A., Underhill, N., & Wicks, A. (2019). Developing a Low Altitude Manned Encounter Model Using ADS-B Observations. *2019 IEEE Aerospace Conference*. Retrieved from <https://doi.org/10.1109/AERO.2019.8741848>